MECHANISMS FOR EXTRACELLULAR ELECTRON EXCHANGE BY *GEOBACTER* SPECIES

A Dissertation Presented

by

JESSICA AMBER SMITH

Submitted to the Graduate School of the
University of Massachusetts Amherst in partial fulfillment
of the requirements for the degree of

DOCTOR OF PHILOSOPHY

February 2015

Department of Microbiology

MECHANISMS FOR EXTRACELLULAR ELECTRON EXCHANGE BY *GEOBACTER* SPECIES

A Dissertation Presented

by

JESSICA AMBER SMITH

Approved as to style and content by:

____
Derek R. Lovley, Chair

____
James F. Holden, Member

____
Steven J. Sandler, Member

____
Dawn E. Holmes, Member

____
John M. Lopes, Department Head
Department of Microbiology

ACKNOWLEDGMENTS

I would like to thank my advisor, Derek Lovley, and the members of my committee, James Holden, Steven Sandler, and Dawn Holmes, for supporting and guiding my projects.

I especially thank Dawn Holmes for all of her support, advice, and friendship. Without her I truly wouldn't be where I am today. I also thank Carla Risso and Pier-Luc Tremblay for their invaluable training and mentorship, and not giving up on me.

I thank all of the past and current members of the Lovley lab, and all of my co-authors.

Above all, thanks to my family, particularly my sister Ashley Smith, who was forever there to make me smile. And to my parents, Willard and Christine Smith, who always support my decisions in life, and encourage me to pursue my goals.

ABSTRACT

MECHANISMS FOR EXTRACELLULAR ELECTRON EXCHANGE BY

GEOBACTER SPECIES

FEBRUARY 2015

JESSICA AMBER SMITH

B.S., WESTERN NEW ENGLAND UNIVERSITY

Ph.D., UNIVERSITY OF MASSACHUSETTS AMHERST

Directed by: Professor Derek R. Lovley

Understanding the mechanisms for microbial extracellular electron exchange are of interest because these processes play an important role in the biogeochemical cycles of both modern and ancient environments, development of bioenergy strategies, as well as for bioremediation applications. Only a handful of microorganisms are capable of extracellular electron exchange, one of the most thoroughly studied being the *Geobacter* species. *Geobacter* species are often the predominant Fe(III) reducing microorganisms in many soils and sediments, can exchange electrons directly via interspecies electron transfer, and can both donate or accept electrons with a wide variety of extracellular substrates including the electrode of a microbial fuel cell.

This dissertation describes three research projects that aim to further understand these mechanisms and identify novel components involved in extracellular electron exchange by *Geobacter* species. The first uncovers components involved in extracellular electron transfer to insoluble Fe(III) oxides by *Geobacter metallireducens*. This project identified six *c*-type cytochromes, a NHL-repeat containing protein, and a gene

potentially involved in pili glycosylation that were essential for reduction of insoluble Fe(III) oxide, but not for soluble Fe(III) citrate.

The second research project serves to reveal and examine PilA-pili independent mechanisms for extracellular electron transfer to Fe(III) oxides by *Geobacter sulfurreducen*s. During the course of this study a *pilA*-deficient strain of *G. sulfurreducens* adapted to reduce Fe(III) oxide via production of the *c*-type cytochrome PgcA, which was released into the culture medium, and was required for the newly adapted mechanism of Fe(III) oxide reduction.

The third research project investigates the mechanism(s) utilized by *G. sulfurreducens* for extracellular electron exchange into the cell via the oxidation of the humic substance analog anthrahydroquinone-2,6-disulfonate (AHQDS) in cocultures with *G. metallireducens*. Cocultures initiated with strains of *G. sulfurreducens* deficient in genes for proteins previously identified to be important in extracellular electron exchange grew as well as the wild type strain, suggesting that mechanisms for exchanging electrons with extracellular electron donors are substantially different than for reduction of extracellular electron acceptors.

TABLE OF CONTENTS

LIST OF TABLES

LIST OF FIGURES

CHAPTER 1

INTRODUCTION

1.1 Central Objective and Goals

Understanding the mechanisms for microbial extracellular electron exchange are of interest because these processes play an important role in the biogeochemical cycles of both modern and ancient environments, development of bioenergy strategies, as well as for bioremediation applications (Lovley *et al*., 2004). In one form of extracellular electron exchange microorganisms may transfer electrons from the inner to outer cell surface in order to reduce a terminal insoluble electron acceptor such as Fe(III) oxide, an electrode of a current- producing microbial fuel cell, or to a neighboring microorganism. Extracellular electron exchange can also happen in the reverse direction, in which case electrons are transferred into the cell from an electron donor, for example during direct interspecies electron transfer (DIET) or from a current consuming electrode. Only a handful of microorganisms are capable of extracellular electron exchange, including the thoroughly studied *Geobacter sulfurreducens*. *G. sulfurreducens* forms highly conductive networks of PilA-pili filaments that transfer electrons directly onto extracellular electron acceptors (Malvankar *et al*., 2011; Reguera *et al*., 2005; Vargas *et al*., 2013), however these filaments do not appear to be important for electron transfer into the cell by *G. sulfurreducens* and the mechanisms for this type of extracellular electron exchange remain unclear (Strycharz *et al*., 2011). Additionally, other lesser studied *Geobacter* species such as *G. metallireducens* are more effective at extracellular electron transfer than *G. sulfurreducens* and have other environmentally significant physiological properties not found in *G. sulfurreducens,* such as the ability to anaerobically oxidize aromatic hydrocarbons (Butler *et al*., 2007; Lovley *et al*., 1993b; Zhang *et al*., 2012; Zhang *et al*., 2013; Zhang *et al*., 2014). *G. metallireducens* can also directly transfer electrons to methanogenic species such as *Methanosaeta* (Rotaru *et al*., 2014b) and *Methanosarcina barkeri* (Rotaru *et al*., 2014a).

The main goal of this dissertation is to uncover components involved in extracellular electron transfer in the lesser characterized Fe(III) oxide reducer *Geobacter metallireducens,* and to develop insights into the mechanisms used by *Geobacter sulfurreducens* for PilA-pili independent extracellular electron exchange.

1.2 Organization of the Dissertation

This dissertation is divided into three independent research chapters; each one corresponds to an independent scientific publication. Chapter 1 presents the justification and background of the study. Chapters 2, 3, and 4 are the main research chapters describing results and discussion from each project. Chapter 2 presents results from experiments that uncovered components involved in extracellular electron transfer to Fe(III) oxide by *Geobacter metallireducens*. Chapter 3 presents results from a study that identified PilA-pili independent mechanisms for extracellular electron transfer by *Geobacter sulfurreducen*s. Chapter 4 investigates the mechanism(s) utilized by *G. sulfurreducens* for extracellular electron exchange into the cell. Finally, Chapter 5 summarizes the findings, discusses relevant implications, and suggests directions for future work.

1.3 Extracellular Electron Exchange

Extracellular electron exchange refers to a method by which an organism utilizes electron transfer processes on the outer cell surface. Extracellular electron exchange can occur when an organism is transferring electrons from the inside of the cell to the outside in order to reduce an extracellular terminal electron acceptor. The process can also occur in the reverse direction, whereby an organism may accept electrons for energy generation from an insoluble electron donor. Although there are a limited number of organisms known to carry out these unique processes, there are several types of extracellular electron acceptors and extracellular electron donors. Some of the major examples are discussed below.

1.3.1 Extracellular Electron Acceptors

In aerobic cellular respiration oxygen is free to move across the cellular membrane, where it will be reduced to water when it receives electrons from a terminal oxidoreductase enzyme located in the electron transport chain. Anaerobic cellular respiration utilizes a terminal electron acceptor other than oxygen. For example, a terminal nitrate reductase will transfer electrons to nitrate and reduce it to nitrite. Similarly, sulfate can act as a terminal electron acceptor and be reduced to sulfide. When substrates, such as nitrate and sulfate, are used as terminal electron acceptors for energy generation these processes are said to be dissimilatory. This differs from assimilative metabolism whereby substrates are reduced for use as a nutrient source. Like oxygen, nitrate and sulfate can be reduced on the inside of the cell membrane.

Some terminal electron acceptors are insoluble, meaning they cannot enter the cell and must be reduced on the outer cell surface. These insoluble electron acceptors are therefore called “extracellular electron acceptors” and the transport of electrons to them is known as “extracellular electron transfer”. Some examples of extracellular electron acceptors include insoluble metals such as Fe(III) and Mn(IV) oxides, humic substances, electrodes of current-producing microbial fuel cells, or other microorganisms which can directly accept electrons during direct interspecies electron transfer (DIET).

1.3.1.1 Dissimilatory Metal Reduction

Less than three decades ago it was believed that Fe(III) and other metal reducing processes in the environment resulted primarily from nonenzymatic reactions (Lovley, 1993a). However, this theory was refuted when dissimilatory metal reducing microorganisms, specifically *Geobacter* (Lovley *et al*., 1993b) and *Shewanella* (Myers and Nealson, 1988) species, were isolated in pure cultures. Furthermore, it was uncovered that metal reducing species, such as *Geobacter metallireducens,* can couple the reduction of Fe(III) with the oxidation of aromatic contaminants, including benzene (Butler *et al*., 2007; Lovley *et al*., 1993b; Zhang *et al*., 2012; Zhang *et al*., 2013; Zhang *et al*., 2014). We now know that microorganisms can enzymatically catalyze nearly all metal reducing processes taking place in sedimentary environments (Lovley, 1991a; Lovley *et al*., 1991b). This makes sense as metals such as iron are key components in cellular proteins involved in electron transfer; for example, cytochromes contain heme prosthetic groups consisting of an Fe^{2+} ion.

The study of microbial metal reduction is significant because metals are an important component of the biogeochemistry of the Earth today (Aller *et al*., 1986; Canfield *et al*., 1993; Lovley and Phillips, 1986a), and were likely even more widespread on early Earth (Lovley *et al*., 2004; Vargas *et al*., 1998). Several metals can be reduced by microorganisms coupled to the oxidation of simple organic acids and alcohols, hydrogen, or aromatic compounds for energy conservation (Lovley, 1993a). Therefore, this process influences the biogeochemical cycles of metals and the fate of organic matter and nutrients in the environment (Lovley *et al*., 2004). Two of the most thoroughly studied metals include Fe(III) and Mn(IV), which greatly influence the organic and inorganic geochemistry of anaerobic aquatic sediments and groundwater (Lovley, 1991a).

Fe(III) is one of the most abundant electron acceptors for organic matter decompositions in many aquatic sediments and subsurface environments (Lovley, 1991a). Reduction of Fe(III) can be coupled to the oxidation of hydrogen or to a wide variety of organic compounds that are completely oxidized to carbon dioxide (Coates *et al*., 1995; Lovley, 1993a). Acetate is one of the most significant electron donors and sources of carbon in sedimentary environments where Fe(III) reduction is an important process (Lovley and Phillips, 1989). Some Fe(III) reducers can also oxidize aromatic hydrocarbons and long chain fatty acids (Butler *et al*., 2007; Holmes *et al*., 2011; Holmes *et al*., 2012; Tor and Lovley, 2001; Zhang *et al*., 2012; Zhang *et al*., 2013; Zhang *et al*., 2014). Most of these substrates are the products from fermentation occurring in anaerobic environments (Lovley and Phillips, 1989). Therefore, Fe(III) reducers are typically not in competition with fermentative microorganisms, but instead have a cooperative relationship with them in anoxic sediments.

When electrons are transferred to ferric iron during dissimilatory Fe(III) reduction the compound is reduced to ferrous iron. For example, when acetate is oxidized to carbon dioxide during Fe(III) respiration the overall equation is:

$$CH_3COO^- + 8Fe(III) + 4H_2O \rightarrow 2HCO_3^- + 8Fe(II) + 9H^+$$

Fe(III) can exist in many forms both in the environment and in the laboratory. Crystalline Fe(III) oxides include hematite, goethite, akaganeite, and magnetite. Although crystalline Fe(III) oxides can be reduced by Fe(III) reducing species it is generally difficult to continuously transfer these cultures in the laboratory and the rate of growth is relatively slow; this is likely attributed to the large size and surface area of the particles (Kostka and Nealson, 1995; Lovley, 1991a). Poorly crystalline Fe(III) oxides are typically used in the laboratory for studies on mechanisms for insoluble Fe(III) oxide reduction (Aklujkar *et al*., 2013; Childers *et al*., 2002; Ding *et al*., 2008; Smith *et al*., 2013). Soluble Fe(III) forms are the simplest for laboratory culturing, and rates of growth are considerably faster than poorly crystalline Fe(III) oxides. Soluble Fe(III) forms, such as Fe(III) citrate, are likely more accessible to the cell, but are still reduced on the outer cell surface (Nevin and Lovley, 2002a). Chelators, such as nitrilotriacetic acid (NTA), can serve to further solubilize Fe(III) forms (Lovley *et al*., 1994). The reduced Fe(II) is more soluble than oxidized Fe(III), and thus microbial Fe(III) reduction results in an increase in dissolved iron in the environment. Reduction of Fe(III) also results in the production of magnetite (Fe_3O_4), siderite ($FeCO_3$), and vivianite ($Fe_3PO4 \cdot 8H_2O$) (Lovley, 1991a; Lovley, 1995).

There are three commonly considered mechanisms for Fe(III) oxide reduction which include: (i) direct contact between redox-active proteins on the outer surfaces of the cells and the electron acceptor, (ii) electron transfer via a bacterially produced electron shuttle, and (iii) solubilization of Fe(III) by Fe(III) chelators (Nevin and Lovley, 2002a). Mechanisms for Fe(III) reduction have been most thoroughly studied in bacterial species from the genera *Geobacter* and *Shewanella*. *Geobacter* species must come into direct contact with the insoluble Fe(III) oxide in order to reduce the electron acceptor

(Nevin and Lovley, 2000; Straub and Schink, 2003). On the other hand, *Shewanella* species, such as the thoroughly studied *S. oneidensis*, release riboflavin (B2) and flavin mononucleotide (FMN) to the outside of the cell, which can serve as electron shuttles accelerating the reduction of insoluble substrates (Coursolle *et al*., 2010; Lies *et al*., 2005; Marsili *et al*., 2008; Nevin and Lovley, 2002b; von Canstein *et al*., 2008). *S. oneidensis* can also reduce insoluble electron acceptors by direct contact through the Mtr respiratory pathway (Shi *et al*., 2007), which consists of a conduit of multiheme *c*-type cytochromes and a non-heme outer membrane β-barrel that connects the cytochromes to a cytoplasmic membrane quinol oxidase (Coursolle *et al*., 2010; Hartshorne *et al*., 2009; Ross *et al*., 2007). *Shewanella* species may also produce microbial nanowires involved in long-range electron transport (El-Naggar *et al*., 2010; Leung *et al*., 2013; Pirbadian *et al*., 2014). However, studies on the electrical and biochemical properties of these filaments are still in their infancy.

Geological and microbiological evidence suggests that Fe(III) reduction evolved from Archaea, and was a key form of respiration on early earth (Holm *et al*., 1992; Kashefi *et al*., 2004; McKay *et al*., 1996). Many hyperthermophilic microorganisms can reduce Fe(III) coupled to the oxidation of hydrogen (Kashefi *et al*., 2004; Lin *et al*., 2014; Roling *et al*., 2003; Slobodkin, 2005; Vargas *et al*., 1998). Some hyperthermophiles can also couple the reduction of Fe(III) with the complete oxidation of aromatic and aliphatic hydrocarbons. For example, *Ferroglobus placidus* (Hafenbradl *et al*., 1996) is a hyperthermophilic archaeon that can couple the reduction of Fe(III) with the complete oxidation of benzene (Holmes *et al*., 2011), and several other aromatic compounds (Aklujkar *et al*., 2014; Holmes *et al*., 2012; Tor and Lovley, 2001). *F.*

placidus, along with its relative *Geoglobus ahangari*, both require direct contact in order to reduce insoluble Fe(III) oxides (Manzella *et al*., 2013; Smith *et al*., 2014). *F. placidus* has close to 30 genes encoding for putative *c*-type cytochrome proteins (Anderson *et al*., 2011; Smith *et al*., 2014), and eight of these had higher transcript abundance in *F. placidus* cells grown on insoluble Fe(III) oxide compared with soluble Fe(III) citrate, suggesting a possible role for these proteins in the direct electron transfer to insoluble Fe(III) (Smith *et al*., 2014). Some methanogenic archaea are also capable of reducing Fe(III) (Bond and Lovley, 2002b). However, the general mechanism(s) remain unclear. Uncovering the methods utilized by hyperthermophilic archaea for insoluble metal reduction can help in understanding evolution from life on early earth.

Mn(IV) reduction is similar to Fe(III) reduction in that both compounds get reduced extracellularly and can be coupled to the oxidation of organic compounds (Myers and Nealson, 1988). Mn(IV) oxide is found in many diverse forms in the environment, and the form influences the rate of reduction. Mn(IV) gets reduced to Mn(II), which like Fe(II) is more soluble than the oxidized form (Lovley, 1993a; Morgado *et al*., 2010). An additional side product of Mn(IV) reduction is rhodochrosite ($MnCO_3$) (Lovley, 1991a; Lovley, 1995). Specific mechanisms on the reduction of Mn(IV) are not as widely studied as Fe(III), however most microorganisms that can reduce Fe(III) can also transfer electrons to Mn(IV) compounds (Lovley and Phillips, 1988; Myers and Nealson, 1988).

Uranium is another metal that microorganisms can utilize as a terminal electron acceptor. Microbial reduction of soluble U(VI) to insoluble U(IV) is an important process in the global uranium cycle (Gorby and Lovley, 1992; Lovley and Phillips, 1992a; Lovley and Phillips, 1992b; Lovley *et al*., 1993c), and has been a useful technique for immobilizing uranium from contaminated environments (Phillips *et al*., 1995; Williams *et al*., 2013). For example, *Geobacter* species are naturally occurring U(VI) reducers in many subsurface environments, and can be stimulated with the addition of acetate in the groundwater (Anderson *et al*., 2003; Holmes *et al*., 2002). The reduction of U(VI) to U(IV) by microorganisms such as *Geobacter* precipitates the uranium from the groundwater preventing its further mobility (Williams *et al.*, 2013). Like soluble Fe(III) citrate, the slightly more soluble U(VI) is reduced on the outer cell surface of metal reducing microorganisms. For example, U(VI) reduction by *G. sulfurreducens* occurs via outer cell surface *c*-type cytochromes (Shelobolina *et al.*, 2007; Orellana *et al*., 2013).

Several other metals and metalloids can be microbially reduced (Lovley, 1993a) including selenium (Doran and Alexander, 1977; Maiers *et al*., 1988), chromium (Lovley, 1993a), mercury (Lovley, 1993a), technetium (Lloyd and Macaskie, 1996; Lloyd *et al*., 2000), molybdenum, vanadium (Ortiz-Bernad *et al*., 2004), copper (Caccavo *et al*., 1994), silver (Law *et al*., 2008), gold (Kashefi *et al*., 2001), and arsenic (Giloteaux *et al*., 2013). Dissimilatory reduction of many of these metals is a potential mechanism for removing these toxic metal forms from contaminated environments or waste streams (Lovley, 1993a).

1.3.1.2 Humic Substances and Other Extracellular Quinones

Microorganisms capable of producing energy via extracellular electron transfer to insoluble metals typically also have the ability to transfer electrons to the quinone moieties of humic substances (Lovley *et al*., 1996a; Scott *et al*., 1998) or onto humic analogs such as the synthetic laboratory compound anthraquinone-2,6-disulfonate (AQDS). Humic substances can serve as the sole electron acceptor for energy generation

(Lovley *et al*., 1996a; Lovley *et al*., 1998). Humic substance can also act as an electron shuttle whereby a microorganism transfers electrons to reduce the humic substance, which can then transfer the electrons to an additional electron acceptor, thereby regenerating the oxidized humic compound (Lovley *et al*., 1996a; Lovley *et al*., 1998). This secondary electron acceptor that is reduced by the humic compound can be an insoluble oxidized metal such as Fe(III), or could be another microorganism in the environment (Liu *et al*., 2012). Therefore, addition of humic substances can greatly increase the rate of insoluble metal reduction or interspecies electron transfer.

The humic analog AQDS has been useful in the laboratory for uncovering how microorganisms are capable of extracellular electron transfer to humic substances (Voordeckers *et al*., 2010). Addition of AQDS increases the rate of Fe(III) reduction substantially when added to cultures. AQDS is likely more accessible to cells than the highly insoluble Fe(III) oxide. In this case AQDS is reduced to anthrahydroquinone-2,6,-disulphonate (AHQDS), which can then shuttle electrons to Fe(III), regenerating AQDS for further reduction by the microorganism (Lovley *et al*., 1996a; Lovley *et al*., 1998). AQDS/ AHQDS shuttling has also been observed between two species, such as in cocultures of *G. metallireducens* with *G. sulfurreducens* (Liu *et al*., 2012) .

1.3.1.3 Microbial Fuel Cells

Electrodes of a microbial fuel cell (MFC) can serve as an anaerobic electron acceptor for some microorganisms (Lovley, 2006a; Lovley, 2006b). Many bacteria that can utilize insoluble metals as terminal electron acceptors can, in a similar manner, also transfer electrons beyond the cell surface onto electrodes. Studies of MFCs are of interest because of the possibility they offer in harvesting electricity from organic waste and renewable biomass (Lovley, 2008; Lovley and Nevin, 2011c). MFCs consist of an anode, which accepts electrons from microorganisms, and a cathode, which transfers electrons to a terminal electron acceptor. Electrons are generally supplied to microorganisms via microbially degradable organic matter. Much like Fe(III) reduction, transfer of electrons from microorganisms to the anode of a microbial fuel cell can occur via direct electron transfer, through the release of a biologically produced electron shuttling compound, or via an artificial mediating electron shuttle (Lovley, 2006a).

Although MFC's have the potential to convert organic waste matter to electricity, current outputs are too low for most perceived practical applications. Research efforts have focused on two main ways to improve the efficiency of MFC's (Malvankar *et al*., 2012c). The first way is through engineering better fuel cell architecture and cathode materials. The second way is through improving the biological factors, either through genetic engineering or laboratory adaptation of the microorganisms colonizing the fuel cell.

Most standard electrodes of MFCs consist of graphite (Bond and Lovley, 2003). Recent efforts towards increasing the efficiency and power output of electrodes have identified many materials that can either be added to the MFC or are actually components of the electrode. One of the most commonly used materials is granular activated carbon (GAC). GAC has a high-surface area that can support microbial attachment and growth (Aziz *et al*., 2011). GAC is also often added to methanogenic digesters to increase and accelerate methane production (Aktas and Cecen, 2007). It is highly conductive (Kastening *et al*., 1997), and can possibly serve as an electron acceptor during anaerobic respiration (van der Zee *et al*., 2003). Anodes in MFCs can actually be constructed with

GAC (Gregory *et al*., 2004), and enhance an anodes ability to accept electrons from microorganisms. GAC may also act in the reverse direction and serve as an electron donor for anaerobic respiration (Gregory *et al*., 2004; Nevin *et al*., 2010).

Other efforts to improve electricity production by MFCs have focused on enhancing capabilities of the microorganisms that colonize the fuel cell. One method is through genetic engineering. For example, over-expression of *pilA* and exopolysaccharide proteins in *Geobacter sulfurreducens* calles increases current-producing biofilms and power densities in fuel cells (Leang *et al*., 2013).

Another strategy that has been effective is laboratory adaptive evolution of microorganisms on the electrode. Because electrodes are not naturally occuring electron acceptors, evolutionary pressure has not allowed for selection of microorganisms that are most efficient at electron transfer to electrodes. In one study, *G. sulfurreducens* strain DL-1 was grown on a current producing electrode for an extended period of time. The adapted strain, KN400, had current and power densities substantially higher than that of DL-1 (Yi *et al*., 2009). This type of laboratory adaptive evolution is a useful tool for isolating strains with enhanced capabilities when placed under a selective pressure.

1.3.1.4 Extracellular Interspecies Electron Transfer

In the environment, almost all organisms rely on other species to survive. This type of cooperative or syntrophic relationship is essential in all domains of life, particularly among microorganisms. One of the most thoroughly studied types of interspecies cooperation between microorganisms is hydrogen interspecies transfer (HIT), a process by which electron-donating microorganisms reduce protons to hydrogen and another organism can oxidize the hydrogen for energy generation (McInerney *et al*., 2009; Stams and Plugge, 2009). HIT can often be observed between a bacterial and methanogenic species, whereby the methanogen oxidizes hydrogen and couples it to the reduction of carbon dioxide forming methane (Rotaru *et al.*, 2012). A similar reaction can occur via formate as an electron carrier (McInerney *et al*., 2009; Stams and Plugge, 2009).

Another type of interspecies electron transfer is direct interspecies electron transfer (DIET), whereby electrons are transported from one microorganism to another via direct electrical connections, without the involvement of hydrogen or formate as electron carriers (Lovley, 2011b). DIET was first observed in cocultures of *Geobacter metallireducens* and *Geobacter sulfurreducens* (Summers *et al*., 2010). These cocultures were grown in a medium with ethanol provided as the sole electron donor and fumarate as the sole electron acceptor. In this environment the two species need to exchange electrons in order to grow because *G. metallireducens* can metabolize ethanol, but cannot reduce fumarate and *G. sulfurreducens* cannot utilize ethanol as an electron donor, but can use fumarate as an electron acceptor. *G. metallireducens* is a poor hydrogen former (Cord-Ruwisch *et al*., 1998), and furthermore when cultures with *G. sulfurreducens* in which a hydrogenase gene essential for oxidation of hydrogen was deleted from the genome, the cocultures were still effectively able to oxidize ethanol and reduce fumarate to succinate (Summers *et al*., 2010). These results show that electrons were being directly exchanged between aggregates of the two species in the coculture.

DIET has also been observed between *Geobacter metallireducens* with acetoclastic methanogens (Rotaru *et al.*, 2014a; Rotaru *et al.*, 2014b). Acetoclastic methanogens include the *Methanosaeta* and *Methanosarcina* species. The *Methanosaeta* species are strict acetoclastic methanogens, and cannot use hydrogen for the reduction of carbon dioxide to methane (Rotaru *et al*., 2014b). The *Methanosarcina* have a more diverse physiology and can use a wider of variety of substrates for methane production including acetate, hydrogen and methanol (Rotaru *et al*., 2014a). These acetoclastic methanogens often predominate in many anaerobic digesters, and electrically conductive granules with high abundance of both *Geobacter* and *Methanosaeta* species have been identified in upflow anaerobic sludge blanket (UASB) reactors treating brewery waste (Morita *et al*., 2011), suggesting DIET is an important process in the environment.

When cocultured with *G. metallireducens*, *Methanosaeta harundinacea* directly accepted electrons generated from *G. metallireducens,* after oxidizing ethanol, and reduced carbon dioxide to methane (Rotaru *et al*., 2014b). Like *M. harundinacea*, *Methanosarcina* species are acetoclastic methanogens and are often abundant in methanogenic soils and sediments, coal mines, landfills, and anaerobic digesters. When cocultured with *G. metallireducens*, *Methanosarcina barkeri* was able to directly accept electrons for the reduction of carbon dioxide to methane (Rotaru *et al*., 2014a). Similar to *Geobacter* cocultures, the addition of the electrically conductive granular activated carbon (GAC), can mediate the electron transport between *M. barkeri* and *G. metallireducens*, accelerating the electron transport process (Liu *et al*., 2012).

To date *G. metallireducens* has been the only microorganism found to be capable of donating electrons to another species by DIET. The exact mechanism that allows this to occur is still in its infancy. However it is known that the *pilA* gene (Gmet_1399) which codes for the protein subunit of the type IV geopilin, the *c*-type cytochrome gene Gmet_2896, and the gene *fliC* which encodes for the flagella protein subunit are essential for DIET by *G. metallireducens* (Shrestha *et al*., 2013c). Additionally, *G. metallireducens* is able to utilize ethanol as an electron donor, which many organisms including *G. sulfurreducens* and methanogens cannot do. *Pelobacter carbinolicus*, a member of the *Geobacteraceae* which evolved from an Fe(III) reducer (Aklujkar *et al*., 2012), can also utilize ethanol as an electron donor. However, when it was cocultured with *G. sulfurreducens* electrons were exchanged via hydrogen (Rotaru *et al*., 2012). This is likely because *P. carbinolicus* lacks the ability to make direct electrical connections with extracellular electron acceptors, and, unlike *G. metallireducens*, its ability to effectively generate hydrogen (Aklujkar *et al*., 2012). The specific extracellular electron transport components combined with the ability to oxidize ethanol are the two qualities that enable *G. metallireducens* to donate electrons via DIET. A search for other species capable of donating electrons directly, including other members of the *Geobacteraceae*, could potentially provide further insight towards understanding the specific mechanisms used for DIET.

1.3.2 Extracellular Electron Donors

Along with a terminal electron acceptor being needed for energy generation during cellular respiration, an electron donor is essential for both energy generation and biosynthesis reactions to occur. There are many compounds that can be utilized as electron donors by different organisms. Glucose is most commonly considered, however, many microorganisms can metabolize a wide variety of other electron donors including acetate, others short cahin fatty acids, hydrogen, alcohols, or many soluble organic compounds. Some microorganisms have the unique ability to oxidize insoluble electron donors that cannot freely move across the cell membrane. Some examples of common extracellular electron donors are discussed below.

1.3.2.1 Environmental Compounds

Along with serving as terminal electron acceptors when they are in the oxidized form, humic substances can also serve as electron donors when they are in a reduced state (Lovley *et al*., 1999). For example the humic analog anthrahydroquinone-2,6,-disulphonate (AHQDS) can be utilized as the sole electron donor by Fe(III)- reducing microorganisms including *G. sulfurreducens*. In fact, a wide phylogenetic diversity of microorganisms that can use humic substances as an electron acceptor can also oxidize reduced humic substances coupled to the reduction of many terminal electron acceptors including nitrate, fumarate, and arsenate. Some of these microorganisms include *G. metallireducens*, *G. sulfurreducens*, *Geothrix fermentans*, *Shewanella alga*, and *Wolinella succinogenes* (Lovley *et al*., 1999). Humic substances may also play a role in electron shuttling between microorganisms in the environment (Liu *et al*., 2012). As discussed previously, this type of electron shuttling occurs between *G. metallireducens* and *G. sulfurreducens* (Liu *et al*., 2012). Another example is with cocultures of *G. metallireducens* and *W. succinogenes.* In these cocultures *G. metallireducens* can oxidize acetate coupled to the reduction of AQDS, while *W. succinogenes* cannot oxidize acetate but is able to use reduced AHQDS for fumarate respiration (Lovley *et al*., 1999). The quinone moieties of humic substances found naturally in the environment can likely also serve as electron donors and shuttling compounds in a similar manner.

Reduced metal compounds such as Fe(II) and U(IV) can serve as electron donors for microbial respiration. In this case lithotrophic microorganisms oxidize these electron donors coupled to the reduction of oxygen (Weber *et al.*, 2006a). The mechanism for oxidation of insoluble metals is poorly understood due to the difficulty of laboratory culturing with these inorganic compounds. For example, Fe(II)- oxidizing bacteria oxidize Fe(II) to insoluble Fe(III) oxide precipitates, which makes culturing complicated. Furthermore, maintaining a steady supply of electrons in the form of Fe(II) and maintaining oxygen concentrations in the micromolar range to minimize abiotic Fe(II) oxidation is challenging (Weber *et al.*, 2006a). However, Fe(II)-oxidizing bacteria such as *Mariprofundus ferrooxydans* PV-1 are capable of accepting electrons from an external source such as the electrode of a microbial fuel cell (Summers *et al.*, 2013), suggesting that the oxidation of compounds such as Fe(II) occurs on the outer cell surface. Additionally, some Fe(III) reducing bacteria, including *Geobacter metallireducens,* can oxidize Fe(II) and U(IV) with nitrate as an electron acceptor (Finneran *et al.*, 2002; Weber *et al.*, 2006b). The findings that microorganisms capable of electron transfer onto extracellular electron acceptors, and the ability of Fe(II) oxidizers to accept electrons from other insoluble electron donors suggests that these reduced metals represent a class of insoluble electron donors. Unfortunately, studies on specific mechanisms for oxidation of these compounds are currently stymied by the lack of technical ability in culturing microorganisms with these compounds in the laboratory.

Zero-valent iron (ZVI) is another form of reduced metal that can be utilized as an insoluble electron donor for some microorganisms. ZVI has applications in treating acidic water contaminated with heavy metals, and is also useful for industrial wastewater treatment as it catalyzes the abiotic conversion of a variety of pollutants such as chlorinated aliphatics, chlorinated aromatics, nitrates, and other contaminants (Li *et al.*, 2006; O'Carroll *et al*., 2013; Yan *et al*., 2010). ZVI can also serve as an electron donor coupled to the microbial reduction of many oxidized contaminants such as chlorinated solvents (Gregory *et al*., 2000; Lampron *et al*., 2001; Novak *et al*., 1998). ZVI can be oxidized to Fe(II) when being utilized as an electron donor for sulfate reducing bacteria in anaerobic sludge (Karri *et al*., 2005). Under anaerobic conditions hydrogen is produced from the chemical reaction of ZVI with water, therefore the ultimate electron transfer from ZVI to these microorganisms is likely via hydrogen (Liang *et al*., 2000). However, ZVI has also been shown to be utilized as an electron donor by methanogenic species (Novak *et al*., 1998), facilitating methanogenesis and anaerobic digestion. Many anaerobic digesters are dominated by the acetoclastic methanogenic species *Methanosaeta* and *Methanosarcina* (Morita *et al*., 2011). *Methanosaeta* and some *Methanosarcina* species would not be able to utilize hydrogen as a substrate for methanogenesis. Therefore, it is likely that if these species were utilizing ZVI as an electron donor for methanogenesis, they would not be accepting electrons from hydrogen transfer, but instead by some alternative mechanism.

1.3.2.2 Microbial Fuel Cells as Electron Donors

In addition to the electrodes of a MFC acting as a terminal extracellular electron acceptor they can also serve in the reverse direction as electron donors (Nevin *et al*., 2010; Ross *et al*., 2011). In some cases when electrodes are poised at low potentials they can indirectly donate electrons to microorganisms via hydrogen production or electron shuttles (Lovley, 2008). Alternatively, microorganisms can directly accept electrons from an electrode. In this case the microorganisms accept electrons from the cathode that then allows for the electrons to be transferred to a terminal electron acceptor via anaerobic respiration. This process was first observed in *Geobacter* species utilizing fumarate, nitrate, or U(VI) as an electron acceptor (Dumas *et al*., 2008; Gregory and Lovley, 2005; Gregory *et al*., 2004).

Shewanella species are also capable of utilizing MFC's as electron donors. *S. oneidensis* strain MR-1 uses a reverse Mtr pathway to power reductive reactions (Ross *et al*., 2011). Unlike *Shewanella*, *Geobacter* species do not appear to utilize the same components for electron exchange from the electrode as they do for extracellular electron transfer to electrodes as electron acceptors (Strycharz *et al*., 2011). Understanding the mechanisms used by microorganisms use for electron exchange from electrodes to cells is important industrially for electrosynthesis of high value fuels and chemicals (Lovley and Nevin, 2013).

1.3.2.3 Direct Interspecies Electron Exchange

During DIET, one microorganism in the syntrophic relationship receives electrons from a neighboring species in a direct manner. This type of electron exchange is another example of a cell transporting electrons from the extracellular surface. In cocultures of *G. metallireducens* and *G. sulfurreducens*, it was initially shown that *G. sulfurreducens* requires outer cell surface electron components such as PilA- microbial nanowires (Summers *et al*., 2010). Although the *pilA* gene is essential for effective DIET to occur, it is unclear whether these nanowires participate in direct exchange of electrons or are important for attachment of the cells during aggregate formation allowing for increased rates of direct electron exchange to occur. OmcS is a *c*-type cytochrome that is essential for direct electron exchange by *G. sulfurreducens* in DIET cocultures (Summers *et al*., 2010). OmcS is found localized along the pilin filaments (Leang *et al*., 2010), and is also important for electron transfer from cells onto insoluble Fe(III) oxide (Mehta *et al*., 2005). Although OmcS is required for the direct acceptance of electrons, it is still unclear how electrons cross the cell wall and cell membrane of *G. sulfurreducens*.

As previously mentioned, DIET also occurs between *G. metallireducens* and acetoclastic methanogens (Rotaru *et al*., 2014a; Rotaru *et al*., 2014b). Currently it is unclear how these methanogenic species are able to directly accept electrons during DIET, however some species of methanogens have also been shown to accept electrons from non-biological extracellular surfaces (Liu *et al*., 2012) and donate electrons onto extracellular electron acceptors (Bond *et al*., 2002b).

1.4 Extracellular Electron Exchange by *Geobacter* Species

The *Geobacteraceae* family represents one of the most widely studied groups of microorganisms capable of extracellular electron exchange. *Geobacter* species can be easily cultured and genetically manipulated in the laboratory, and carry out many unique processes such as the ability to donate electrons extracellularly to a wide variety of compounds and surfaces including electrodes, other organisms, and insoluble metals including Fe(III) and Mn(IV) oxides. Studies of several *Geobacter* species, including the model organisms *G. sulfurreducens* and *G. metallireducens*, have shown that the cell must come into direct contact with the extracellular electron acceptor in order to transfer electrons (Nevin and Lovley, 2000; Straub and Schink, 2003). Although *Geobacter* may lack the ability to reduce Fe(III) oxide at a distance, they surprisingly have been found to be the predominate metal-reducing species in many soils and subsurface environments (Holmes *et al*., 2007). Therefore, understanding the mechanism(s) by which they are able to transfer electrons through extracellular exchange is of importance.

Much of the research on extracellular electron exchange in *Geobacter* species has been conducted with *G. sulfurreducens*. *G. sulfurreducens* has served as the species of choice up until now because it was the first to have a genome sequence (Methé *et al*., 2003) and methods for genetic manipulation (Coppi *et al*., 2001). *G. sulfurreducens* has many metabolic traits that make it easy for study in the laboratory including fumarate reduction (Butler *et al*., 2006), hydrogen oxidation (Coppi *et al*., 2004), and direct interspecies electron transfer (Summers *et al*., 2010). However, *G. sulfurreducens* lacks the ability to metabolize aromatic compounds, does not reduce Fe(III) oxide as effectively as some of the other *Geobacter* species such as *G. metallireducens* (Aklujkar *et al*., 2009; Caccavo *et al*., 1994; Lovley *et al*., 1993b), and is non-motile (Childers *et al*., 2002).

G. metallireducens strain GS-15 was the first *Geobacter* species isolated in pure culture (Lovley *et al*. 1993b), the first microorganism found to conserve energy to support growth from the oxidation of organic compounds coupled to the reduction of Fe(III) or Mn(IV) oxides (Lovley and Phillips,1988), and the first microorganism found to oxidize organic compounds completely to carbon dioxide with electron transfer to an electrode (Bond *et al.* 2002a). Although there are some extracellular electron transport components that are well conserved between *G. sulfurreducens* and *G. metallireducens*, many of the genes involved in extracellular electron transfer by *G. sulfurreducens*, including some essential *c*-type cytochromes, do not have homologs in *G. metallireducens*. Few studies have focused on the mechanism(s) for extracellular electron transfer in *G. metallireducens*, mostly because a genetic system for this organism was unavailable. However, availability of putative electron transfer proteins from several other *Geobacter* species (Butler *et al*., 2010), and the recent development of a genetic system for *G. metallireducens* (Tremblay *et al*., 2012) have facilitated the study of *G. metallireducens*. Information acquired from these studies should provide further insights into direct extracellular electron transfer, including Fe(III) and Mn(IV) oxide reduction in the environment.

1.4.1 Cytochromes

Previous studies in *G. sulfurreducens* have revealed some factors that play an important role in direct extracellular electron transfer. Initial studies suggested that *b*-type cytochrome(s) were involved (Gorby and Lovley, 1991), however, this was quickly ruled out and later studies demonstrated a role for *c*-type cytochromes (Lovley *et al*. 1993c). The importance of *c*-type cytochromes has been further shown through transcriptomic (Aklujkar *et al*., 2013; Holmes *et al*., 2006; Holmes *et al*., 2009), comparative genomics (Aklujkar *et al*., 2009; Butler *et al*., 2010), and genetic studies (Aklujkar *et al*., 2013; Kim *et al*., 2005; Kim *et al*., 2006; Leang *et al*., 2003; Mehta *et al*., 2005) . *c*-type cytochromes are a hallmark feature of *Geobacter* species due to their abundance and diversity (Butler *et al*., 2010; Ding *et al*., 2006; Methé *et al*., 2003). For example, the *G. sulfurreducens* genome encodes for roughly 103 *c*-type cytochromes, of which 65 have homologs among the 91 putative *c*-type cytochromes in its close relative *G. metallireducens* (Aklujkar *et al*., 2009). Although *c*-type cytochromes are abundant among all *Geobacter* species, the only family that is well conserved is the PpcA family of triheme periplasmic cytochromes (Butler *et al*., 2010). This family of *c*-type cytochromes is located in the periplasmic space of the cell, and predicted to carry electrons from the inner to outer membranes by heme groups that are oriented in parallel or perpendicular to each other (Morgado *et al*., 2010), an arrangement expected to facilitate rapid electron transfer within and between proteins (Mowat and Chapman, 2005).

Outer membrane and extracellular *c*-type cytochromes play an important role in direct electron transfer from the cell to an extracellular electron acceptor. Several outer surface *c*-type cytochromes have been identified and extensively studied in *G. sulfurreducens*. Some of these include OmcB, OmcE, and OmcT which are expected to be embedded in the outer membrane (Mehta *et al*., 2005). Of these, the 12-heme, 89kDa *c*-type cytochrome protein OmcB has been purified (Qian *et al*., 2007). OmcB is embedded in the outer membrane, with a portion of the protein exposed to the outer surface (Qian *et al*., 2007). When the gene coding for OmcB was deleted from G. sulfurreducens, cells were unable to reduce insoluble Fe(III) oxide. Initially, this mutant strains was also unable to reduce soluble Fe(III) citrate, but adapted to reduce this soluble electron acceptor over time (Leang *et al*., 2003).

One of the most important and thoroughly studied *c*-type cytochromes involved in extracellular electron transfer by *G. sulfurreducens* is OmcS. OmcS, is a six-heme *c*-type cytochrome (Qian *et al*., 2011) found to be specifically associated with the pili of *G. sulfurreducens* (Leang *et al*., 2010) and required for growth on insoluble Fe(III) oxide, but not soluble Fe(III) citrate (Mehta *et al*., 2005). Purified OmcS can reduce a wide diversity of insoluble electron acceptors including Fe(III) oxide, U(VI), and humic substances (Qian *et al*., 2011). OmcS is also essential for the directly accepting electrons in DIET cocultures of *G. sulfurreducens* with *G. metallireducens* (Summers *et al*., 2010). However, the deletion of OmcS has no effect on electron transfer to the electrode of a

MFC, indicating that there is a different mechanism for extracellular electron transfer to MFC's (Lovley, 2011c).

PgcA (*p*eriplasmic *G*EMM-regulated *c*ytochrome *A*) is another *c*-type cytochrome that has been previously shown to play a role in Fe(III) oxide reduction by *G. sulfurreducens* (Tremblay *et al*., 2011). *pgcA* is under the regulation of a cyclic-di-GMP sensing riboswitch known as the GEMM (genes related to the environment, membranes and motility) riboswitch (Sudarsan *et al*., 2008). PgcA is a member of one of the cytochromes families that is conserved across many *Geobacter* species (Butler *et al*., 2010). PgcA exhibited higher transcript abundance in *G. sulfurreducens* strain DL-1 cells grown with insoluble Fe(III) oxide as an electron acceptor in comparison with Fe(III) citrate (Aklujkar *et al*., 2013), and the PgcA protein was more abundant in cells grown on insoluble Fe(III) oxide than soluble Fe(III) citrate in a proteomic studies (Ding *et al*., 2008). In addition a strain of *G. sulfurreducens* adapted over an extended period of time for enhanced rates of Fe(III) oxide reduction selected for mutations that increased the expression of PgcA (Tremblay *et al*., 2011).

OmcZ is a *c*-type cytochrome found to be necessary for electron transfer to electrodes but not to insoluble Fe(III) oxides (Nevin *et al*., 2009), and is specifically localized at the biofilm-anode interface in high current density biofilms (Inoue *et al*., 2011). The extracellular form of OmcZ contains 8 hemes, has a molecular weight of 30kDa, and is poorly soluble in water, which likely helps maintain the protein within the extracellular matrix (Inoue *et al*., 2010). Although OmcZ is essential for high-density current production, it is not important for cells grown on a current-consuming electrode (Strycharz *et al*., 2011). The *omcZ* gene showed lower transcript abundance in current-consuming compared with current-producing biofilms (Strycharz *et al*., 2011). Furthermore, a mutant strain deficient in the gene for OmcZ had no impact on electron transfer from the electrode to *G. sulfurreducens* cells (Strycharz *et al*., 2011). These results further suggest that the mechanism(s) for extracellular electron transfer from the electrodes to *G. sulfurreducens* cells are very different from the mechanism for electron transfer from cells to electrodes.

Understanding how *G. sulfurreducens* is able to directly accept electrons is important for optimizing microbial electrosynthesis, a strategy for producing fuels and other organic biocommodities from carbon dioxide with electricity as the energy source (Lovley and Nevin, 2011c). Additionally, uncovering components necessary for extracellular electron exchange into the cell will help in understanding and identifying DIET in the environment, which can be an important process in the anaerobic food chain and wastewater treatment (Lovley, 2011b). Previously, in order to evaluate how electrons enter *G. sulfurreducens* cells from the cathode to support fumarate respiration, gene transcript abundance and gene deletion studies were utilized to compare components involved in electron transfer into the cell (current consuming) with electron transfer out of the cell (current producing) (Strycharz *et al*., 2011). The study identified one *c*-type cytochrome, GSU3274, which was essential for *G. sulfurreducens* to directly accept electrons from the cathode. Deletion of GSU3274 completely inhibited the capacity for electron transfer from electrodes, but had no impact on cell growth when acetate was utilized as the electron donor coupled to the reduction of fumarate (Strycharz *et al*., 2011).

GSU3274 is predicted to be a monoheme *c*-type cytochrome located in the periplasm (Strycharz *et al*., 2011). This makes it unlikely that GSU3274 serves as the direct electrical connection between *G. sulfurreducens* cells and the electrode. Additionally, this preliminary study had several limitations, one being that the cathode biofilm current consumption was low indicating poor electron transfer to the cells. Secondly, the interpretation of the results was complicated by the fact that it was necessary to add acetate as a source of organic carbon to maintain biofilms, which could also potentially have acted as an electron donor. Therefore, understanding and identifying components involved in the uptake of electrons from extracellular electron donors by *G. sulfurreducens* warrants further investigation.

As previously mentioned, most of the well studied *c*-type cytochromes in *G. sulfurreducens* do not contain homologous genes in other *Geobacter* species such as *G. metallireducens* (Aklujkar *et al*., 2009; Butler *et al*., 2010). For example, *G. metallireducens* does not have homologs for *omcS* or *omcT*, and different *c*-type cytochrome sequences are found in syntenous locations where *omcB*, *omcC*, and *omcE* would be expected to be located (Aklujkar *et al*., 2009). However, other *Geobacter* species also contain upwards of 100 genes encoding for *c*-type cytochrome proteins. This suggests that although the *c*-type cytochrome genes are not all well conserved, they are important across the genus.

1.4.2 Microbial Nanowires

Another component known to play a vital role in effective extracellular electron transfer by *Geobacter* species are the electrically conductive pili (Malvankar *et al*., 2011; Reguera *et al*., 2005). Studies on *Geobacter* pili have shown that they are unique in that they possess metallic-like conductivity comparable to synthetic conducting polymers, such as the organic metal polyaniline (Malvankar *et al*., 2011), and are not used for twitching motility as is the case in other microorganisms (Reguera *et al*., 2005).

The pili "microbial nanowires" of *Geobacter* were initially of interest when found to be expressed by *G. metallireducens* when grown on insoluble Fe(III) or Mn(IV) oxides, but not when grown with soluble or chelated Fe(III) as the electron acceptor (Childers *et al*., 2002). The main structural protein of the pili is encoded by a gene known as *pilA* and deletion of this gene inhibits Fe(III) oxide reduction in *G. sulfurreducens* (Reguera *et al*., 2005) and *G. metallireducens* (Tremblay *et al*., 2012). Along with being essential for effective extracellular electron transfer onto insoluble metals, the microbial nanowires are also essential for DIET by both *G. sulfurreducens* and *G. metallireducens* (Shrestha *et al*., 2013c; Summers *et al*., 2010). Surprisingly, electron transport along the pili appears to be more similar to the metal-like conductivity observed in synthetic organic conducting polymers, rather than traditional biological electron transfer in which electrons hop/tunnel between discrete redox carriers (Malvankar *et al*., 2011).

The pili of *G. sulfurreducens* are capable of long-range (>1 cm) electron transport via a metallic-like conductivity (Malvankar *et al*., 2011). Five aromatic amino acids located on the carboxyl end of PilA are required for pili conductivity. Replacing these five aromatic amino acids with non-aromatic alanines yielded a strain, known as Aro-5, which produced pili with greatly diminished conductivity (Vargas *et al*., 2013). The Aro-5 strain was not able to produce highly conductive biofilms required for generating high current densities on MFCs, and was unable to effectively reduce insoluble Fe(III) oxides (Vargas *et al*., 2013).

It is presumed that the role of microbial nanowires is conserved amongst *Geobacter* species. Most genes attributed to pilus biogenesis in *G. sulfurreducens* have orthologs in several other *Geobacter* species, including the *pilA* gene (Aklujkar *et al*., 2009). However, to date *Geobacter sulfurreducens* has been the only species found to contain these electrically conductive pili. Furthermore, it appears that pili are only essential for extracellular electron transfer from the cell to an extracellular electron acceptor. A mutant strain deficient in the PilA gene had no impact on electron transfer from a current-consuming electrode to *G. sulfurreducens* (Strycharz *et al*., 2011), indicating there is likely an alternative direct electrical contact made for electron transfer in the reverse direction.

1.4.3 Exopolysaccharides

Components other than *c*-type cytochromes and microbial nanowires are also known to be involved in the extracellular electron exchange mechanism of *Geobacter* species. These include exopolysaccharides (EPS) and multi-copper proteins. Until recently, the EPS of *Geobacter* had not been considered vital in the process of extracellular electron transfer; however, it is now hypothesized that the EPS may play a role in the anchoring of *c*-type cytochromes in the extracellular matrix (Rollefson *et al*. 2011).

The type IV pili play a secondary role in attachment of *G. sulfurreducens* cells to the electrode (Reguera *et al*., 2006). However, the *pilA*- deficient mutant in *G. sulfurreducens* still produced thin biofilms and generated small amounts of current on a current- consuming electrode (Reguera *et al*., 2006), which lead to the belief that there were other mechanisms that allowed attachment and cell surface electron transfer by

Geobacter species. Studies in the *Geobacter* relative *Myxococcus xanthus* have shown that along with type IV pili, extracellular polysaccharides also play a key role in biofilm growth (Arnold and Shimkets, 1988). *G. sulfurreducens* also contains a genetic region encoding for synthesis of extracellular anchoring polysaccharides (*xapA* to *xapK*), and these genes seem to be important for biofilm formation, cell-surface electron transfer, and for *c*-type cytochrome anchoring (Rollefson *et al*. 2009). One of these genes, the extracellular anchoring polysaccharide GSU1501 (*xap*), was specifically involved in attachment of *G. sulfurreducens* to insoluble material, and possibly plays a role the in anchoring of outer cell surface *c*-type cytochromes (Rollefson *et al*. 2011). However, GSU1501 is in close proximity to the *pilA* gene (GSU1496) in the *G. sulfurreducens* genome, and therefore this mutation may affect expression of *pilA*. Further studies concerning the role of GSU1501, and other components of the EPS, in extracellular electron transfer, and its possible affect on *pilA* expression are needed to understand the involvement of the EPS in extracellular electron exchange.

CHAPTER 2

OUTER CELL SURFACE COMPONENTS ESSENTIAL FOR FE(III) OXIDE REDUCTION BY *GEOBACTER METALLIREDUCENS*

2.1 Abstract

Geobacter species are important Fe(III) reducers in a diversity of soils and sediments. Mechanisms for Fe(III) oxide reduction have been studied in detail in *Geobacter sulfurreducens*, but a number of the most thoroughly studied outer surface components of *G. sulfurreducens*, particularly *c*-type cytochromes, are not well conserved among *Geobacter* species. In order to identify cellular components potentially important for Fe(III) oxide reduction in *Geobacter metallireducens*, gene transcript abundance was compared in cells grown on Fe(III) oxide or soluble Fe(III) citrate with whole-genome microarrays. Outer-surface cytochromes were also identified. Deletion of genes for *c*-type cytochromes that had higher transcript abundance during growth on Fe(III) oxides and/or were detected in the outer-surface protein fraction identified six *c*-type cytochrome genes, that when deleted removed the capacity for Fe(III) oxide reduction. Several of the *c*-type cytochromes which were essential for Fe(III) oxide reduction in *G. metallireducens* have homologs in *G. sulfurreducens* that are not important for Fe(III) oxide reduction. Other genes essential for Fe(III) oxide reduction included a gene predicted to encode an NHL (Ncl-1–HT2A–Lin-41) repeat-containing protein and a gene potentially involved in pili glycosylation. Genes associated with flagellum-based motility, chemotaxis, and pili had higher transcript abundance during growth on Fe(III) oxide, consistent with the previously proposed importance of these components in Fe(III) oxide reduction. These results demonstrate that there are similarities in extracellular electron transfer between *G. metallireducens* and *G.*

sulfurreducens but the outer-surface *c*-type cytochromes involved in Fe(III) oxide reduction are different.

2.2 Introduction

The mechanisms for electron transfer to Fe(III) oxide in *Geobacter* species are of interest because *Geobacter* species play an important role in Fe(III) reduction in a wide diversity of soils, aquatic sediments, and subsurface environments (Lovley *et al*., 2011d). Furthermore, an understanding of the mechanisms for Fe(III) oxide reduction is expected to provide insights into other important types of extracellular electron transfer in *Geobacter*, such as electron transfer to electrodes (Lovley, 2012a) and interspecies electron transfer (Morita *et al*., 2011; Summers *et al*., 2010). Initial studies on the mechanisms for Fe(III) oxide reduction in *Geobacter* species were conducted with *G. sulfurreducens* because it was the first *Geobacter* species for which a genetic system was developed (Coppi *et al*., 2001). However, *G. metallireducens* is a more effective Fe(III) oxide reducer than *G. sulfurreducens* and has other environmentally significant physiological properties not found in *G. sulfurreducens*, such as the ability to anaerobically oxidize aromatic hydrocarbons, including benzene (Zhang *et al*., 2012; Zhang *et al*., 2013). Therefore, understanding how Fe(III) oxides are reduced in *G. metallireducens* aids in understanding the physiology of this important model organism and provides the opportunity to find conserved mechanisms for Fe(III) oxide reduction in *Geobacter* species. A genetic system has recently been developed for *G. metallireducens*, which now makes such studies feasible (Tremblay *et al*., 2012).

Initial studies suggested that like *G. sulfurreducens* (Reguera *et al*., 2005), *G. metallireducens* requires type IV pili for Fe(III) oxide reduction (Tremblay *et al*., 2012).

The pili of *G. sulfurreducens* possess metal-like conductivity (Malvankar *et al*., 2011), which is distinct from the electron hopping/tunneling associated with other known forms of biological electron transport (Malvankar and Lovley, 2012b). Measurements of the conductivity of the pili of *G. metallireducens* have not been reported, but the PilA sequence of *G. metallireducens* is 76% similar to the *G. sulfurreducens* PilA sequence. The *G. sulfurreducens* pili are decorated with the multi-heme *c*-type cytochrome OmcS (Leang *et al*., 2010), which is required for Fe(III) oxide reduction (Mehta *et al*., 2005). The spacing of OmcS on pili is too great to contribute to conduction of electrons along the length of the pili (Leang *et al*., 2010; Malvankar *et al*., 2012c) and multiple lines of additional evidence rule out this possibility (Leang *et al*., 2010; Malvankar *et al*., 2012a; Malvankar *et al*., 2012b; Malvankar *et al*., 2011). Therefore, it has been proposed that the role of OmcS is to facilitate electron transfer from the pili to Fe(III) oxides (Lovley, 2011a). However, there is no homolog of OmcS in *G. metallireducens*, in line with the overall poor conservation of outer surface *c*-type cytochromes in *Geobacter* species (Butler *et al*., 2010).

The only other *G. sulfurreducens* outer-surface *c*-type cytochrome known to be essential for Fe(III) oxide reduction is OmcB, which appears to be embedded in the outer membrane (Qian *et al*., 2007) and is speculated to facilitate electron transfer from the periplasm to the outer surface (Lovley, 2012b). There is no homolog to *omcB* in *G. metallireducens*, although another *c*-type cytochrome is found in a syntenous location (Aklujkar *et al*., 2009). The only *c*-type cytochromes known to be involved in Fe(III) reduction that are well conserved between *G. sulfurreducens* and *G. metallireducens* are

PpcA and MacA, which are located in the periplasm (Aklujkar *et al*., 2009; Butler *et al*., 2004; Lloyd *et al*., 2003).

Comparing gene expression during growth on insoluble electron acceptors versus growth on soluble electron acceptors has been a productive strategy for identifying components involved in extracellular electron transfer in *G. sulfurreducens* (Holmes *et al*., 2006; Nevin *et al*., 2009). Here, we report on components of *G. metallireducens* likely to be important in electron transfer to Fe(III) oxides identified from gene expression, protein localization, and gene deletion studies.

2.3 Materials and Methods

2.3.1 Bacterial strains and growth conditions.

Geobacter metallireducens (ATCC 53774 and DSM 7210) was routinely cultured under strict anaerobic conditions with 10 mM acetate provided as the sole electron donor as previously described (Lovley *et al*., 1993b). Either Fe(III) citrate (56 mM) or Fe(III) oxide (100 mM) were provided as the sole terminal electron acceptor for Fe(III) reduction studies. Samples of Fe(III) oxide cultures were dissolved in 0.5 N HCl and Fe(II) concentrations were measured using the ferrozine assay as previously described (Anderson and Lovley, 1999).

For genetic manipulations Fe(III) citrate (56 mM) was provided as the electron acceptor along with the addition of ferrous ammonium sulfate (500 μM) and yeast extract (0.1%) to liquid medium and agar plates (Tremblay *et al*., 2012). Genetic manipulations were carried out in an anaerobic chamber containing $N_2/CO_2/H_2$ (in percent, 83/10/7) atmosphere and at a temperature of 30°C. *Escherichia coli* was cultivated with Luria-Bertani medium with or without antibiotics (Sambrook *et al.*, 1989). All bacterial strains and plasmids are listed in Appendix A (Table A2).

2.3.2 SDS-PAGE and protein identification.

The loosely bound surface proteins fraction of *G. metallireducens* was isolated during mid-exponential growth as previously described (Mehta *et al.*, 2005). Cells grown with Fe(III) oxide provided as the electron acceptor were treated with equal volumes of TPE and oxalate solution prior to cell fractionation. The outer membrane protein fraction was isolated using a previously described method (Inoue *et al.*, 2010). Loosely bound and outer membrane protein fractions were combined, and protein concentration was determined with the bicinchoninic acid (BCA) assay (Pierce, Rockford, IL). *c*-type cytochromes were identified by separation with SDS-PAGE, and stained for heme as previously described (Thomas *et al.*, 1976). Equal amount of proteins were loaded in each lane. Differentially expressed *c*-type cytochrome bands from the Tris-Tricine polyacrylamide gel were excised and sent to the Laboratory for Proteomic Mass Spectrometry at the University of Massachusetts Medical School for liquid chromatography coupled with tandem mass spectrometry (LC-MS/MS) analysis.

2.3.3 DNA microarrays.

Total RNA for microarray analysis was extracted from quadruplicate cultures of *G. metallireducens* cells grown with acetate (10 mM)-Fe(III) citrate(55 mM) or acetate (10mM)-Fe(III) oxide (100 mM) during exponential growth using methods previously described (Holmes *et al*., 2012). RNA samples were purified with the RNeasy MinElute Clean-Up kit (Qiagen, Valencia, CA) according to the manufacturer's instructions, and treated with the TURBO DNA-free DNase (Ambion, Austin, TX, USA). The RNA samples were tested for genomic DNA contamination by PCR amplification of the 16S rRNA gene. The concentration and quality of the RNA samples were determined using a NanoDrop ND-1000 spectrophotometer (NanoDrop Technologies, Wilmington, DE). All RNA samples had A260/280 ratios, of 1.8–2.0, indicating high purity. cDNA was generated with the TransPlex Whole Transcriptome Amplification Kit (Sigma-Aldrich, St-Louis, MO, USA) according to manufacturer's instructions.

Whole-genome microarray hybridizations were carried out by Roche NimbleGen, Inc. (Madison, WI). Quadruplicate biological and triplicate technical replicates were conducted for all microarray analyses. Cy3-labeled cDNA was hybridized to oligonucleotide microarrays based on *G. metallireducens* genome and resident plasmid sequences (accession number NC007515 and NC007517 at GenBank). The microarray results were analyzed with Array 4 Star (DNASTAR, Madison, WI). A gene was considered differentially expressed only if the *P* value determined by using the Student *t* test analysis was ≤ 0.01.

2.3.4 RT-qPCR.

Microarray results were confirmed with reverse transcription-quantitative PCR (RT-qPCR). The Power SYBR green PCR Master Mix (Applied Biosystems, Foster City, CA) and the ABI 7500 Real-Time PCR System were used to amplify and to quantify PCR products. Each reaction consisted of forward and reverse primers at a final concentration of 200 nM, 5 ng of cDNA, and 12.5 µl of Power SYBR green PCR Master Mix (Applied Biosystems). Primer pairs were designed with amplicon size of 100 to 200 bp for the following: Gmet 0557, Gmet 2896, Gmet 0909, Gmet 0930, Gmet 1868, and Gmet 2029. Expression of these genes was normalized with *proC* expression, a gene shown to be constitutively expressed in *Geobacter* species (Holmes *et al*., 2005). The relative levels of expression of the studied genes were calculated by the $2^{-\Delta\Delta CT}$ method (Livak and Schmittgen, 2001). Sequences from all primers used for RT-qPCR are listed in Table A3 in Appendix A.

2.3.5 Deletion mutant construction and complementation.

The primers used for the construction of mutants are listed in Table A3 in Appendix A. All mutants were made by replacing the gene of interest with a spectinomycin resistance gene as previously described (Tremblay *et al*., 2012). All restriction digestions were carried out according to the manufacturer's instructions. PCRs were performed with the JumpStart *Taq* DNA polymerase (Sigma-Aldrich). Briefly, primer pairs were used to amplify by PCR flanking regions of approximately 500 bp downstream and upstream of the target genes using *G. metallireducens* genomic DNA as a template. PCR products were digested with the AvrII (CCTAGG) (NEB, Beverly, MA) restriction endonuclease, ethanol precipitated, and ligated with the T4 DNA ligase (NEB). The ligation reaction was loaded onto a 1% agarose gel, and a 1-kb band was purified using the Qiaquick gel extraction kit (Qiagen) and cloned into pCR2.1 TOPO cloning vector resulting in pCR2.1up5′+3′dn. Sequences of the cloned products were verified by Sanger sequencing. The spectinomycin resistance cassette was digested with

XbaI (TCTAGA) (NEB) from pUC19-*Sp*^{r}*loxP* (Tremblay *et al*., 2012), and the recombinant plasmid pCR2.1up5′+3′dn was digested with AvrII. The spectinomycin resistance cassette was cloned into pCR2.1up5′-′+3′dn to complete the construction of the mutant alleles. Plasmids bearing mutant alleles were linearized by digesting with either KpnI (GGTACC) (NEB) or XhoI (CTCGAG) (NEB) and concentrated by ethanol precipitation. The linearized plasmids were electroporated into *G. metallireducens* as described previously (Tremblay *et al*., 2012). Replacement of wild-type alleles by mutant alleles in *G. metallireducens* was verified by PCR. Deletion mutants made in this study were complemented by amplifying the respective genes with their native ribosome binding site (RBS) using *G. metallireducens* genomic DNA as a template. The resulting PCR products were digested and cloned under the control of a constitutive *lac* promoter into pCM66 (Marx and Lidstrom, 2001).

2.3.6 Microarray data accession number.

Microarray data have been deposited with NCBI GEO under accession number GSE40316.

2.4 Results and Discussion

In order to gain insight into which genes coding for outer cell surface proteins might be important for insoluble Fe(III) oxide reduction in *G. metallireducens,* gene transcript abundance was compared in cells grown on Fe(III) oxide or Fe(III) citrate (see Table A1 in Appendix A). The microarray analysis revealed 792 genes differentially expressed at 2-fold change and 95% confidence. A total of 437 of these genes were upregulated with growth on Fe(III) oxide, whereas 355 were downregulated. Additional focus was placed on genes with higher transcript abundance during growth on Fe(III) oxide based on the assumption that genes more highly expressed during growth on Fe(III) oxide are likely to play an important role in this process.

2.4.1 Cytochromes.

The microarray analysis revealed 23 genes coding for *c*-type cytochromes that had higher transcript abundance in cells grown on Fe(III) oxide (Table 1). In order to identify additional cytochromes that might have roles in Fe(III) oxide reduction, proteins were isolated from the outer surface protein fraction and stained for heme because cytochromes localized on the outer surface of the cell have the potential to directly interact with extracellular electron acceptors. Heme staining of outer-surface proteins separated by SDS-PAGE revealed numerous protein bands with a stronger signal in preparations of cells grown on Fe(III) oxide versus cells grown on Fe(III) citrate, six of which could be identified via liquid-chromatography/mass spectrometry (Figure 1). Four of the genes identified (Gmet 0679, Gmet 0825, Gmet 0909, and Gmet 2896) were genes that had higher transcript abundance in cells grown on Fe(III) oxide than in Fe(III) citrate-grown cells (Table 1).

The function of *c*-type cytochromes whose genes had higher transcript abundance during growth on Fe(III) oxide and/or were identified as outer-surface cytochromes was analyzed by constructing mutant strains in which one of the cytochrome genes was deleted. Six of the *c*-type cytochrome deletion mutants were unable to grow with Fe(III) oxide as the sole electron acceptor but could grow on Fe(III) citrate (Table 2; see also Figure 2). In each case complementation of the deletion mutants with expression of the appropriate gene in *trans* partially restored the capacity for Fe(III) oxide reduction (Table 2 and Figure 2).

Gmet 2896, which was one of the genes required for Fe(III) oxide reduction, had higher transcript abundance during growth on Fe(III) oxide (Table 1), and the Gmet 2896 protein was localized outside the cell (Figure 1). Gmet 2896 is predicted to encode a tetraheme *c*-type cytochrome in the same family as OmcE of *G. sulfurreducens* with 44% amino acid sequence identity (Butler *et al*., 2010), which is also found on the outer surface and is predicted to contain four hemes. Gmet 2896 appeared in a band located around 14 kDa (Figure 1) even though its predicted molecular mass is 24.9 kDa. This suggests that Gmet_2896 might be processed after translation in a manner similar to OmcZ of *G. sulfurreducens* (Inoue *et al*., 2010; Nevin *et al*., 2009). Long initial lag periods in growth on Fe(III) oxide (Mehta *et al*., 2005) and current production (Holmes *et al*., 2006) have suggested a role for OmcE in extracellular electron transfer in *G. sulfurreducens*, but the ability of this strain to adapt for growth on Fe(III) oxide (Mehta *et al*., 2005) and current production (Malvankar *et al*., 2011) have demonstrated that OmcE is not essential for these functions.

Like Gmet 2896, Gmet 0930 had higher transcript abundance in Fe(III) oxide-grown cells (Table 1) and is required for Fe(III) oxide reduction (Table 2 and Figure 2). Gmet 0930 is in the same family as the gene for OmcZ (Inoue *et al*., 2010) of *G. sulfurreducens* (Butler *et al*., 2010). Unlike the Gmet 0930 protein, OmcZ is not required for Fe(III) oxide reduction (Nevin *et al*., 2009). However, it is also an outer-surface protein (Inoue *et al*., 2011) and is required for optimal current production (Nevin *et al*., 2009; Richter *et al*., 2009). Its localization at the interface between anode biofilms and electrodes suggests that it facilitates electron transfer to electrodes in *G. sulfurreducens* (Inoue *et al*., 2011).

Gmet 0909 was the most highly upregulated gene coding for a *c*-type cytochrome in cells grown on Fe(III) oxide (Table 1) and the Gmet 0909 protein was detected outside the cell (Figure 1). Along with Gmet 0534, Gmet 0909 is the only cytochrome gene with higher transcript abundance during growth on Fe(III) oxide that is conserved across all sequenced *Geobacter* species (Butler *et al*., 2010). Numerous attempts to construct a strain in which Gmet 0909 was deleted failed, suggesting that this gene might also be required for growth on Fe(III) citrate.

The proteins of Gmet 0557 and Gmet 0558 were not detected in the outer surface, but both of these genes, which were predicted to be in the same operon, had much higher transcript levels in cells grown on Fe(III) oxide (Table 1), and are required for Fe(III) oxide reduction (Table 2 and Figure 2). Both proteins are predicted to be localized either in the periplasm or in the extracellular fraction (Table 1). Gmet 0557 is predicted to have four heme binding sites, whereas Gmet 0558 is predicted to have between 23 and 27 heme binding sites. The closest homolog to Gmet 0557 in *G. sulfurreducens* is OmcP (GSU2913) with 59% amino acid sequence identity. The closest homolog to Gmet 0558 in *G. sulfurreducens* is OmcO (GSU2912) with 67% amino acid sequence identity. Neither OmcP nor OmcO are essential for Fe(III) oxide reduction by *G. sulfurreducens*, although transcript levels were higher for both genes during growth on Fe(III) oxide compared to Fe(III) citrate (Aklujkar *et al*., 2013).

Gmet 0557 and Gmet 0558 are located in the same operon as Gmet 0556, which is predicted to encode an NHL (Ncl-1–HT2A–Lin-41) repeat-containing protein localized in the extracellular matrix (Yu *et al.*, 2010) and had higher transcript abundance in cells grown on Fe(III) oxide (Table A1, in Appendix A). Gmet 0556 is predicted to contain conserved immunoglobulin-like fold domains, which are considered to play a possible role in cell adhesion in other microorganisms (Bork *et al.*, 1994). The homolog to Gmet 0556 in *G. sulfurreducens*, GSU2914, was also more highly expressed with growth on Fe(III) oxide compared to Fe(III) citrate (Aklujkar *et al*., 2013). Furthermore, the homologous gene in *G. uraniireducens*, Gura 3430, was more highly expressed during growth in sediments in which insoluble Fe(III) was expected to be the electron acceptor, compared to cells grown with fumarate as the electron acceptor (Holmes *et al*., 2009). Deletion of Gmet 0556 produced a strain that could not reduce Fe(III) oxide but was capable of reducing soluble Fe(III) citrate (Table 2 and Figure 3). Expressing Gmet 0556 in *trans* restored the capacity for Fe(III) oxide reduction (Table 2 and Figure 2). Further functional analysis of this protein seems warranted.

Like Gmet 0557 and Gmet 0558, Gmet 1867 and Gmet 1868 are both located in the same operon, had higher transcript levels in cells grown on Fe(III) oxide (Table 1), and their proteins were not detected in the outer-surface proteins. Both Gmet 1867 and Gmet 1868 are required for Fe(III) oxide reduction (Table 2 and Figure 2). Localization of Gmet 1867 is unclear, whereas Gmet 1868 is predicted to be found in the extracellular matrix (Table 1). Gmet 1867 is predicted to contain 7 to 8 heme-binding sites, and Gmet 1868 is predicted to have 4. The closest homolog to Gmet 1867 and Gmet 1868 in *G. sulfurreducens* are, respectively, GSU1786 (57% amino acid sequence identity) and GSU1787 (69% amino acid sequence identity). Neither of these genes have been previously reported to be involved with Fe(III) oxide reduction in *G. sulfurreducens*, although GSU1787 had higher transcript abundance with growth on Fe(III) oxide compared to Fe(III) citrate (Aklujkar *et al*., 2013).

Several *c*-type cytochrome deletion mutants exhibited no phenotype on Fe(III) oxide or Fe(III) citrate (Table 2). Gmet 0910 and Gmet 0913 have no homologs in *G. sulfurreducens* (Butler *et al*., 2010). None of the *G. sulfurreducens* homologs for Gmet 0534, Gmet 0571, Gmet 0580, Gmet 0581, Gmet 0679, Gmet 0825, Gmet 0912, Gmet 1866, Gmet 2470, and Gmet 2839 have been found to be essential for optimal Fe(III) oxide reduction (Aklujkar *et al*., 2013).

2.4.2 Extracellular polysaccharide genes.

A number of genes annotated as contributing to polysaccharide biosynthesis had higher transcript abundance in Fe(III) oxide-grown cells (Table 3). The most highly expressed were Gmet 2028 through Gmet 2032. Genes coding for homologs of Gmet 2028 (GSU1983), Gmet 2029 (GSU1984), Gmet 2030 (GSU1985), Gmet 2031 (GSU1986), and Gmet 2032 (GSU1987) all had higher transcript abundance in *G. sulfurreducens* when grown on Fe(III) oxide compared to Fe(III) citrate (Aklujkar *et al*., 2013). Furthermore, homologs of Gmet 2030 (Gura 1669), Gmet 2029 (Gura 1670), Gmet 2028 (Gura 1670), Gmet 2003 (Gura 2342), and Gmet 0458 (Gura 1672) were upregulated in *G. uraniireducens* grown on sediments in which insoluble Fe(III) was expected to be the electron acceptor, compared to cells grown with fumarate as the electron acceptor (Holmes *et al*., 2009), suggesting conserved functions for these proteins in the process of extracellular electron transfer among *Geobacter* species. It has recently been proposed that another gene (*xapD*; GSU1501) involved in an extracellular polysaccharide network in *G. sulfurreducens* contributes to insoluble Fe(III) reduction, biofilm formation, and *c*-type cytochrome anchoring (Rollefson *et al*., 2009; Rollefson *et al*., 2011). The homolog of *xapD* in *G. metallireducens* (Gmet 1403) was not differentially expressed on Fe(III) oxide compared to ferric citrate.

The potential role of the highly expressed Gmet 2029, Gmet 2030, Gmet 2031, and Gmet 2032 in Fe(III) oxide reduction was investigated by gene deletion. Only the loss of Gmet 2029 resulted in a *G. metallireducens* strain incapable of reducing Fe(III) oxide (Table 2; Figure 4).

Gmet 2029 is predicted to encode a polysaccharide chain length determinant protein of the Wzz family. The Wzz proteins of several bacterial species (Burrows *et al*., 1996; Daniels and Morona, 1999; Guo *et al*., 2005a; Guo *et al*., 2005b) are implicated in the length determination of the O polysaccharide, a major component of lipopolysaccharide (LPS). However, members of the Wzz protein family are found throughout the *Geobacteraceae* family, including *G. sulfurreducens* (amino acid sequence identity = 39%) which produces a rough LPS without the O polysaccharide (Vinogradov *et al*., 2004). The Wzz protein of *Pseudomonas aeruginosa* also appears to determine the chain length of polysaccharides involved in pilin glycosylation (Faridmoayer *et al*., 2007; Horzempa *et al*., 2006). Thus, a potential role of Gmet 2029 is modification of the pili known to play a role in long-range electron transport.

2.4.3 Expression of genes previously Identified as important in Fe(III) reduction.

In some instances gene expression patterns were consistent with previous observations of *G. metallireducens* physiological differences between cells grown on Fe(III) oxide and Fe(III) citrate.

For example, G. *metallireducens* grown on Fe(III) oxide produces flagella, whereas cells grown on Fe(III) citrate do not (Childers *et al*., 2002), and chemotaxis and motility are thought to be important in Fe(III) oxide reduction (Childers *et al*., 2002; Tremblay *et al*., 2012; Ueki *et al*., 2012). Genes coding for flagellar or chemotaxis proteins represented a high proportion of the genes with the greatest increase in transcript abundance in Fe(III) oxide-grown cells (Table 4). Gmet 0442, a gene coding for the flagellin protein FliC, was the most highly upregulated gene during growth on Fe(III) oxide.

The type IV pili of *Geobacter sulfurreducens* have metallic-like conductivity (Malvankar *et al*., 2011) and are considered to be conduits for electron transfer to Fe(III) oxide (Lovley, 2011a; Reguera *et al*., 2006). *G. metallireducens* produces type IV pili during growth on Fe(III) oxide, but not on Fe(III) citrate, which was attributed to differences in the expression of the gene for the structural PilA protein (Childers *et al*., 2002). Microarray results indicated a slight increase in *pilA* transcript abundance in Fe(III) oxide-grown cells (1.7-fold; P value = 0.19). The difference in transcript abundance for other genes associated with pili functions was somewhat higher (Table 5). A strain of *G. metallireducens* in which *pilA* was deleted was unable to reduce Fe(III) oxide but retained the capacity for Fe(III) citrate reduction, further suggesting the importance of pili in Fe(III) oxide reduction by *G. metallireducens* (Tremblay *et al*., 2012).

2.5 Implications

These studies demonstrate that although *G. metallireducens* is closely related to *G. sulfurreducens,* the outer surface *c*-type cytochromes that are essential for Fe(III) oxide reduction in these two species are distinct. The identification of a select few outer surface cytochromes from the 90 putative *c*-type cytochrome genes in the *G. metallireducens* genome (Aklujkar *et al*., 2009) generates a manageable list for future studies on mechanisms for electron transfer to Fe(III) oxide in this organism. Most important will be the development of antibodies or other reagents that will make it possible to determine the localization of the cytochromes as determining whether cytochromes required for Fe(III) oxide reduction are associated with the outer membrane, pili, or in the outer matrix will provide further insights into their functional role.

The identification of an NHL repeat-containing protein and of a Wzz family protein as being essential for Fe(III) oxide reduction demonstrates that there are still unknown components involved in extracellular electron transfer in *Geobacter* species and that the current understanding of this phenomenon is not complete.

Figures:

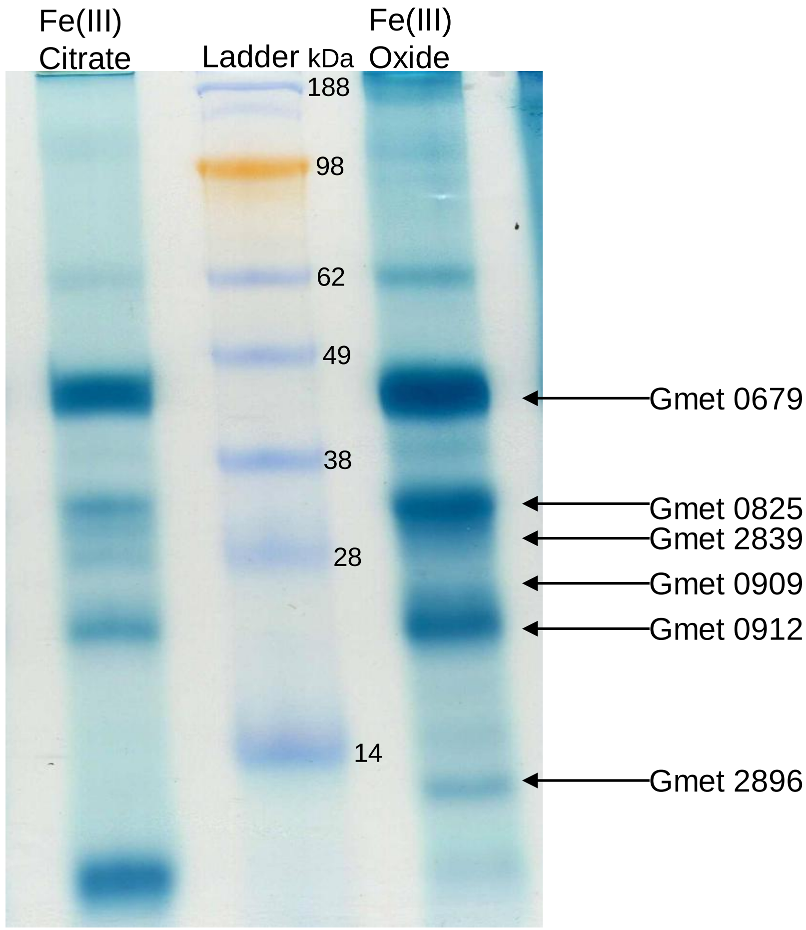

Gene	Annotation	Predicted subcellular localization	Predicted MW (kDa)	Predicted No. of heme groups
Gmet 0679	cytochrome c	Unknown	53.9	5
Gmet 0825	cytochrome c	Extracellular	34.0	11-12
Gmet 2839	cytochrome c	Periplasmic	31.0	12
Gmet 0909	cytochrome c	Unknown	29.5	9
Gmet 0912	cytochrome c	Unknown	25.4	8
Gmet 2896	cytochrome c	Extracellular or periplasmic	24.9	4

Figure 1. *c*-type cytochrome content of outer membrane and loosely bound fractions from Fe(III) oxide and Fe(III) citrate cultures. Proteins (2 µg/lane) were separated by SDS-PAGE and stained for heme (A). Protein marker was SeeBlue Plus2 Pre-Stained Standard (Invritrogen, Carlsbad, CA)**.** Characteristics of identified *c*-type cytochrome (B).

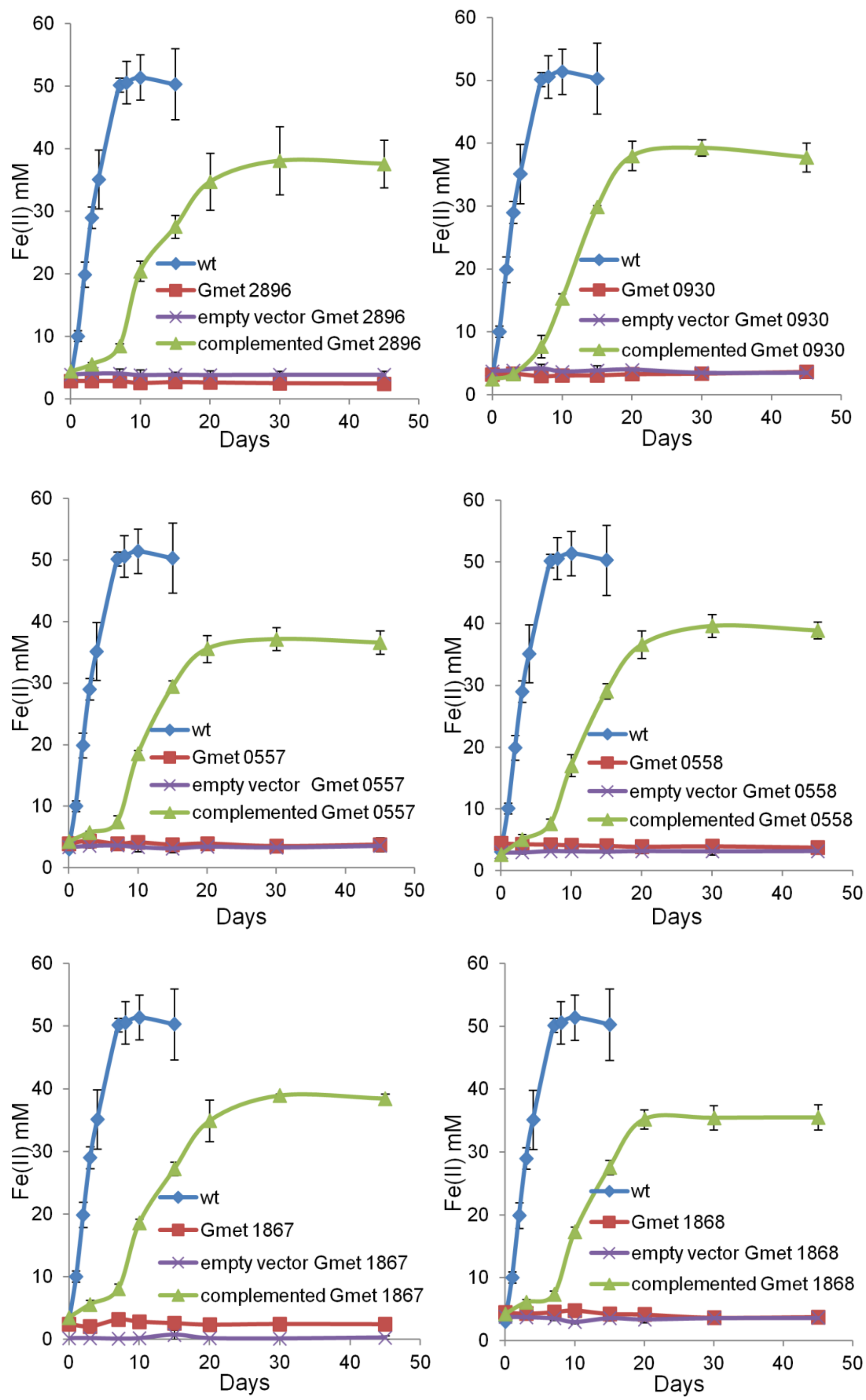

Figure 2. Reduction of Fe(III) oxide by *G. metallireducens c*-type cytochromes mutants and complementation. Each curve is the mean of at least three independent experiments.

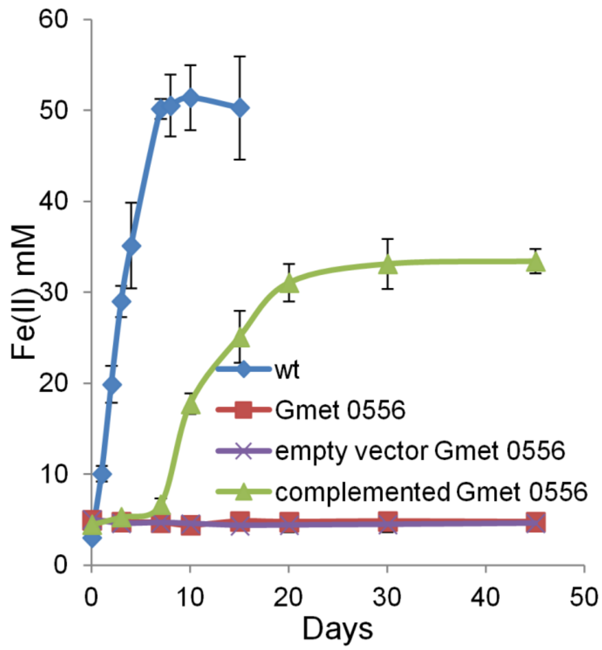

Figure 3. Reduction of Fe(III) oxide by *G. metallireducens* Gmet 0556 mutant and complementation. Each curve is the mean of at least three independent experiments.

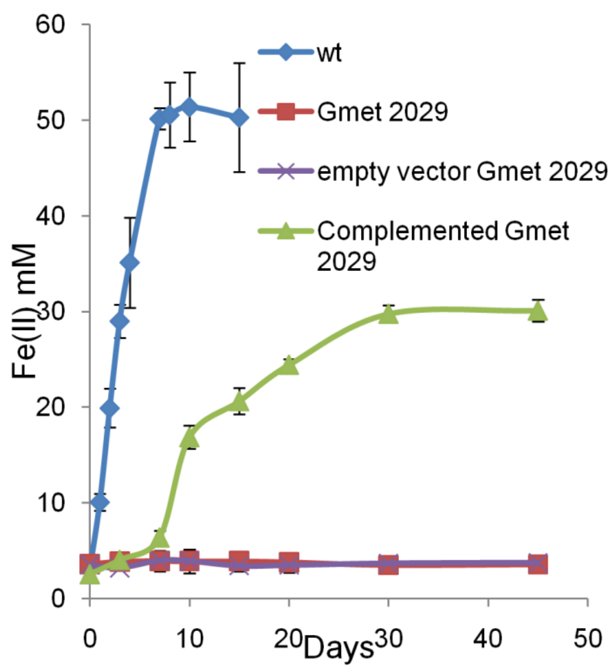

Figure 4. Reduction of Fe(III) oxide by *G. metallireducens* Gmet 2029 mutant and complementation. Each curve is the mean of at least three independent experiments.

Tables:

Table 1. Genes coding for *c*-type cytochrome up-regulated at least two-fold in *G. metallireducens* when Fe(III) oxide is the electron acceptor (P-value cutoff ≤ 0.01)

Gene	Annotation	Predicted subcellular localization[a]	Fold change
Gmet 0909	cytochrome c, 9 heme-binding sites	Unknown	37.8
Gmet 0910	lipoprotein cytochrome c, 10 heme-binding sites	Unknown	32.7
Gmet 0557	cytochrome c, 4 heme-binding sites	Extracellular or periplasmic	18.5
Gmet 0679	cytochrome c, 5 heme-binding sites	Unknown	18.0
Gmet 0558	cytochrome c27 heme-binding sites	Extracellular or periplasmic	17.1
Gmet 0571	cytochrome c, 26 heme-binding sites	Extracellular or periplasmic	16.5
Gmet 3091	cytochrome c, 2 heme-binding sites	Periplasmic	13.9
Gmet 1088	lipoprotein cytochrome c, 1 heme-binding site	Periplasmic	11.1
Gmet 0534	cytochrome c, 5 heme-binding sites	Unknown	8.7
Gmet 0155	cytochrome c, 1 heme-binding site	Periplasmic	8.4
Gmet 2470	cytochrome c, 27 heme-binding sites	Extracellular or periplasmic	6.8
Gmet 1868	cytochrome c, 4 heme-binding sites	Extracellular	5.6
Gmet 1866	cytochrome c, 3-4 heme-binding sites	Unknown	5.0
Gmet 0170	cytochrome c, 8 heme-binding sites	Periplasmic	5.0
Gmet 2896	cytochrome c, 4 heme-binding sites	Extracellular or periplasmic	4.4
Gmet 0580	lipoprotein cytochrome c, 14 heme-binding sites	Extracellular	4.2
Gmet 1867	cytochrome c, 7-8 heme-binding sites	Unknown	4.1
Gmet 0142	cytochrome c, 8 heme-binding sites	Periplasmic	3.6
Gmet 1924	cytochrome c, 5 heme-binding sites	Unknown	3.4
Gmet 0913	cytochrome c, 9 heme-binding sites	Extracellular	3.1
Gmet 0581	lipoprotein cytochrome c, 27-34 heme-binding sites	Extracellular	3.0
Gmet 0825	cytochrome c, 11-12 heme-binding sites	Extracellular	2.5
Gmet 0930	cytochrome c, 6-8 heme-binding sites	Extracellular or periplasmic	2.5

[a]Subcellular localization predictions were done with PSORTb 3.0 (50).

Table 2. Fe(III) reduction rate of mutants and complemented strains grown on Fe(III) oxide or Fe(III) citrate[a]

Strain	Fe(III) oxide (mM Fe(II)/day)	Fe(III) citrate (mM Fe(II)/hour)	Complementation Fe(III) oxide (mM Fe(II)/day)
wild type	6.1 ± 0.6	3.7 ± 0.2	
c-type cytochrome mutants			
Gmet 2896	0.0 ± 0.0	3.5 ± 0.2	4.0 ± 0.2
Gmet 0930	0.0 ± 0.0	3.6 ± 0.2	3.7 ± 0.4
Gmet 0557	0.0 ± 0.0	3.6 ± 0.1	3.9 ± 0.2
Gmet 0558	0.0 ± 0.0	3.1 ± 0.2	3.6 ± 0.1
Gmet 1867	0.0 ± 0.0	3.8 ± 0.2	3.5 ± 0.1
Gmet 1868	0.0 ± 0.0	3.9 ± 0.1	3.3 ± 0.2
Gmet 0534	5.7 ± 0.5		
Gmet 0571	4.9 ± 0.4		
Gmet 0580	5.3 ± 0.5		
Gmet 0581	6.4 ± 0.6		
Gmet 0679	5.7 ± 0.5		
Gmet 0825	4.4 ± 0.4		
Gmet 0910	6.0 ± 0.6		
Gmet 0912	5.5 ± 0.5		
Gmet 0913	5.7 ± 0.4		
Gmet 1866	6.2 ± 0.5		
Gmet 2470	5.5 ± 0.5		
Gmet 2839	6.4 ± 0.5		
Other mutant			
Gmet 0556	0.0 ± 0.0	3.9 ± 0.3	3.7 ± 0.3
Polysaccharide-associated mutants			
Gmet 2029	0.0 ± 0.0	3.8 ± 0.3	3.5 ± 0.3
Gmet 2030	5.9 ± 0.5		
Gmet 2031	6.1 ± 0.5		
Gmet 2032	6.2 ± 0.5		

[a]Each value is the mean and standard deviation of at least three replicates.

Table 3. Polysaccharide biosynthesis-associated genes up-regulated at least two-fold in *G. metallireducens* when Fe(III) oxide is the electron acceptor (P-value cutoff ≤ 0.01)

Gene	Annotation	Fold change
Gmet 2030	periplasmic polysaccharide biosynthesis/export protein	20.9
Gmet 2029	polysaccharide chain length determinant protein, putative; Wzz family	14.3
Gmet 2032	TPR domain lipoprotein	12.3
Gmet 2028	polysaccharide biosynthesis protein, putative	11.8
Gmet 2031	glycosyltransferase domain protein	7.9
Gmet 2003	exopolysaccharide synthesis multitransmembrane protein H (exosortase); EpsH	4.9
Gmet 2023	polysaccharide deacetylase domain protein	4.7
Gmet 2013	polysaccharide deacetylase, putative	3.8
Gmet 0458	polysaccharide biosynthesis protein; CapD	2.5

Table 4. Motility genes up-regulated at least 30-fold in *G. metallireducens* when Fe(III) oxide is the electron acceptor (P-value cutoff ≤ 0.01)

Gene	Annotation	Fold change
Gmet 0442	flagellin FliC	94.5
Gmet 0719	conserved hypothetical protein	77.0
Gmet 0438	flagellar hook-associated protein FlgK	56.9
Gmet 0430	flagellar basal body rod protein FlgF	55.8
Gmet 0439	flagellar hook-filament junction protein FlgL	52.7
Gmet 0432	flagellar basal body P-ring formation protein FlgA	49.0
Gmet 0431	flagellar basal body rod protein FlgG	43.8
Gmet 3115	flagellar basal-body rod protein FlgB	43.1
Gmet 3112	flagellar M-ring mounting plate protein FliF	42.5
Gmet 3104	flagellar operon protein of unknown function DUF3766	39.5
Gmet 3098	flagellar biogenesis protein FliO	39.1
Gmet 0427	flagellar biogenesis protein FlhF	37.6
Gmet 0444	flagellar filament cap protein FliD	32.1
Gmet 3101	flagellar basal body-associated protein FliL	31.0

Table 5. Pilus-associated genes up-regulated at least two-fold in *G. metallireducens* when Fe(III) oxide is the electron acceptor (P-value cutoff ≤ 0.05)

Gene	Annotation	Fold change
Gmet 0967	Type IV pilus tip-associated adhesion PilY1-2	4.6
Gmet 1395	Type IV pilus biogenesis protein PilC	4.0
Gmet 0974	Type IV pilus assembly lipoprotein PilP	3.6
Gmet 3400	Twitching motility pilus retraction protein; PilT 3	3.4
Gmet 0975	Type IV pilus secretion lipoprotein PilQ	3,2
Gmet 0959	Type IV prepilin peptidase	2.0

CHAPTER 3
GOING WIRELESS: FE(III) OXIDE REDUCTION WITHOUT PILI BY GEOBACTER SULFURREDUCENS STRAIN JS-1

3 .1 Abstract

Previous studies have suggested that the conductive pili of *Geobacter sulfurreducens* are essential for extracellular electron transfer to Fe(III) oxides and for optimal long-range electron transport through current-producing biofilms. The KN400 strain of *G. sulfurreducens* reduces poorly crystalline Fe(III) oxide more rapidly than the more extensively studied DL-1 strain. Deletion of the gene encoding PilA, the structural pilin protein, in strain KN400 inhibited Fe(III) oxide reduction. However, low rates of Fe(III) reduction were detected after extended incubation (>30 days) in the presence of Fe(III) oxide. After seven consecutive transfers, the PilA-deficient strain adapted to reduce Fe(III) oxide as fast as the wild type. Microarray, whole-genome resequencing, proteomic, and gene deletion studies indicated that this adaptation was associated with the production of larger amounts of the *c*-type cytochrome PgcA, which was released into the culture medium. It is proposed that the extracellular cytochrome acts as an electron shuttle, promoting electron transfer from the outer cell surface to Fe(III) oxides. The adapted PilA-deficient strain competed well with the wild-type strain when both were grown together on Fe(III) oxide. However, when 50% of the culture medium was replaced with fresh medium every 3 days, the wild-type strain out-competed the adapted strain. A possible explanation for this is that the necessity to produce additional PgcA, to replace the PgcA being continually removed, put the adapted strain at a competitive disadvantage, similar to the apparent selection against electron shuttle-producing Fe(III) reducers in many anaerobic soils and sediments. Despite increased extracellular

cytochrome production, the adapted PilA-deficient strain produced low levels of current, consistent with the concept that long-range electron transport through *G. sulfurreducens* biofilms is more effective via pili.

3.2 Introduction

The mechanisms for microbial extracellular electron transfer to Fe(III) minerals are of interest because of the importance of this process in the biogeochemical cycles of both modern and ancient environments, as well as for bioremediation applications (Lovley *et al*., 2004). Accessing these insoluble electron acceptors is a physiological challenge and can be the rate-limiting step in Fe(III) reduction (Lovley *et al*., 1994). In some instances, natural organic matter may chelate Fe(III) or Fe(III)-reducing microorganisms can produce their own chelators (Nevin and Lovley, 2002b). Furthermore, redox-active organics, such as humic substances, can function as electron shuttles between cells and Fe(III) minerals, alleviating the need for direct electron transfer (Lovley *et al*., 1996a; Roden *et al*., 2010). Some organisms, such as *Shewanella* and *Geothrix* species, produce their own electron shuttles (Marsili *et al*., 2008; Mehta-Kolte and Bond, 2012; Newman and Kolter, 2000; Nevin and Lovley, 2002a; Nevin and Lovley, 2002b; von Canstein *et al*., 2008). For example, electron shuttling via flavin accounted for ca. 75% of the Fe(III) reduction in cultures of *Shewanella oneidensis*, with the remaining Fe(III) reduction being attributed to the direct reduction of Fe(III) oxide via outer membrane-associated *c*-type cytochromes (Kotloski and Gralnick, 2013).

Geobacter species do not appear to produce electron shuttles, relying instead on direct electron transfer from cells to Fe(III) oxides (Nevin and Lovley, 2000). Direct electron transfer may be one of the physiological features explaining why *Geobacter* species are often the predominant Fe(III) reducers in soils and sediments with high rates of Fe(III) reduction (Lovley *et al*., 2011d). Although producing an electron shuttle may be an adaptive response to the need to reduce an insoluble electron acceptor in a closed environment, such as a culture tube, its suitability for open environments, such as soils and sediments, has been questioned (Nevin and Lovley, 2002b). This is because multiple moles of Fe(III) have to be reduced to yield enough energy to biosynthesize even the simplest organic shuttles, and once released into soils or sediments, the electron shuttle is unlikely to diffuse back to the cell that produced it and is susceptible to uptake and metabolism by other species. Shuttle production is most likely to be beneficial in high-energy environments that can promote the growth of thick biofilms, which are rare in most soils and sediments (Nevin and Lovley, 2002b).

Studies on the mechanisms for Fe(III) oxide reduction in *Geobacter* species have primarily focused on *Geobacter sulfurreducens* strain DL-1 (Coppi *et al*., 2001), which was derived as a reisolate from the original culture (Caccavo *et al*., 1994) strain PCA (Lovley *et al*., 2011d). The DL-1 genome encodes many (>100) *c*-type cytochromes (Methé *et al*., 2003), a number of which are localized in the periplasm and outer membrane and are essential for optimal Fe(III) oxide reduction (Butler *et al*., 2004; Kim *et al*., 2005; Kim *et al*., 2006; Leang *et al*., 2003; Mehta *et al*., 2005). However, the terminal electron transfer in DL-1 appears to take place through electrically conductive pili (Lovley, 2011a; Lovley, 2012b). The pili have homology to the type IV pili of other

Gram-negative bacteria, but PilA, the structural pilin protein, is truncated compared to the PilA of other well-studied organisms, such as *Pseudomonas aeruginosa*, whose pili do not appear to be conductive (Vargas *et al*., 2013). Deletion of *pilA* prevents Fe(III) oxide reduction in DL-1, but the mutant can be rescued with the addition of an electron shuttle or Fe(III) chelator, demonstrating that the pili are specifically required for Fe(III) oxide reduction (Reguera *et al*., 2005). Electrons move along the pili through a metallic-like conduction (Malvankar *et al*., 2011; Malvankar and Lovley, 2012) that can be attributed to overlapping pi-pi orbital's of aromatic amino acids in the carboxyl terminus of PilA (Vargas *et al*., 2013). The multiheme *c*-type cytochrome OmcS (Mehta *et al*., 2005; Qian *et al*., 2011) is associated with the pili (Leang *et al*., 2010a) and is essential for Fe(III) oxide reduction, presumably facilitating electron transfer from the pili to the Fe(III) oxides (Lovley, 2011a; Lovley, 2012b).

Another strain of *G. sulfurreducens*, designated KN400, was recovered as a rare variant (1 in 100,000 cells) (Shrestha *et al*., 2013a) in DL-1 cultures, when the culture that was predominately DL-1 was grown with a graphite electrode poised at a low potential (−200 mV versus standard hydrogen electrode [SHE]) as the sole electron acceptor (Yi *et al*., 2009). KN400 produces higher current densities than DL-1 in microbial fuel cells (Yi *et al*., 2009). This has been attributed to its greater production of electrically conductive pili, which confer higher biofilm conductivity (Malvankar *et al*., 2011; Malvankar *et al*., 2012d). Furthermore, KN400 is motile, whereas DL-1 is not, which can be attributed to a regulatory defect in DL-1 (Ueki *et al*., 2012). Motility is beneficial for Fe(III) oxide reduction because once the Fe(III) in one microenvironment is reduced it is necessary for cells to find a fresh source of electron acceptor (Childers *et al*., 2002). Restoring the capacity for motility enhanced the rates of Fe(III) oxide reduction by DL-1 (Ueki *et al*., 2012). Genetically eliminating motility in KN400 (Ueki *et al*., 2012) or *Geobacter metallireducens* (Tremblay *et al*., 2012) decreased the capacity for Fe(III) oxide reduction.

Initial studies demonstrated that KN400 reduced Fe(III) oxides faster than DL-1 (Ueki *et al*., 2012). To evaluate the potential role of increased pilus production in this phenotype, a strain in which *pilA* was deleted was constructed. The results demonstrate that the conductive pili of KN400 are required for optimal Fe(III) oxide reduction but that the *pilA*-deletion mutant adapted an alternative strategy for Fe(III) oxide reduction that was effective in the closed environment of a culture tube.

3.3 Materials and Methods

3.3.1 Bacterial strains and growth conditions.

All *G. sulfurreducens* KN400 strains were routinely cultured under strict anaerobic conditions with 10 mM acetate provided as the sole electron donor and either 100 mmol liter^{-1} Fe(III) oxide or fumarate (40 mM) provided as the sole terminal electron acceptor, as previously described (Lovley *et al*., 1993b; Coppi *et al*., 2001). Samples of Fe(III) oxide cultures were dissolved in 0.5 N HCl, and Fe(II) concentrations were measured using the ferrozine assay as previously described (Lovley and Phillips, 1986b).

For genetic manipulations, cells were grown in either liquid or agar-solidified acetate-fumarate medium (Coppi *et al*., 2001). Genetic manipulations were carried out in an anaerobic chamber with an N_2-CO_2-H_2 (83%, 10%, and 7%, respectively) atmosphere at a temperature of 30°C. *Escherichia coli* was cultivated with Luria-Bertani medium with or without antibiotics (Sambrook *et al.*, 1989). All bacterial strains and plasmids are listed in Table B1 in Appendix B.

3.3.2 Alginate bead assays.

Poorly crystalline Fe(III) oxide was incorporated into microporous alginate beads (diameter, 5 mm) with a nominal molecular mass cutoff of 12 kDa, as previously described (Nevin and Lovley, 2000). Beads were added to freshwater medium to provide Fe(III) at 100 mmol liter$^{-1.}$ The production of Fe(II) was determined with the ferrozine assay, after the beads had been extracted for 12 h in 0.5 N HCl.

3.3.3 DNA microarrays.

Total RNA for microarray analysis was extracted from quadruplicate cultures of JS-1 and KN400 cells during exponential growth in acetate (10 mM)-Fe(III) oxide (100 mmol liter^{-1}) medium, as previously described (Holmes *et al*., 2012; Smith *et al*., 2013). RNA was purified with an RNeasy MinElute cleanup kit (Qiagen, Valencia, CA) according to the manufacturer's instructions and treated with Turbo DNA-free DNase (Ambion, Austin, TX). The RNA samples were tested for genomic DNA (gDNA) contamination by PCR amplification of the 16S rRNA gene. The concentration and quality of the RNA samples were determined with a NanoDrop ND-1000 spectrophotometer (NanoDrop Technologies, Wilmington, DE). All RNA samples had A_{260}/A_{280} ratios of 1.8 to 2.0, indicating high purity. cDNA was generated with a TransPlex whole-transcriptome amplification kit (Sigma-Aldrich, St. Louis, MO) according to the manufacturer's instructions.

Whole-genome microarray hybridizations were carried out by Roche NimbleGen, Inc. (Madison, WI). Quadruplicate biological and triplicate technical replicates were conducted for all microarray analyses. Cy3-labeled cDNA was hybridized to oligonucleotide microarrays based on the KN400 genome (GenBank accession number NC_017454 at the National Center for Biotechnology Information). The microarray results were analyzed with Array 4 Star software (DNASTAR, Madison, WI). A gene was considered differentially expressed only if the *P* value determined by Student's *t* test analysis was less than or equal to 0.01 or 0.05.

3.3.4 Quantitative PCR.

Microarray results were confirmed with quantitative PCR. Primer pairs with amplicon sizes of 100 to 200 bp were designed for the following genes: KN400_1784, KN400_1319, KN400_2603, KN400_2641, KN400_2978, and KN400_1523. Expression of these genes was normalized with the expression of *proC*, a gene shown to be constitutively expressed in *Geobacter* species (Holmes *et al*., 2005). Relative levels of expression of the studied genes were calculated by the $2^{-\Delta\Delta CT}$threshold cycle (C_T) method (Livak and Schmittgen, 2001).

The proportion of JS-1 and KN400 cells in cocultures was determined by quantitative PCR on genomic DNA with the following primer sets: (i) KN400-specific primer set pilAF/pilAR, which amplifies a section of the *pilA* gene, and (ii) JS-1-specific primer set kmF/kmR, which amplifies a section of the kanamycin resistance cassette. Both primer sets had 100% efficiency. Standards were made using gDNA from KN400 for the *pilA* gene and gDNA from JS-1 for the kanamycin resistance cassette. Genomic DNA was extracted using a FastDNA 2-ml SPIN kit for soil (MP, Solon, OH).

Power SYBR green PCR master mix (Applied Biosystems, Foster City, CA) and an ABI 7500 real-time PCR system were used to amplify and to quantify the PCR products. Each reaction mixture consisted of forward and reverse primers at a final concentration of 200 nM, 5 ng of cDNA or gDNA, and 12.5 μl of Power SYBR green PCR master mix (Applied Biosystems). The sequences of all primers used for quantitative PCR are listed in Table B2 in Appendix B.

3.3.5 Cell-free filtrate SDS-PAGE and protein identification.

The cell-free proteins in the medium were collected from JS-1 and KN400 cells grown with Fe(III) oxide provided as the electron acceptor when Fe(II) concentrations reached 30 mmol liter^{-1}. One hundred milliliters of culture was centrifuged at 10,000 × *g* for 20 min to remove cells and insoluble Fe(III) oxide. The supernatant was collected, and 30 ml was concentrated with an Amicon Ultra-15 centrifugal filter unit (Millipore, Billerica, MA). Protein was quantified with a Micro BCA protein assay kit (Thermo Scientific, Rockford, IL). *c*-type cytochromes were identified by separation by SDS-PAGE and staining for heme as previously described (Thomas et al., 1976). *c*-type cytochrome bands from the Tris-Tricine polyacrylamide gel were excised and sent to the Laboratory for Proteomic Mass Spectrometry at the University of Massachusetts Medical School for liquid chromatography coupled with tandem mass spectrometry (LC-MS/MS) analysis.

3.3.6 Mutant construction.

Primers used for the construction of mutants are listed in Table B2 in Appendix B. Deletion mutants were made by replacing the gene of interest with an antibiotic resistance cassette. All restriction digestions were carried out according to the manufacturer's instructions. PCRs were done with JumpStart *Taq* DNA polymerase (Sigma-Aldrich). Briefly, primer pairs were used to amplify flanking regions of approximately 500 bp downstream and upstream of the target genes by PCR using KN400 genomic DNA as the template. PCR products were digested with the AvrII restriction endonuclease (CCTAGG; NEB, Beverly, MA), ethanol precipitated, and ligated with T4 DNA ligase (NEB). The ligation reaction mixture was loaded onto a 1% agarose gel, and a 1-kb band was purified using a QIAquick gel extraction kit (Qiagen) and cloned into the pCR2.1 TOPO cloning vector, resulting in pCR2.1up5′+3′dn. The sequences of the cloned products were verified by Sanger sequencing. The gentamicin cassette was digested with XbaI (TCTAGA; NEB) from pUC19-Gm^r *loxP* (Aklujkar and Lovley, 2010), and the recombinant plasmid pCR2.1up5′+3′dn was digested with AvrII. The gentamicin resistance cassette was cloned into pCR2.1up5′-′+3′dn to complete the construction of the mutant alleles. Plasmids bearing mutant alleles were linearized by digesting with either KpnI (GGTACC; NEB) or XhoI (CTCGAG; NEB) and concentrated by ethanol precipitation. The linearized plasmids were electroporated as described previously (Coppi et al., 2001). Antibiotics were added for selection purposes only. Replacement of wild-type alleles by mutant alleles was verified by PCR.

3.3.7 Current production and anode biofilm visualization.

Strains were grown in H-cell culturing systems as previously described (Bond *et al.*, 2002; Bond and Lovley, 2003). Graphite block cathodes and anodes (65 cm^2; Mersen, Greenville, MI) were suspended in two chambers, each of which contained 200 ml of medium, that were separated with a Nafion 117 cation-exchange membrane (Electrolytica, Amherst, NY). The cathode chamber was continually gassed with N_2-CO_2 (80:20). The anode was poised at +500 mV (versus a standard hydrogen electrode). Acetate (10 mM) was provided as the electron donor and fumarate (40 mM) was provided as the electron acceptor for pregrowth to an optical density (OD) at 600 nm of 0.2. Once this OD was reached, the medium in the anode chamber was swapped for medium with only 10 mM acetate.

Confocal microscopy with a Leica TCS SP5 microscope was performed on biofilm samples as previously described using LIVE/DEAD BacLight stain (Reguera *et al.*, 2006).

3.3.8 Fe(III) oxide competition growth assays.

When Fe(II) concentrations were 25 mmol liter^{-1}, equal volumes (0.5 ml) of the JS-1 and KN400 isolates grown in Fe(III) oxide medium were transferred into triplicate tubes containing 10 ml of Fe(III) oxide medium. The initial culture was incubated at 30°C for 7 days, at which point 5 ml of the medium was removed from the tube and replaced with 5 ml of fresh Fe(III) oxide medium. Replacement with 5 ml of fresh Fe(III) oxide medium was continued every 3 days for a total of 30 days.

3.3.9 Microarray data accession number.

Microarray data have been deposited with NCBI GEO under accession number GSE47868.

3.4 Results and Discussion

3.4.1 Adaptation of the pilA-deletion mutant for Fe(III) oxide reduction.

Deletion of *pilA* in *G. sulfurreducens* KN400 severely inhibited the capacity for insoluble Fe(III) oxide reduction (Figure 5A), suggesting, as previously observed for the DL-1 strain (Methé *et al*., 2003), that pili are important for this form of respiration. However, with extended incubation, some Fe(III) was reduced (Figure 5A). Transfer (10% inoculum) into fresh medium resulted in a higher rate of Fe(III) reduction (Figure 5B), and with successive transfers, the rate of Fe(III) oxide reduction increased to a rate comparable to that of the wild type (Figure 5B-C). A strain obtained as an isolated colony from the adapted *pilA*-deficient culture, designated strain JS-1, conserved the capacity to reduce Fe(III) at this high rate (Figure 5D). The growth rates of strains JS-1 and KN400 with fumarate as the electron acceptor were not significantly different (Figure 6).

In order to evaluate the potential for flavin or other small soluble electron shuttles to be released into the medium by JS-1, poorly crystalline Fe(III) oxide was incorporated into microporous alginate beads with a molecular mass cutoff of 12 kDa (Nevin and Lovley, 2000). Approximately 6 mmol liter^{-1} of Fe(II) was produced after 20 days of incubation in both JS-1 and KN400 (Figure 7), corresponding to the amount that is likely to be exposed on the surface of the beads (Nevin and Lovley, 2000). When the electron shuttling compound anthraquinone 2,6,-disulfonate (AQDS) was added to the medium at 50 μM, JS-1 was able to produce up to approximately 60 mmol liter^{-1}of Fe(II) within 15 days (Figure 7). These results suggest that JS-1 does not release a low-molecular-weight electron shuttling compound to promote Fe(III) oxide reduction.

3.4.2 Increased expression of PgcA in JS-1.

In order to further evaluate how JS-1 adapted for effective Fe(III) oxide reduction, transcript abundance during growth on Fe(III) oxide was assessed with whole-genome microarrays. KN400_1784, a gene encoding the 3-heme 50-kDa *c*-type cytochrome PgcA, had the greatest relative increase in transcript abundance in JS-1 compared to that in KN400 (Table 6).

Previous studies have suggested that PgcA is involved in Fe(III) oxide reduction. The PgcA protein (Ding *et al*., 2008) and *pgcA* transcripts (Aklujkar *et al*., 2013) were more abundant in cells grown on Fe(III) oxide than in cells grown on Fe(III) citrate in *G. sulfurreducens* strain DL-1. *pgcA* contains a riboswitch sequence for genes related to the environment, membranes, and motility (GEMM) (Tremblay *et al*., 2011; Weinberg *et al*., 2007), which senses cyclic-di-GMP (Sudarsan *et al*., 2008). Mutations within this riboswitch that resulted in increased transcription of *pgcA* were selected for in the adaptive evolution of *G. sulfurreducens* strain DL-1 for enhanced Fe(III) oxide reduction (Tremblay *et al*., 2011). A draft genome sequence of strain JS-1 (P. M. Shrestha and J. A. Smith, unpublished data) indicated that there is an insertion of a transposase and a transposase-associated protein (KN400_0540 and KN400_0541) between the 89th and 90th base pairs of the GEMM riboswitch sequence upstream of the *pgcA* sequence that was not reported in the genome of strain KN400 (Butler *et al*., 2012). Sanger sequencing of this region of the JS-1 and KN400 genomes confirmed this difference (Figure 8). It is likely that the mutation in strain JS-1 accounted for the increased number of *pgcA* transcripts compared to that in strain KN400.

PgcA was previously recovered in the periplasmic fraction in proteomic studies (Ding *et al*., 2006), but according to the PSORTb subcellular localization prediction tool (version 3.0) (Yu *et al*., 2010), its ultimate localization is the extracellular fraction. Therefore, in order to evaluate whether increased transcript abundance for *pgcA* translated into the increased production of extracellular PgcA, cell-free filtrates from late-log-phase cultures grown on Fe(III) oxide were analyzed on SDS-polyacrylamide gels. One band that stained intensely for heme was apparent in JS-1, but not KN400 (Figure 9). This band was excised and identified as PgcA via liquid chromatography-mass spectrometry.

The extracellular fraction contained another protein, which stained for heme, that was present in KN400 but more abundant in JS-1 (Figure 9). This band was identified as OmcZ via liquid chromatography-mass spectrometry. OmcZ is an 8-heme *c*-type cytochrome which is produced in strain DL-1 and is processed to a 30-kDa form that is excreted from the cell (Inoue *et al*., 2010; Inoue *et al*., 2011). OmcZ was essential for optimum current production by strain DL-1, but deleting *omcZ* had no impact on Fe(III) oxide reduction (Nevin *et al*., 2009).

Other genes highly expressed in JS-1 included genes encoding proteins involved in sulfate assimilation (Table 6; see Table B3 in Appendix B) (Mahadevan *et al*., 2008). A potential explanation for this response is that the greater production of PgcA in JS-1 creates an increased demand for biosynthesis of cysteine, which is found in the heme attachment site of *c*-type cytochromes (Daltrop *et al*., 2002).

3.4.3 PgcA is essential for Fe(III) oxide reduction in JS-1 but not KN400.

In order to further examine the potential role of PgcA and OmcZ in the adaptation for enhanced Fe(III) oxide reduction in the absence of *pilA*, strains in which *pgcA* or *omcZ* was disrupted with an antibiotic resistance cassette were generated in JS-1 and KN400. Deletion of *omcZ* had no effect on Fe(III) oxide reduction in either strain (Figure 10A), consistent with the previous finding with DL-1 (Nevin *et al*., 2009).

The *pgcA*-deficient KN400 strain reduced Fe(III) oxide at a rate similar to that for wild-type KN400, but deletion of *pgcA* in JS-1 significantly inhibited Fe(III) oxide reduction (Figure 10B). These results demonstrate that *pgcA* is essential for Fe(III) oxide reduction in JS-1 and suggest that the mechanism for Fe(III) reduction is significantly different in JS-1 and KN400.

3.4.4 Inability of increased PgcA expression to recover capacity for high current densities.

KN400's superior current-producing capability has been attributed, at least in part, to enhanced production of pili (Malvankar *et al*., 2011; Yi *et al*., 2009). As expected, the *pilA*-deletion strain of KN400 produced substantially less current than the wild type (Figure 11A).

Strain JS-1 was also deficient in current production (Figure 11A). With extended incubation (~15 days), both the unadapted *pilA*-deficient strain (Figure 11C) and strain JS-1 (Figure 11D) produced biofilms that were nearly as thick as the wild-type KN400 biofilm produced within 2 days (Figure 11B). Cells of both *pilA*-deficient strains appeared to be packed more tightly within their biofilms than cells in the wild-type biofilm. These results demonstrate that the low current output of the *pilA*-deficient strains could not be attributed to an inability to produce biofilms.

The finding that the best genetic strategies for improving biofilm conductivity and current density are either to delete cytochrome genes and decrease content (Malvankar *et al.*, 2012c) or increase pilus production (Leang *et al*., 2013) strongly suggests that pilus conductivity is the important feature in long-range electron transport through *G. sulfurreducens* biofilms. Thus, the finding that strain JS-1 was deficient in current production, despite its increased expression of PgcA, may not be surprising.

3.4.5 Competition in coculture.

When equal amounts of Fe(III) oxide-grown JS-1 and KN400 were inoculated into the same tubes of Fe(III) oxide medium, approximately half of the available Fe(III) oxide was reduced in 7 days. JS-1 outcompeted KN400 during this period, accounting for approximately 90% of the community (Figure 12). This demonstrated that in the closed environment of a culture tube, JS-1's pilus-independent strategy for Fe(III) oxide reduction was highly competitive with the pilus-based strategy of KN400.

In order to simulate a more open environment, after day 7, half of the medium was removed and exchanged with fresh Fe(III) oxide medium every third day. Despite the predominance of JS-1 on day 7, with successive medium swaps, KN400 increased in relative abundance and eventually dominated the culture (Figure 12). It is expected that the loss of extracellular mediators in a truly open environment, such as soils and sediments, would be much greater than that resulting from the modest removal of half of the culture medium every third day.

3.5 Implications

These studies demonstrate that increased extracellular expression of the *c*-type cytochrome PgcA is an alternative to pilus-mediated electron transport to Fe(III) oxide in *Geobacter sulfurreducens*. The possibility of a *c*-type cytochrome functioning as an electron shuttle in *G. sulfurreducens* was previously proposed (Seeliger *et al*., 1998), but further study demonstrated that the cytochrome proposed to function as the electron shuttle was, in fact, not abundant in the extracellular matrix (Lloyd *et al*., 1999) and the cytochrome shuttle hypothesis was subsequently rescinded (Straub and Schink, 2003). A series of subsequent studies has provided evidence that *Geobacter* species directly contact Fe(III) oxides in order to reduce them and that conductive pili are required for optimal Fe(III) oxide reduction (Lovley, 2012b; Nevin and Lovley, 2000; Nevin and Lovley, 2002b; Reguera *et al*., 2005; Vargas *et al*., 2013).

The initial inability of the *pilA*-deficient strain of KN400 to reduce Fe(III) oxide suggests that pili are involved in Fe(III) reduction by the wild-type strain, but the adaptation of releasing PgcA is clearly an effective remedy for the loss of pili during growth in culture tubes. High concentrations of PgcA in the extracellular matrix could promote Fe(III) oxide reduction by facilitating electron transfer between electron carriers bound in the outer membrane and Fe(III) oxide. PgcA could potentially function in this manner while still being held in the extracellular matrix, but the recovery of PgcA in cell supernatants suggests that it may function as an electron shuttle. The lower abundance of transcripts for genes involved in flagellum function in JS-1 than in KN400 (see Table B4 in Appendix B) further supports this conclusion because previous studies have suggested that flagellum-mediated motility is most necessary when cells need to directly contact Fe(III) oxides (Childers *et al*., 2002; Ueki *et al*., 2012). Presumably, once Fe(III) oxide is reduced in one location, the cell must move to a fresh Fe(III) oxide source. In contrast, motility is not required when a soluble electron shuttle is available (Childers *et al*., 2002).

However, as previously discussed in detail (Nevin and Lovley, 2002b), Fe(III) reducers that function via release of electron shuttles are unlikely to be competitive in open soil and sediment environments. Furthermore, in those instances in which release of a shuttle may be advantageous, the production of shuttles less complex than PgcA, such as the flavins released by *Shewanella* (Kotloski and Gralnick, 2013; Marsili *et al*., 2008; von Canstein *et al*., 2008) and *Geothrix* (Mehta-Kolte and Bond, 2012; Nevin and Lovley, 2002a) species, is likely to be a more effective strategy.

It has been suggested that one reason for the predominance of *Geobacter* species in a wide diversity of environments in which Fe(III) reduction is an important biogeochemical process is that *Geobacter* species do not produce electron shuttles (Lovley *et al*., 2011d). The long period necessary for the *pilA*-deficient strain of KN400 to adapt for effective Fe(III) oxide reduction and the fact that deleting *pgcA* in the wild type had no impact on Fe(III) oxide reduction suggest that pilus-mediated Fe(III) oxide reduction is more representative of the mechanism by which *G. sulfurreducens* reduces Fe(III) oxide in soils and sediments.

There are now several examples of strains of Fe(III)-reducing microorganisms undergoing mutations to develop alternative strategies for extracellular electron transfer following gene deletions (Bucking *et al*., 2012; Schicklberger *et al*., 2013) or simply in response to strong selective pressure for rapid electron transfer (Tremblay *et al*., 2011). The ability of KN400 to adapt to the loss of pili demonstrates that caution may be warranted in extrapolating to natural environments the mechanisms for Fe(III) oxide reduction elucidated in studies with cultures maintained for long periods under laboratory conditions that do not mimic those found in soils and sediments. The substantial plasticity encoded in the genomes of microorganisms capable of extracellular electron transfer, coupled with unnatural laboratory selection pressures, has the potential to lead to physiological responses that might not be found in natural environments.

Figures:

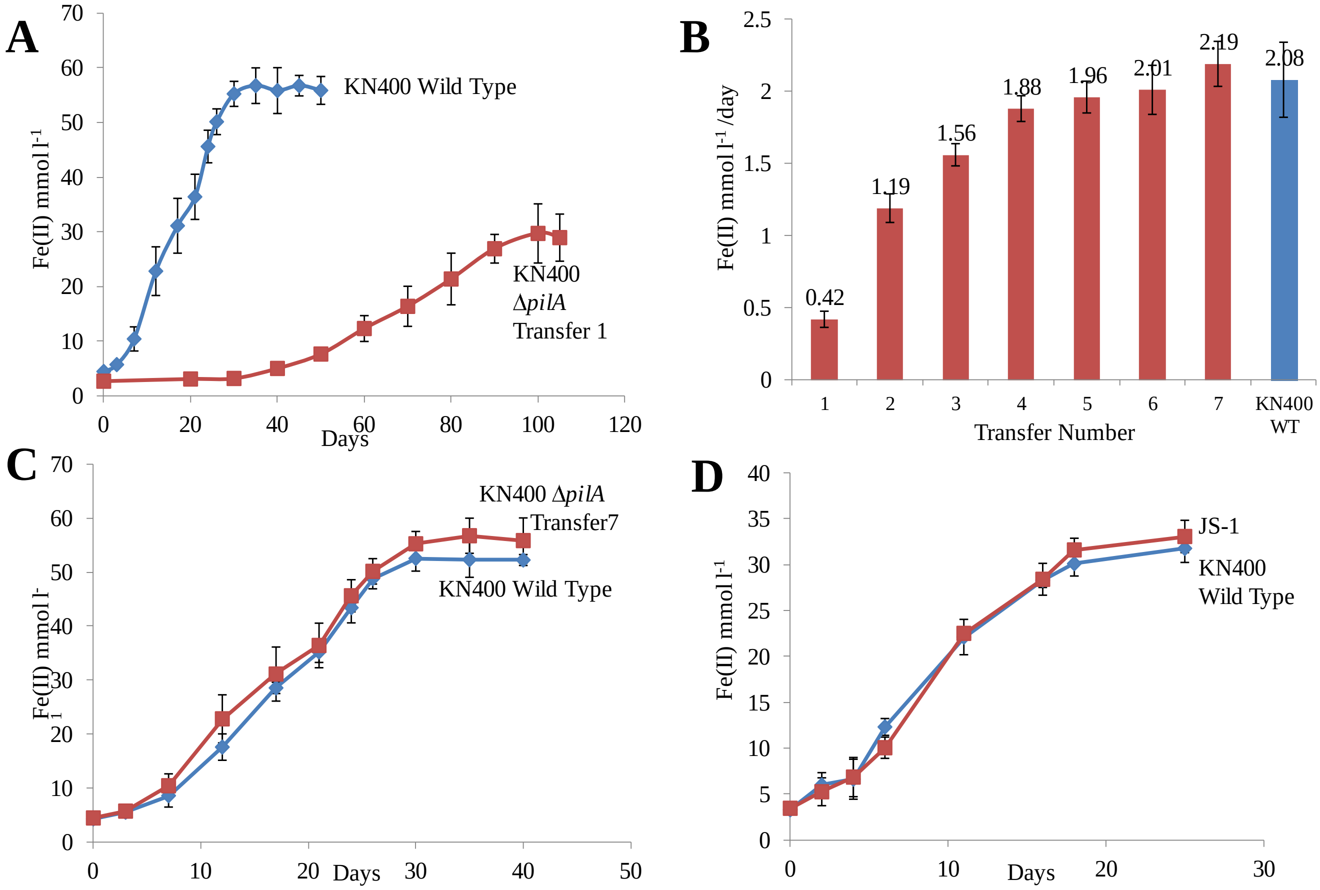

Figure 5. Adaptation of *pilA*-deletion mutant for Fe(III) oxide reduction. (A) Fe(II) produced from Fe(III) oxide over time in KN400 wild type and the first transfer of the KN400 *pilA*-deficient strain into Fe(III) oxide medium. (B) Rates of Fe(II) production over time from Fe(III) oxide in each consecutive transfer of the KN400 *pilA*-deficient mutant, and in KN400 wild type. (C) Fe(II) produced from Fe(III) oxide over time in KN400 wild type and the KN400 *pilA*-deficient mutant after seven transfers in Fe(III) oxide medium. (D) Fe(II) produced from Fe(III) oxide over time in KN400 wild type and JS-1, an isolate from the seventh transfer of the KN400 *pilA*-deficient mutant on Fe(III) oxide medium. Results are the means and standard deviation for triplicate cultures of each strain.

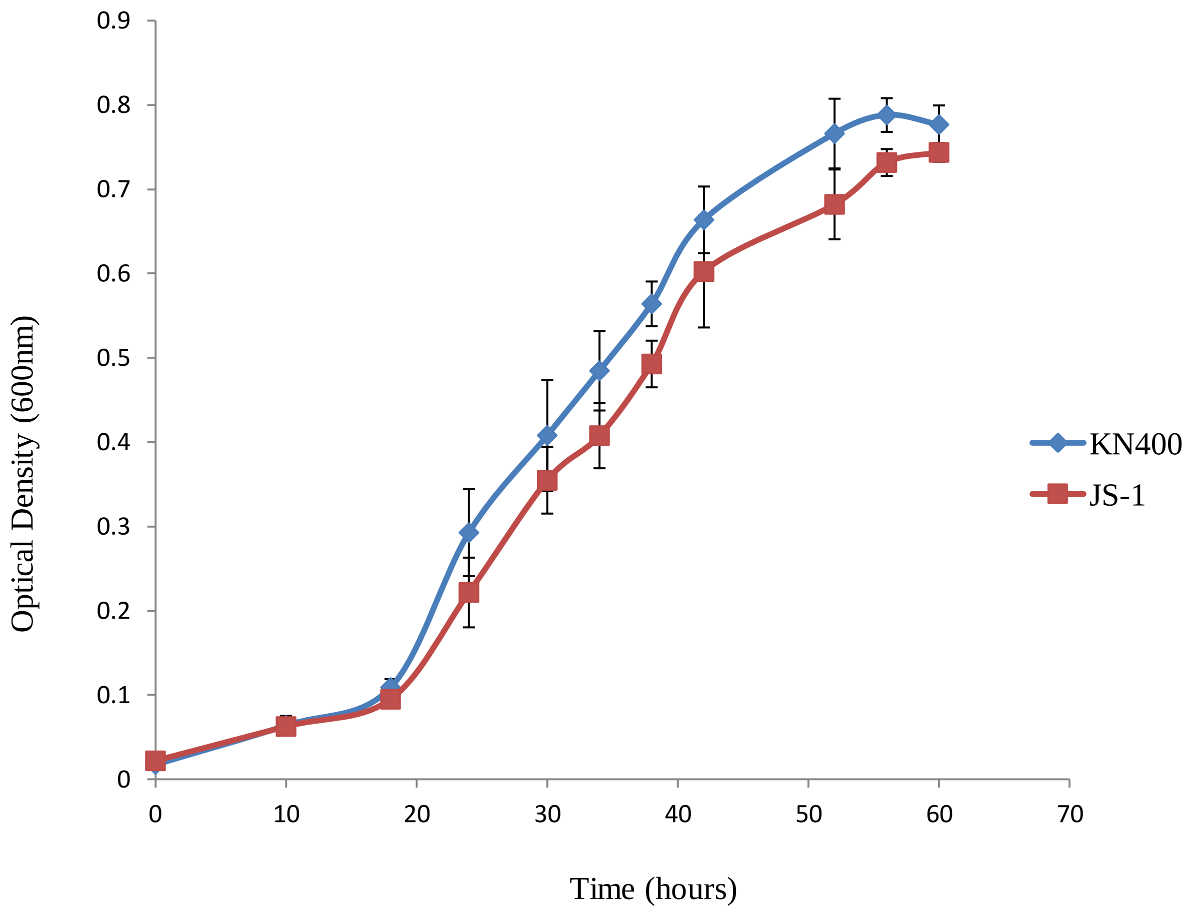

Figure 6. Growth of KN400 and JS-1 with 40mM fumarate as the sole electron acceptor and 10mM acetate as the sole electron donor.

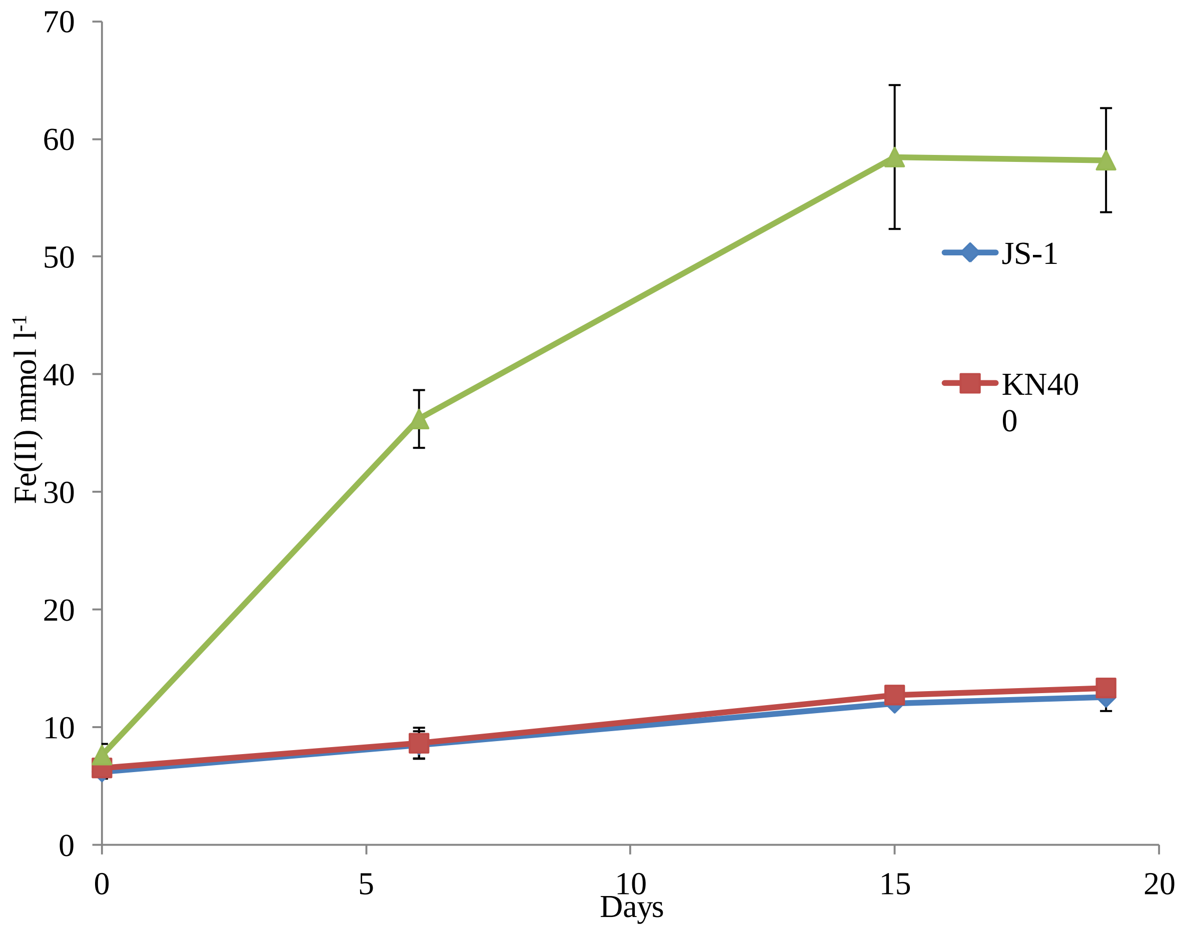

Figure 7. Production of Fe(II) when Fe(III) oxide within alginate beads was provided as the electron acceptor. Anthraquinone 2,6,-disulfonate (AQDS) was added at 50 µM where noted. The results are the means and standard deviation for triplicate cultures.

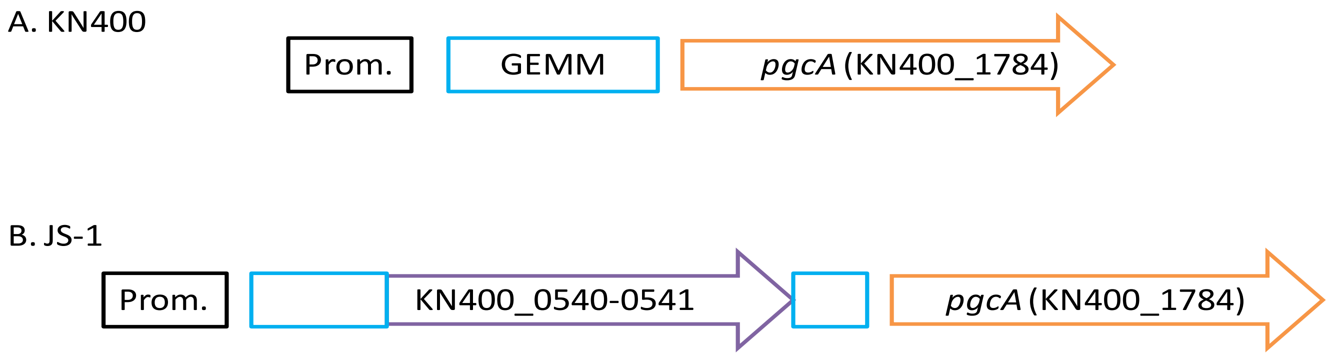

Figure 8. Schematic of the KN400 *pgcA* gene which follows the GEMM riboswitch and *pgcA* promoter (A), and JS-1 in which two transposases have been inserted between the 89th and 90th base pair of the GEMM riboswitch preceding the *pgcA* gene (B).

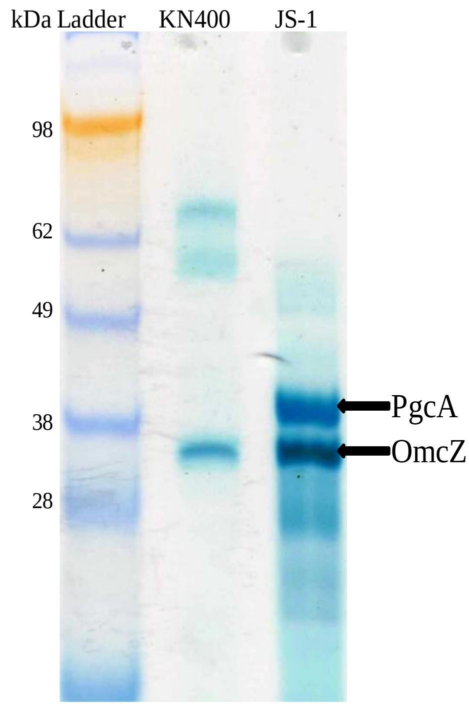

Figure 9. *c*-type cytochrome content of cell-free filtrates from KN400 and JS-1 cultures grown with Fe(III) oxide as the electron acceptor. Proteins were separated with SDS-PAGE and stained for heme. Labeled bands were determined to contain the specified cytochromes with LC/MS/MS. Left lane: SeeBlue Plus2 Pre-Stained Standard (Invritrogen, Carlsbad, CA).

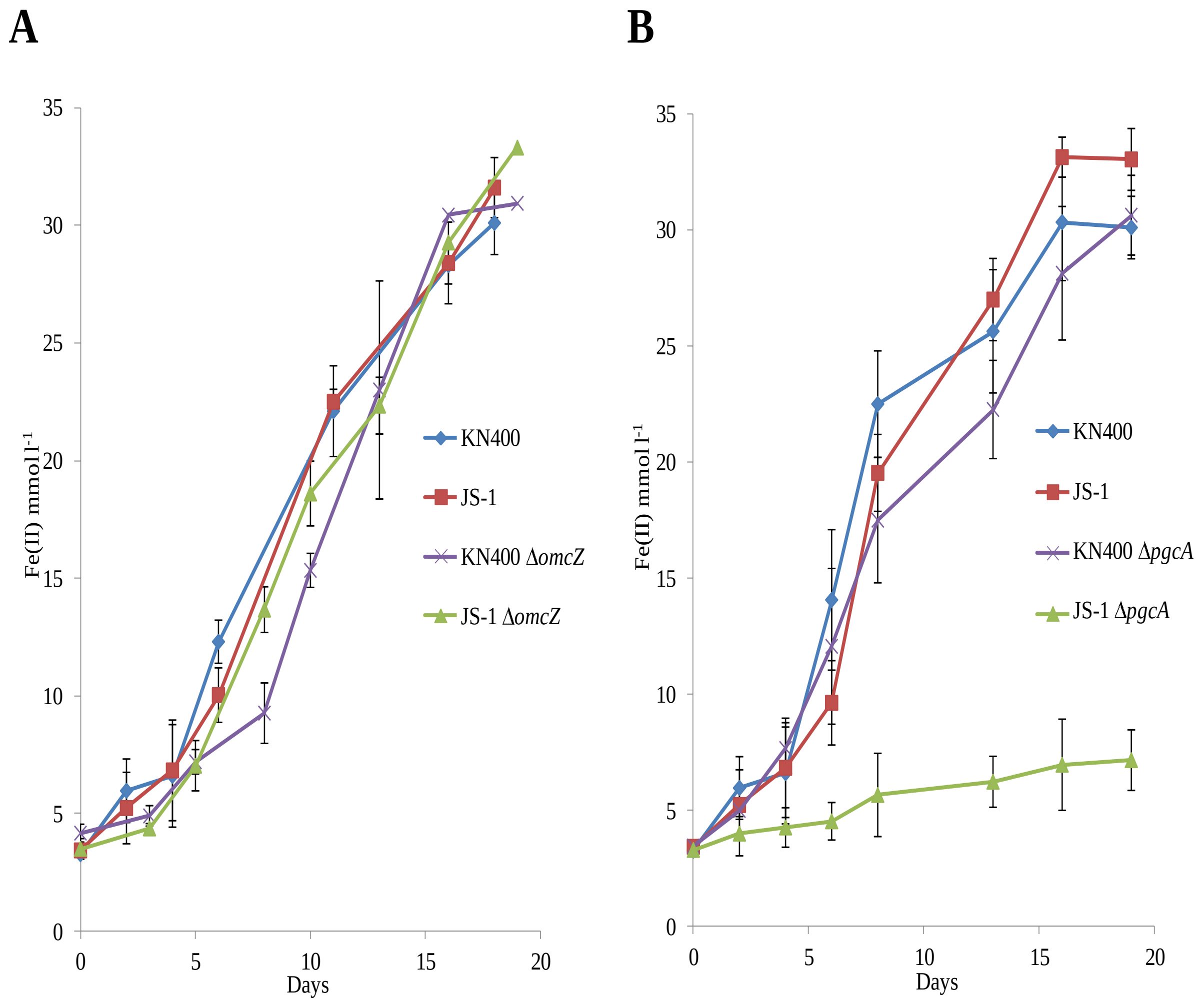

Figure 10. Fe(III) oxide reduction by *omcZ* and *pgcA* mutants. (A) Fe(II) produced from Fe(III) oxide over time in KN400, JS-1, *omcZ*-deficient KN400, and *omcZ*-deficient JS-1. (B) Fe(II) produced from Fe(III) oxide over time in KN400, JS-1, *pgcA*-deficient KN400, and *pgcA*- deficient JS-1. Results are the means and standard deviation of results from triplicate cultures for each strain.

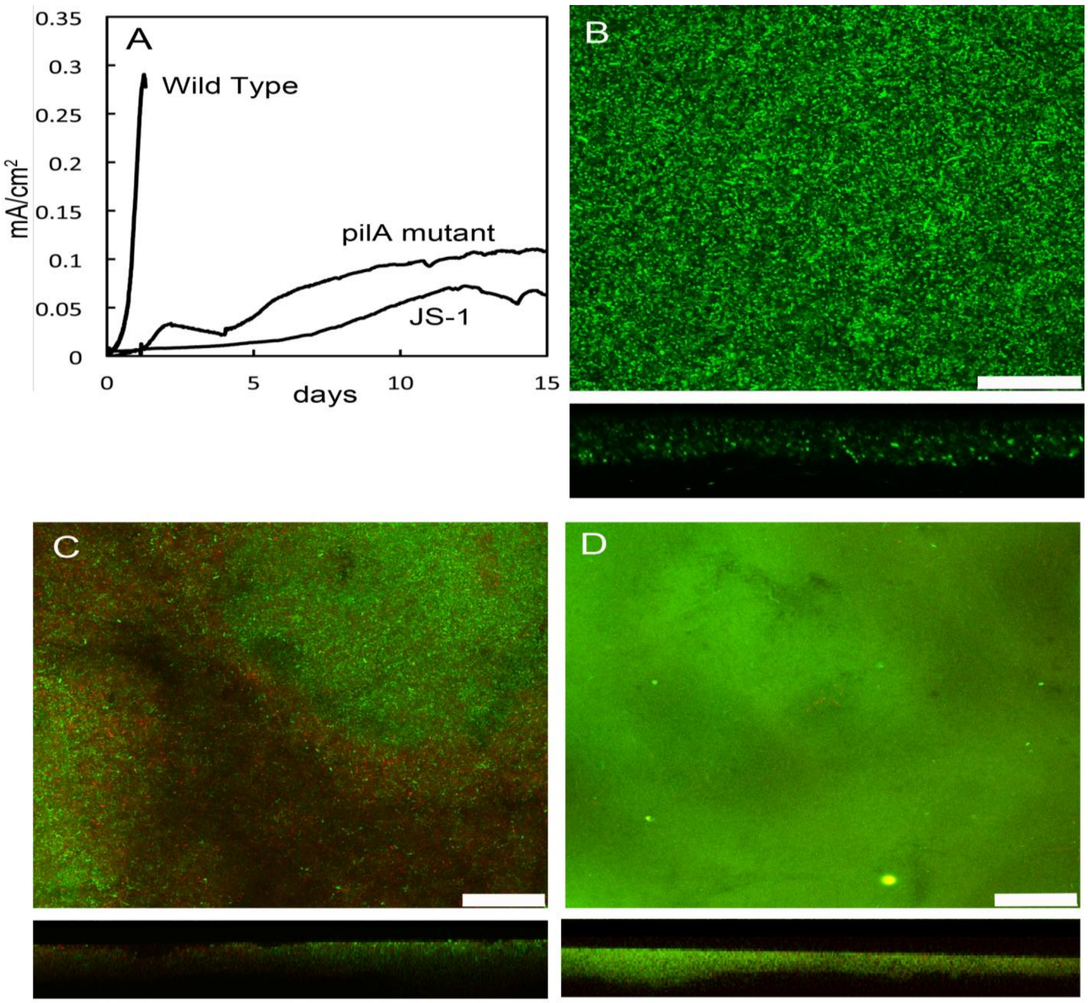

Figure 11. (A) Current production per area by KN400, the KN400 *pilA*-deficient mutant, and JS-1. Data are representative of three independent experiments with each strain. (B-D) Confocal scanning laser images from biofilms of (B) KN400, (C) the KN400 *pilA*-deficient mutant, and (D) JS-1. The large square panels represent a 3D projection and the smaller rectangular panels represent a side view. Scale bar is 25 microns. Images were taken at maximum current, i.e. 2 days for KN400 wild-type; 18 days for the KN400 *pilA*-deficient mutant; and 22 days for JS-1.

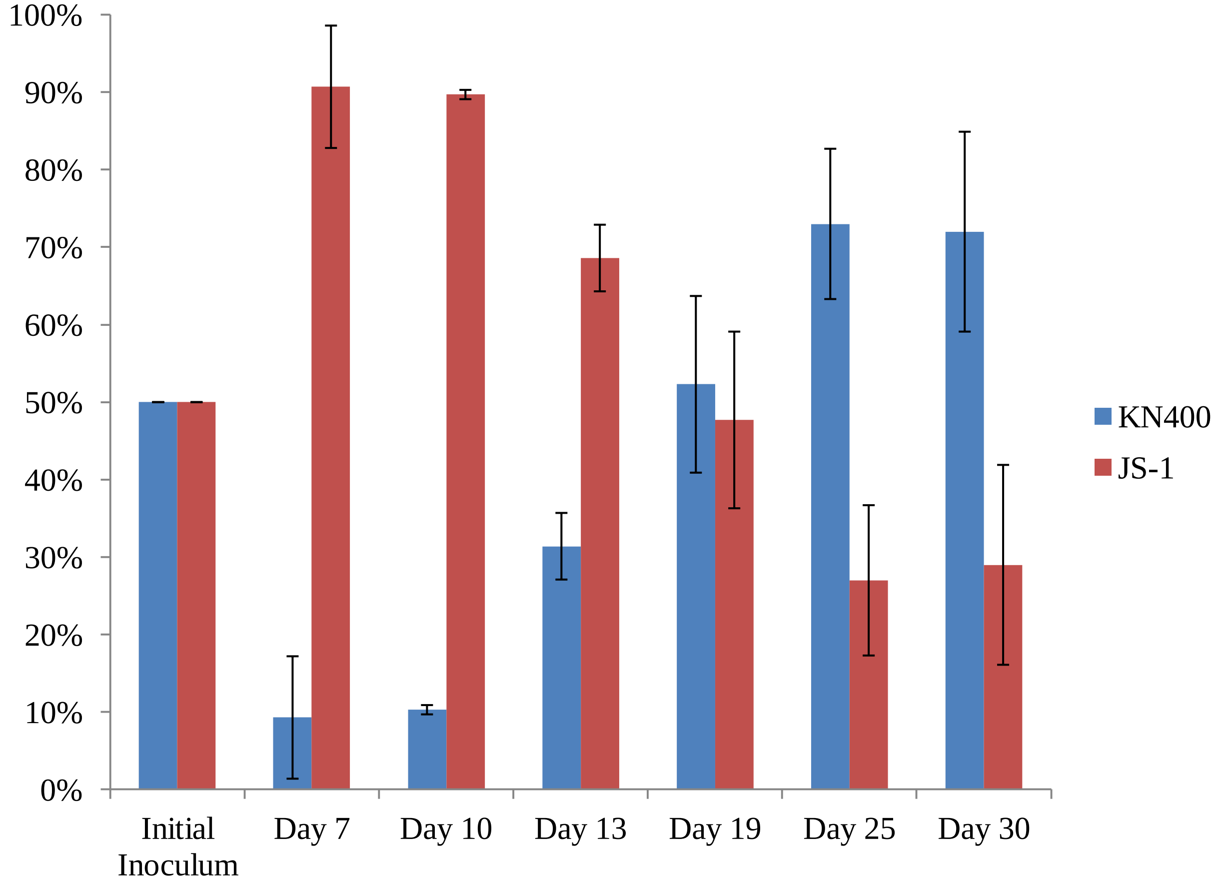

Figure 12. Percentages of JS-1 or KN400 in a mixed Fe(III) oxide culture in which 50% of the medium was swapped out with fresh Fe(III) oxide every 3 days after an initial 7 day incubation.

Tables:

Table 6. Genes up-regulated at least eight-fold in JS-1 compared with KN400 (P-value cutoff ≤ 0.01)

Gene	Annotation	Fold Change
KN400_1784	PgcA- lipoprotein cytochrome c, 3 heme-binding sites	57.2
KN400_0540	protein of unknown function of ISGsu7	21
KN400_1319	sulfate ABC transporter, periplasmic sulfate-binding protein	17.4
KN400_2603	conserved hypothetical protein	13.5
KN400_1318	winged helix-turn-helix transcriptional regulator, Rrf2 family	11.1
KN400_2690	hypothetical protein	10.5
KN400_3415	hypothetical protein	10.1
KN400_2691	anaerobic C4-dicarboxylate antiporter, Dcu family	9.9
KN400_1211	iron-sulfur cluster-binding oxidoreductase	9.9
KN400_1038	conserved hypothetical protein	9.8
KN400_2687	conserved hypothetical protein	9.5
KN400_1785	TPR domain lipoprotein	9.1
KN400_1693	conserved hypothetical protein	9.0
KN400_2641	efflux pump, RND family, outer membrane protein	8.7

CHAPTER 4

SYNTROPHIC GROWTH VIA QUINONE-MEDIATED INTERSPECIES ELECTRON TRANSFER

4.1 Abstract

The mechanisms by which microbial species exchange electrons are of interest because interspecies electron transfer can expand the metabolic capabilities of microbial communities. Previous studies with the humic substance analog anthraquinone-2,6-disulfonate (AQDS) suggested that quinone-mediated interspecies electron transfer (QUIET) is feasible, but it was not determined if sufficient energy is available from QUIET to support the growth of both species. Furthermore, there have been no previous studies on the mechanisms for the oxidation of anthrahydroquinone-2,6-disulfonate (AHQDS). A coculture of *Geobacter metallireducens* and *Geobacter sulfurreducens* metabolized ethanol with the reduction of fumarate much faster in the presence of AQDS, and there was an increase in cell protein. *G. sulfurreducens* was more abundant, consistent with *G. sulfurreducens* obtaining electrons from acetate that *G. metallireducens* produced from ethanol, as well as from AHQDS. Cocultures initiated with a citrate synthase-deficient strain of *G. sulfurreducens* that was unable to use acetate as an electron donor also metabolized ethanol with the reduction of fumarate and cell growth, but acetate accumulated over time. *G. sulfurreducens* and *G. metallireducens* were equally abundant in these co-cultures reflecting the inability of the citrate synthase-deficient strain of *G. sulfurreducens* to metabolize acetate. Evaluation of the mechanisms by which *G. sulfurreducens* accepts electrons from AHQDS demonstrated that a strain deficient in outer-surface *c*-type cytochromes that are required for AQDS reduction was

as effective in QUIET as the wild-type strain. Deletion of additional genes previously implicated in extracellular electron transfer also had no impact on QUIET. These results demonstrate that QUIET can yield sufficient energy to support the growth of both syntrophic partners, but that the mechanisms by which electrons are derived from extracellular hydroquinones require further investigation.

4.2 Introduction

Interspecies electron transfer (IET) may be an important mechanism for energy exchange in a range of anaerobic microbial communities, but the diversity of microbial strategies for IET has yet to be fully explored. The best-known mechanism for IET is hydrogen interspecies electron transfer (HIT) in which the electron-donating species reduces protons to H_2 and the electron-accepting partner oxidizes H_2 with the reduction of an electron acceptor (McInerney *et al.*, 2009; Shrestha and Rotaru, 2014; Sieber *et al.*, 2014; Stams and Plugge, 2009). In some instances formate may substitute for H_2 as the electron carrier (i.e. formate interspecies formate transfer (FIT)) (McInerney *et al.*, 2009; Shrestha and Rotaru, 2014; Sieber *et al.*, 2014; Stams and Plugge, 2009). HIT has been documented with a wide diversity of H_2-producing and H_2-consuming microbes (McInerney *et al.*, 2009; Shrestha and Rotaru, 2014; Sieber *et al.*, 2014; Stams and Plugge, 2009).

An alternative to HIT and FIT is direct interspecies electron transfer (DIET), in which syntrophic partners forge biological electrical connections to exchange electrons (Lovley, 2011b; Rotaru *et al.*, 2014a; Shrestha *et al.*, 2013b; Summers *et al.*, 2010). To date DIET has only been documented with *Geobacter* species as the electron-donating species with either another *Geobacter* species (Shrestha *et al*., 2013b; Summers *et al*., 2010) or a methanogen (Rotaru *et al*., 2014a; Rotaru *et al*., 2014b) as the electron-accepting species. The ability of *Geobacter* species to participate in DIET can be attributed to their ability to make extracellular electrical connections via pili that have metallic-like conductivity (Malvankar *et al*., 2011; Reguera *et al*., 2005; Shrestha *et al*., 2013b; Summers *et al*., 2010). Conductive materials such as granular activated carbon (Liu *et al*., 2012), biochar (Chen *et al*., 2014b), and carbon cloth (Chen *et al*., 2014a) can substitute for the conductive pili to form interspecies electrical connections. The conductive mineral magnetite can also promote DIET (Kato *et al*., 2012; Liu *et al*., 2014), by functioning as an outer-surface *c*-type cytochrome substitute (Liu *et al*., 2014).

A less explored mechanism of IET is electron exchange via quinone-mediated interspecies electron transfer (QUIET) in which compounds with quinone moieties serve as electron shuttles between the electron-donating and the electron-accepting partner. Quinone moieties are components of humic substances, which are abundant in many soils and sediments and can serve as electron acceptors for microbial respiration (Gralnick and Newman, 2007; Lovley *et al*., 1996a; Scott *et al*., 1998). The hydroquinones produced can abiotically reduce Fe(III) oxides, regenerating the quinone moieties. The humics-catalyzed electron shuttling between Fe(III)-reducing microorganisms and Fe(III) oxides can greatly accelerate the rate of Fe(III) oxide reduction and the degradation of organic contaminants in subsurface sediments by Fe(III) reducers (Lovley *et al*., 1998). Anthraquione-2,6-disulfonate (AQDS) can serve as a humic substances analog which microbes can reduce to the humics analog anthrahydroquinone-2,6-disulfonate (AHQDS). Reduced humics or AHQDS can also serve as an electron donor for microbial reduction of a diversity electron acceptors including: nitrate, selenite, and arsenate (Lovley *et al*. 1999). Providing AQDS as an electron shuttle promoted interspecies electron transfer in cell suspensions of *G. metallireducens* and *Wolinella succinogenes* (Lovley *et al*., 1999) and in co-cultures of *G. metallireducens* and *G. sulfurreducens* (Liu *et al*., 2012), but it was not determined in these studies whether either of the partners conserved energy to support growth from QUIET.

Co-cultures of *G. metallireducens* and *G. sulfurreducens* grown in a medium with ethanol as the electron donor and fumarate as the electron acceptor provide a good model system for investigating IET mechanisms because: 1) the two species can only grow in ethanol/fumarate medium if they exchange electrons (Summers *et al*., 2010); 2) *G. metallireducens* does not produce H_2 or formate when metabolizing ethanol to acetate, eliminating the possibility of HIT or FIT (Shrestha *et al*., 2013c); 3) both species can be genetically manipulated (Coppi *et al*., 2001; Tremblay *et al*., 2012) facilitating functional studies; and 4) a citrate synthase-deficient mutant of *G. sulfurreducens* which can not use acetate as an electron donor is available, making it possible to determine if electrons derived from IET can serve as sole electron donor to promote respiration and growth (Shrestha *et al*., 2013b).

Studies with gene deletion mutants demonstrated that genes for five outer-surface *c*-type cytochromes had to be deleted in order to substantially diminish the ability of *G. sulfurreducens* to reduce humic substances or AQDS (Voordeckers *et al*., 2010). It is expected that reduced humics and AHQDS are also oxidized at the outer cell surface. Humic substances are too large to enter the cell and like AQDS the size and charge of AHQDS are expected to prevent it from crossing the outer membrane. However, it is unknown what outer-surface proteins may be involved in accepting electrons from reduced humics or AHQDS.

In order to learn more about the potential for QUIET to support growth, and the mechanisms for AHQDS oxidation, studies were carried out with *G. metallireducens/G. sulfurreducens* co-cultures. The results demonstrate that growth of both syntrophic partners via QUIET is possible and that the hypothesized electron acceptors for the oxidation of AHQDS at the outer surface are proteins different than those involved in AQDS reduction.

4.3 Materials and Methods

4.3.1 Laboratory strains and culture conditions.

All *Geobacter* strains were obtained from our laboratory culture collection and routinely cultured under strict anaerobic conditions as previously described (Balch *et al*., 1979; Coppi *et al*., 2001). All pure culture strains of *G. metallireducens* were regularly transferred into FC medium (Lovley *et al*., 1993b) with 20 mM ethanol provided as the sole electron donor and 56 mM ferric citrate as the sole electron acceptor. All pure culture strains of *G. sulfurreducens* were regularly transferred into NBF medium (Coppi *et al*., 2001) with 10 mM acetate provided as the sole electron donor and 40 mM fumarate as the sole electron acceptor. Co-cultures were initiated with equal amounts of both organisms in anaerobic pressure tubes containing 10 mL of NBF medium, with 10 mM ethanol provided as the sole electron donor and 40 mM fumarate as the electron acceptor. Cysteine was omitted from all cultures to eliminate the possibility of a cysteine/cystine electron shuttle between the organisms. DL vitamins were also omitted from the media to eliminate any other possible electron shuttling compounds. Additions of anthraquinone-2,6,-disulphonate (AQDS) were made from a concentrated stock to provide a final concentration of 500 μM.

4.3.2 Analytical techniques.

Organic acids were monitored with high performance liquid chromatography (HPLC) as previously described (Nevin *et al*., 2008). Changes in ethanol concentration were monitored with gas chromatography as previously described (Morita *et al.*, 2011).

4.3.3 Protein determination.

Protein concentrations were determined with previously described methods (Rotaru *et al.*, 2012). Equal volumes of culture were harvested at different time intervals during growth, washed in an isotonic wash buffer, then resuspended in 5% sodium dodecyl sulfate (SDS) and steamed for 5 minutes. The cell lysate was diluted for protein determination with the bicinchoninic acid assay (Sigma Aldrich), according to the manufacturer's instructions.

4.3.4 Quantitative PCR.

The proportion of *G. sulfurreducens* and *G. metallireducens* cells in co-cultures was determined by quantitative PCR with genomic DNA serving as the template as previously described (Summers *et al.*, 2010). The *G. metallireducens* specific primer set Gmet_F 5'- ATGGCCCACATCTTCATCTC-3', Gmet_R 5'-

TGCATGTTTTCATCCACGAT-3’, and the *G. sulfurreducens* specific primer set Gsulf_F 5’-CCAGCTACGCCTACTTCTTCTTT-3’, Gsulf_R 5’-AAGCTGTGGTTCAGGAGGTATTT-3’ were used to determine proportions of each species in the co-culture. Genomic DNA was extracted using the Epicenter Master Pure DNA Purification kit (Epicentre Biotechnologies, Madison, WI, USA) following the manufacturer’s instructions.

Power SYBR green PCR master mix (Applied Biosystems, Foster City, CA) and an ABI 7500 real-time PCR system were used to amplify and to quantify PCR products. Each reaction mixture consisted of forward and reverse primers at a final concentration of 200 nM, 5 ng of gDNA, and 12.5 µl of Power SYBR green PCR master mix (Applied Biosystems).

4.4 Results and Discussion

4.4.1 QUIET-based growth of both syntrophic partners.

In the absence of extracellular electron transport mediators, co-cultures of *G. metallireducens* and *G. sulfurreducens* require ca. 30 days to metabolize ethanol when first initiated, which has been attributed to the time necessary for the co-cultures to initially adapt to produce the biological electrical connections required for DIET (Summers *et al*., 2010). Faster initial rates of succinate production were observed when AQDS was added to co-cultures as a potential electron shuttle (Liu *et al*., 2012), but it was not determined whether this QUIET also supported cell growth.

Further evaluation confirmed that QUIET supported growth of both species (Figure 13). Unlike co-cultures participating in DIET, the cells did not aggregate and remained planktonic. The culture medium had an orange tinge characteristic of AHQDS, suggesting that *G. metallireducens* maintained a constant source of AHQDS to serve as an electron donor for *G. sulfurreducens* respiration. Cell protein accumulated over time (Figure 13A), coincident with ethanol metabolism (Figure 13B) and the reduction of fumarate to succinate (Figure 13C). Low levels of acetate accumulated (Figure 13D), indicating that *G. sulfurreducens* was consuming most of the acetate that *G. metallireducens* produced from ethanol metabolism. Quantitative PCR revealed that *G. sulfurreducens* accounted for 62 $\pm$ 4.5 % (mean $\pm$ standard deviation; n=3) of the *Geobacter* cells in the co-culture, consistent with *G. sulfurreducens* receiving electrons from the interspecies electron transfer via the AQDS/AHQDS electron shuttle, as well as from the acetate released from *G. metallireducens* metabolism of ethanol. With continued transfer of the AQDS-amended co-culture the lag period decreased and the growth rate increased (Figure 14), suggesting that the co-culture adapted to optimize QUIET-based growth.

In order to determine whether *G. sulfurreducens* could conserve energy to support growth solely from electrons derived from AHQDS, a co-culture was initiated with the previously described (Ueki and Lovley, 2010a) strain of *G. sulfurreducens* in which the gene for citrate synthase was deleted. This strain is unable to use acetate as an electron donor. This co-culture grew, as demonstrated by continued fumarate reduction in successive transfers of a 5% inoculum. Analysis of the fourth transfer of the AQDS-amended *G. metallireducens/G. sulfurreducens* co-culture with the citrate synthase-deficient strain of *G. sulfurreducens* demonstrated that cell protein increased over time (Figure 15A), co-incident the ethanol metabolism (Figure 15B), and the reduction of fumarate to succinate (Figure 15C). There was a steady accumulation of acetate over time (Figure 15D), in accordance with the inability of citrate synthase-deficient strain of *G. sulfurreducens* to use acetate as an electron donor. In these co-cultures, the citrate synthase-deficient strain of *G. sulfurreducens* accounted for 51 ± 3.9 % of the total cells, comparable to the proportion of *G. sulfurreducens* in the previously described (Shrestha *et al*., 2013b) co-culture in which *G. metallireducens* and the citrate synthase-deficient *G. sulfurreducens* strain shared electrons via DIET.

In order to further evaluate the potential for AHQDS to serve as the sole electron donor for *G. sulfurreducens*, a co-culture was initiated with the citrate synthase-deficient strain of *G. sulfurreducens* and the previously described (Tremblay *et al*., 2012), genetically modified strain of *G. metallireducens* that can not produce the electrically conductive pili required for DIET (Shrestha *et al*., 2013c). This co-culture grew as well as the co-culture with wild-type *G. metallireducens* (Figure 16) with a similar abundance of *G. sulfurreducens* (54 ± 3.7%).

4.4.2 Evaluation of outer surface electron transport components involvement in AHQDS oxidation during QUIET.

In order to evaluate potential mechanisms for the hypothesized AHQDS oxidation at the outer cell surface of *G. sulfurreducens*, the impact of deleting genes for outer-surface redox-active proteins on the growth of the co-culture in the presence AQDS was investigated. Co-cultures were initiated with wild-type *G. metallireducens* and the previously described (Voordeckers *et al.*, 2010) BESTZ strain of *G. sulfurreducens* that is deficient in the outer-surface *c*-type cytochromes OmcB, OmcE, OmcS, OmcT, and OmcZ. This strain reduced AQDS at rates less than 5 % of the wild-type strain (Voordeckers *et al*., 2010). However, co-cultures initiated with the BESTZ strain grew with continued transfer in AQDS-amended medium reducing fumarate to succinate at a maximum rate (16.9 ± 1.55 mM succinate produced per day) comparable (Figure 17A) to co-cultures initiated with wild-type *G. sulfurreducens* (17.6 ± 1.09 mM succinate produced per day). In contrast, just the deletion of OmcS inhibited DIET in *G. metallireducens/G. sulfurreducens* co-cultures (Summers *et al*., 2010). Co-cultures in AQDS-amended medium initiated with a strain of *G. sulfurreducens* deficient in only *omcS* also produced succinate at a rate comparable to wild-type (16.7 ± 1.19 mM succinate produced per day). As might be expected, co-cultures in AQDS-amended medium initiated with a strain of *G. sulfurreducens* in which *pilA* had been deleted (Reguera *et al*., 2005), also functioned well with rates of succinate production of 18.2 ± 1.78 mM succinate produced per day, confirming that conductive pili are not necessary for interspecies electron exchange when AQDS/AHQDS serve as an electron shuttle.

In addition to *c*-type cytochromes, the putative multi-copper, redox-active outer surface proteins OmpB and OmpC have also been implicated in electron transfer to extracellular electron acceptors (Holmes *et al*., 2008; Mehta *et al*., 2006; Qian *et al*., 2007). However, co-cultures initiated with strains of *G. sulfurreducens* deficient in either OmpB or OmpC effectively reduced fumarate as well as co-cultures initiated with wild-type *G. sulfurreducens* (Figure 17B), with rates of succinate production of 17.1 ± 1.4 and 17.2 ± 1.4 mM succinate produced per day, respectively.

OmpJ is a putative porin that is one of the most abundant outer-membrane proteins of *G. sulfurreducens* (Afkar *et al*., 2005). Deletion of the gene encoding for OmpJ in *G. sulfurreducens* reduces the heme content of the cell ca. 50%, particularly reducing the abundance of outer-surface *c*-type cytochromes, but also influencing the relative abundance of cytochromes in other fractions, with increased abundance of some cytochromes and reduced abundance of others (Afkar *et al*., 2005). The OmpJ-deficient strain reduces fumarate as well as the wild-type, but is deficient in the reduction of soluble Fe(III) citrate, as well as insoluble Fe(III) oxide. Yet, co-cultures in AQDS-amended medium initiated with the OmpJ-deficient strain of *G. sulfurreducens* readily reduced fumarate after multiple transfers (Figure 17C) with a succinate production rate (15.1 $\pm$ 1.01 succinate produced per day) just slightly lower than co-cultures initiated with wild-type *G. sulfurreducens*.

In addition to extracellular proteins, periplasmic constituents are presumably also required for electron transport from extracellular electron donors to intracellular electron carriers. GSU3274 encodes a putative, periplasmic, mono-heme cytochrome (Strycharz *et al*., 2011). Wild-type *G. sulfurreducens* can directly accept electrons from a negatively poised graphite electrode for the reduction of fumarate (Gregory *et al*., 2004), but a strain of *G. sulfurreducens* in which the gene GSU3274 was deleted could not (Strycharz *et al*., 2011), suggesting that the protein encoded by GSU3274 was an important intermediary in electron transfer from extracellular electron donors. However, AQDS-amended co-cultures initiated with the GSU3274-deficient strain of *G. sulfurreducens* reduced fumarate to succinate as well as wild-type (Figure 17D) with a rate of succinate production of 21.6 $\pm$ 1.8 mM succinate produced per day. These results suggest that the protein encoded by GSU3274 is not required for *G. sulfurreducens* to effectively oxidize AHQDS. Additional studies of the GSU3274-deficient strain could not replicate previously reported results (Strycharz *et al*., 2011) as this strain accepted current from a negatively poised graphite electrode as well as wild-type (K. Nevin and T. Woodard, unpublished data).

4.5 Implications

The results demonstrate for the first time that syntrophic partners can conserve energy to support growth via QUIET. This is an important finding because humic substances, which contain abundant quinone moieties that can be reversibly oxidized and reduced may be important electron carriers in a diversity of anoxic soils and sediments (Gralnick and Newman, 2007). Previously, the primary focus has been on the role of humic substances as an electron shuttle from microorganisms to insoluble Fe(III) oxides, but the results presented here suggest that quinone-bearing organics such as humic substances may also promote interspecies electron transfer.

Reduced humic substances clearly must be extracellular electron donors because their size precludes crossing the outer membrane. It was hypothesized that AHQDS is oxidized on the outer cell surface as well because: 1) gene deletion studies have demonstrated that AQDS is reduced on the outer cell surface of *G. sulfurreducens* (Voordeckers *et al*., 2010) as well as in *Shewanella oneidensis* (Gralnick and Newman, 2007) and 2) the reduced form of the molecule is expected to be excluded from crossing the outer membrane due to similar size and charge considerations. However, none of the outer-surface proteins that have been identified as being important in electron transfer to extracellular electron acceptors were essential for the reverse reaction of oxidizing AHQDS. Further evidence that the route(s) for AHQDS oxidation may differ from those for AQDS reduction is the previous finding that *Paracoccus denitrificans* was incapable of reducing AQDS, but oxidized AHQDS with nitrate as the electron acceptor (*Lovley et al*., 1999). A better understanding of the mechanisms by which *G. sulfurreducens* oxidizes AHQDS and humic substances could aid in screening the microbial world for other microorganisms that may be capable of functioning as the electron-accepting microorganism in QUIET and may provide insight into the mechanisms for practical applications such as bioremediation and microbial electrosynthesis (Lovley, 2011e; Lovley and Nevin, 2013) in which electrodes serve as the electron donor for anaerobic respiration.

Figures:

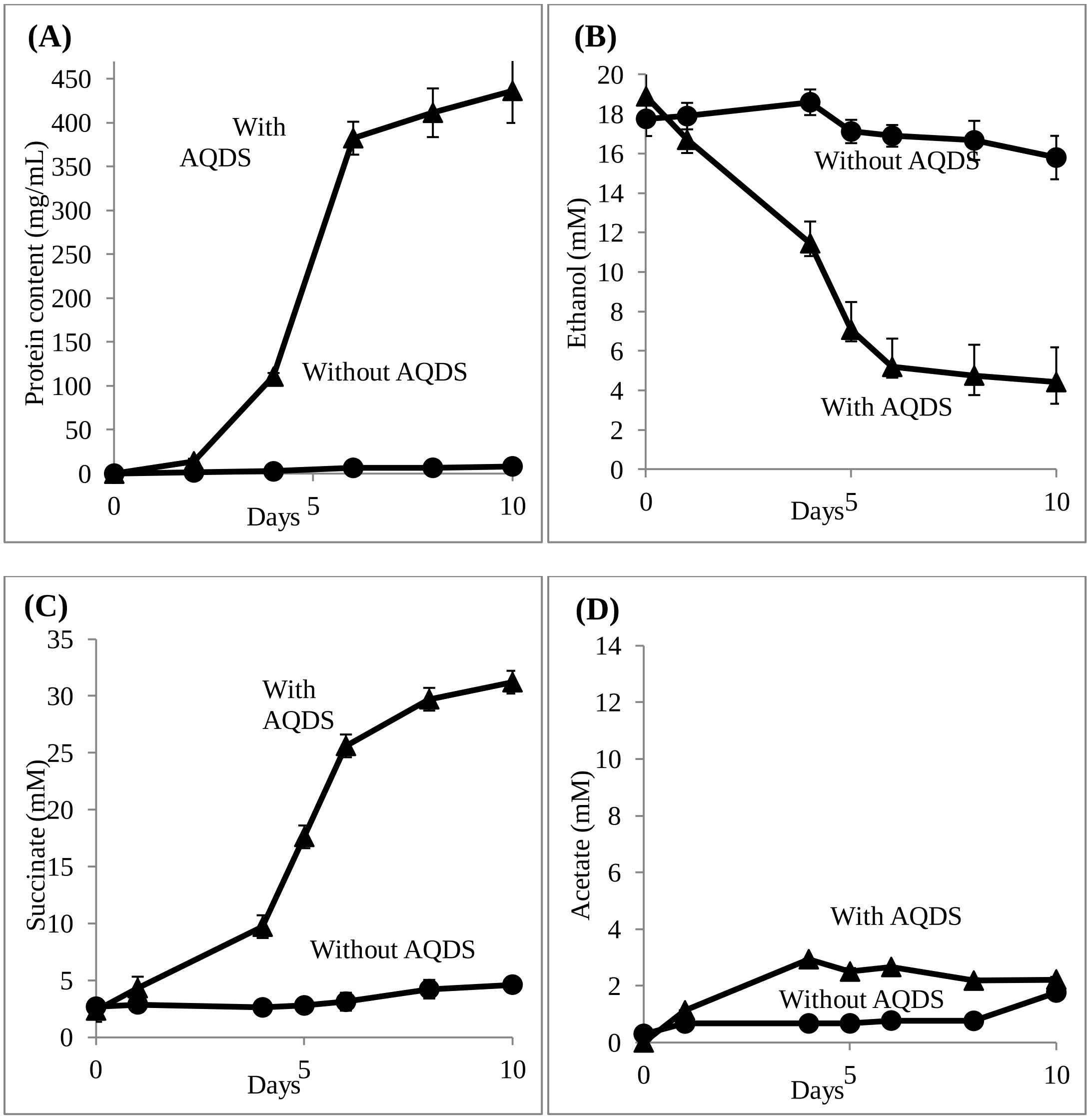

Figure 13. Growth and metabolism of *Geobacter metallireducens* and *Geobacter sulfurreducens* with and without the addition of AQDS when initially established. A) cell protein; (B) ethanol; (C) succinate; and (D) acetate over time.

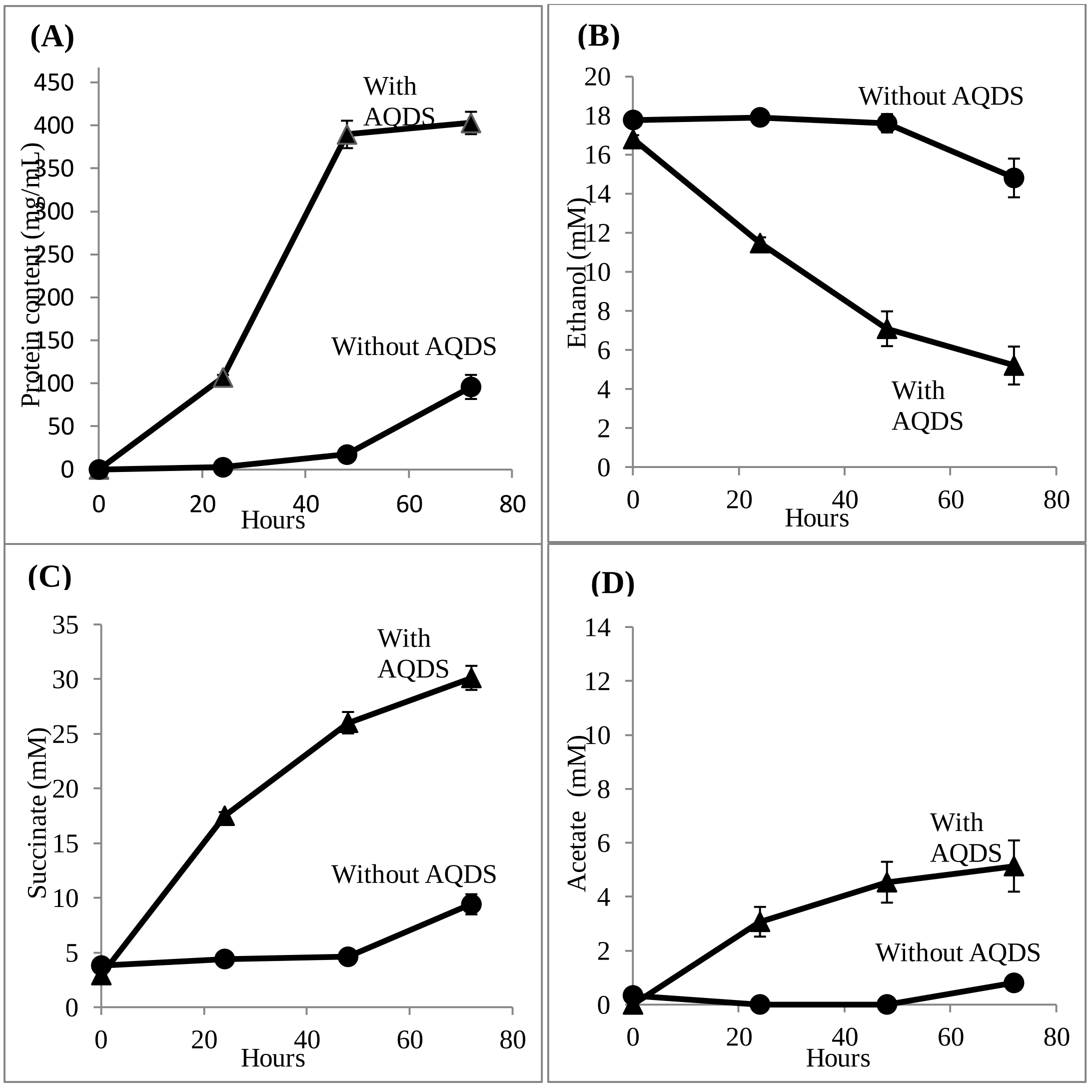

Figure 14. Growth and metabolism of *Geobacter metallireducens* and *Geobacter sulfurreducens* co-cultures with or without AQDS after four successive transfers. (A) cell protein; (B) ethanol; (C) succinate; and (D) acetate over time.

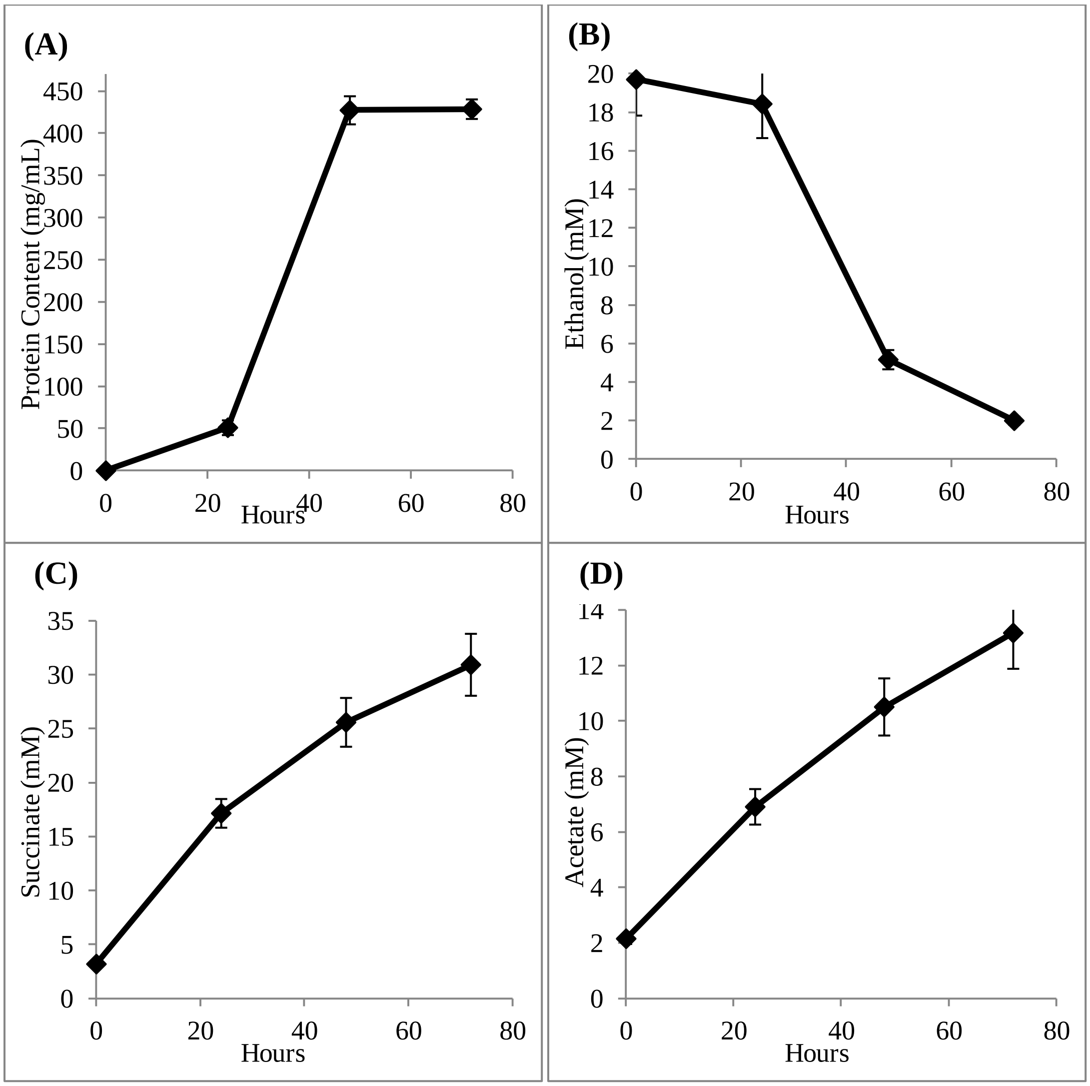

Figure 15. Growth and metabolism of co-cultures initiated with wild-type *Geobacter metallireducens* and the citrate synthase-deficient strain of *Geobacter sulfurreducens* in AQDS-amended medium after four successive transfers. A) cell protein; (B) ethanol; (C) succinate; and (D) acetate over time.

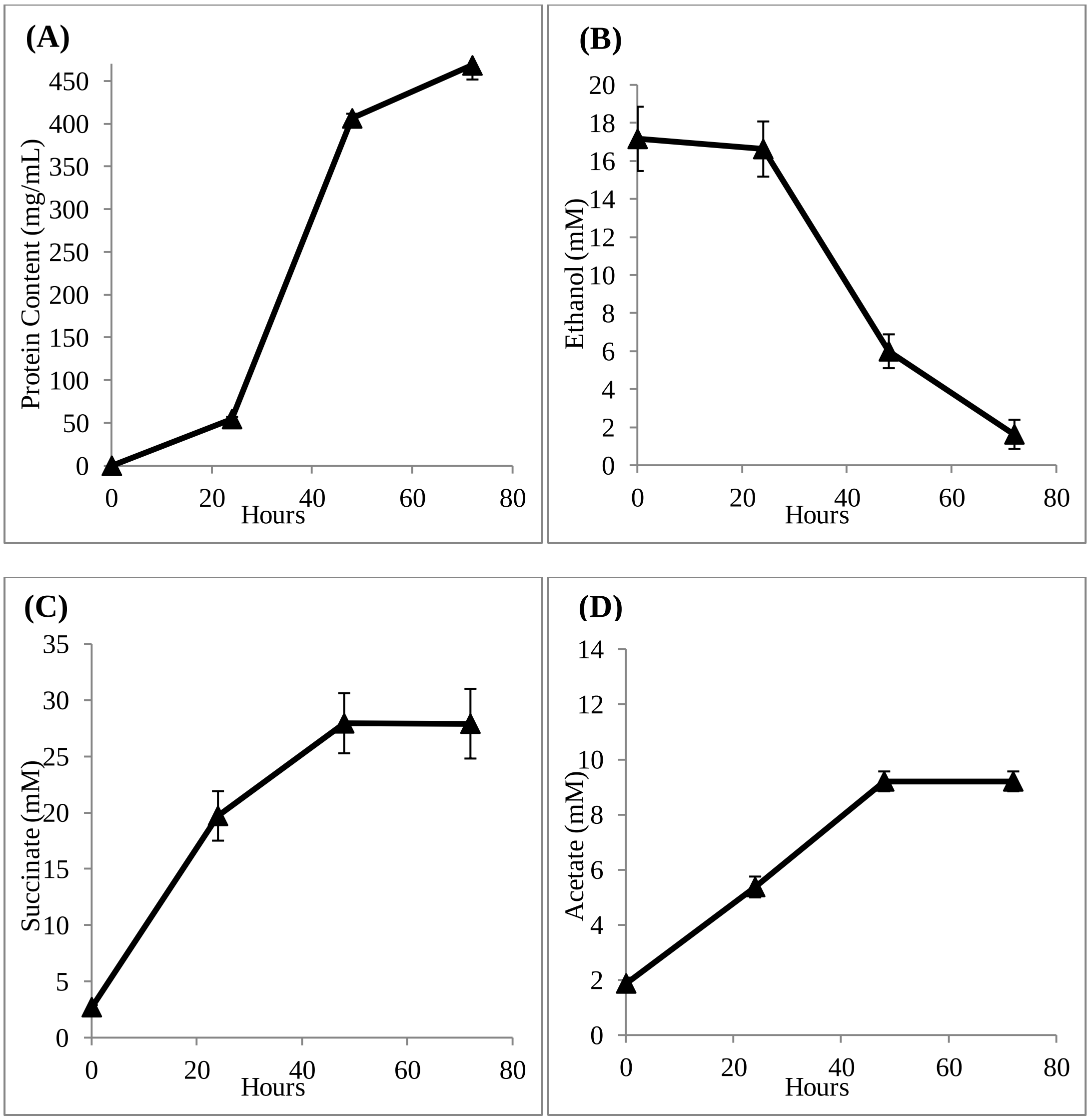

Figure 16. Growth and metabolism of co-cultures initiated with the pilin-deficient strain of *Geobacter metallireducens* and the citrate synthase-deficient strain of *Geobacter sulfurreducens* in AQDS-amended medium after four successive transfers. A) cell protein; (B) ethanol; (C) succinate; and (D) acetate over time.

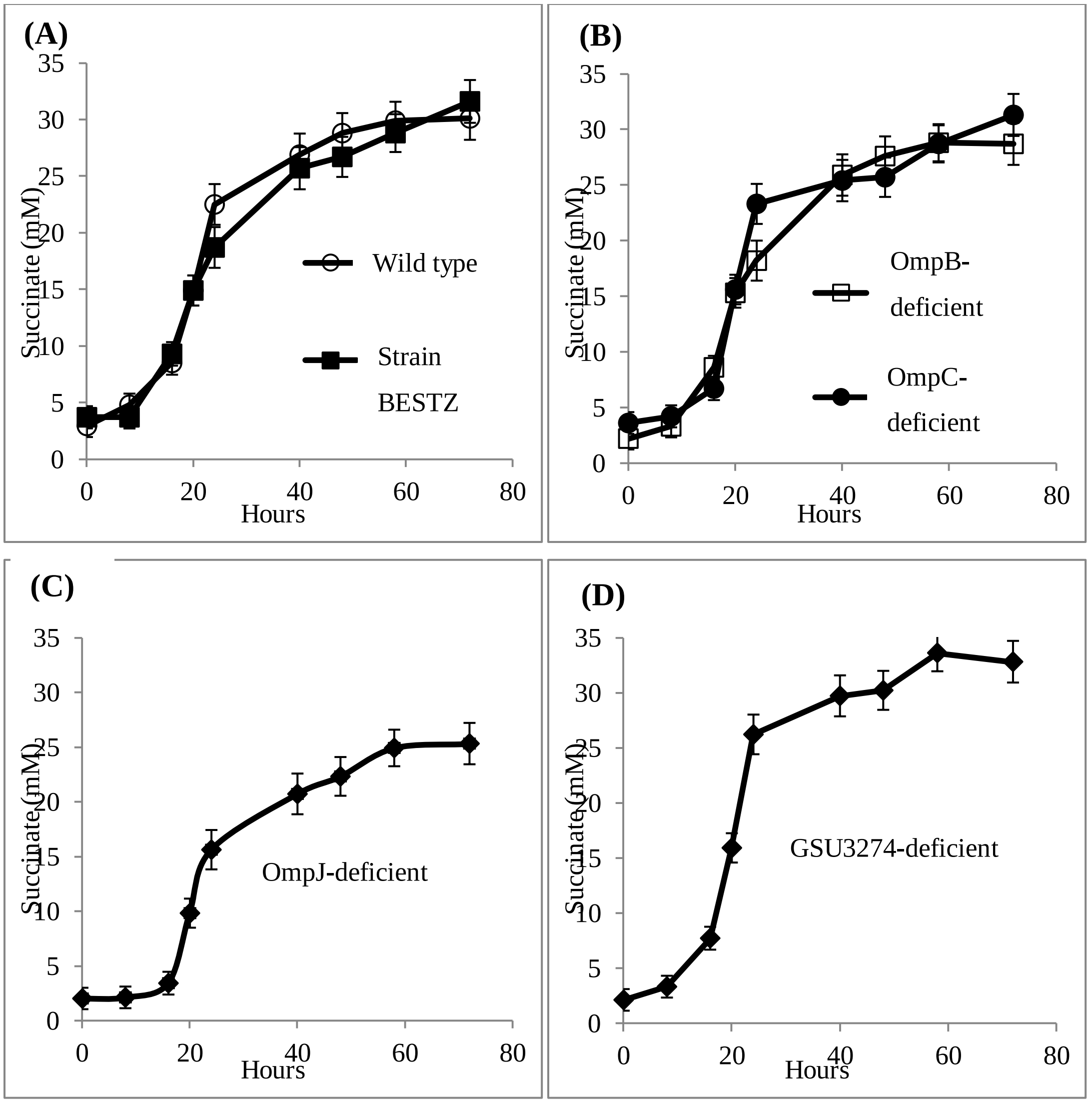

Figure 17. Growth and metabolism of co-cultures initiated with wild-type *Geobacter metallireducens* and strains of *Geobacter sulfurreducens* in which genes for putative electron transport genes were deleted in AQDS-amended medium after four successive transfers. *G. sulfurreducens* strains evaluated were: A) wild-type and the BESTZ strain deficient in the outer-surface *c*-type cytochromes OmcB, OmcE, OmcS, OmcT, and OmcA; (B) strains deficient in the putative outer-surface multi-copper proteins OmpB of OmpC; (C) strain deficient in the putative porin OmpJ; and (D) strain deficient in the putative periplasmic *c*-type cytochrome encoded by gene GSU3274.

CHAPTER 5
CONCLUSIONS AND FUTURE DIRECTIONS

This dissertation has presented three research projects with the goal of (1) investigating components involved in extracellular electron transfer to insoluble Fe(III) oxides by the environmentally relevant *Geobacter* species, *G. metallireducens*, (2) evaluating PilA-pili independent mechanisms for extracellular electron transfer to Fe(III) oxides by a strain of *G. sulfurreducens*, and (3) providing insights into the mechanism(s) utilized by *G. sulfurreducens* for extracellular electron transfer into the cell via electron exchange through an electron shuttling compound. Studies investigating these goals aim to improve our understanding on how extracellular electron exchange occurs during important biogeochemical cycles in the environment, during interspecies electron transfer, as well as for practical applications such as electrosynthesis and wastewater treatment.

The first research project identified components involved in extracellular electron transfer to insoluble Fe(III) oxides by *G. metallireducens*. Although many studies on the mechanisms for extracellular electron transfer have been conducted in *G. sulfurreducens*, many of the most thoroughly studied components are not well conserved among *Geobacter* species; furthermore *G. sulfurreducens* lacks the ability for many environmentally relevant processes, including oxidation of aromatic compounds. *G. metallireducens* is able to couple the reduction of Fe(III) with the oxidation of aromatic compounds, including benzene, making it important to understand the mechanisms for extracellular electron transfer in this species. We identified six *c*-type cytochromes, a NHL-repeat containing protein, and a gene potentially involved in pili glycosylation that were essential for reduction of insoluble Fe(III), but not for soluble Fe(III) citrate.

This research demonstrated that there are similarities in the mechanisms for extracellular electron transfer between the thoroughly studied *G. sulfurreducens* and the environmentally relevant *G. metallireducens*, but that the outer- surface *c*-type cytochromes involved in Fe(III) oxide reduction are different. Further experiments are required to biochemically analyze these individual *c*-type cytochromes and also determine their exact cellular location. These studies will help to further understand the pathway of electron transport from the cytoplasmic space to extracellular surface of *G. metallireducens*. Additionally, this study identified a potential gene involved in glycosylation of *G. metallireducens* pili. Future experiments are necessary to determine the exact function of this gene, and identify if it is important in other *Geobacter* species.

The second research projected indentified that *G. sulfurreducens* is capable of adapting PilA-pili independent mechanism for extracellular electron transfer to Fe(III) oxides. The adaptation was associated with greater production of the *c*-type cytochrome PgcA, which was required for Fe(III) oxide reduction, and released into the culture medium. It is hypothesized that PgcA is acting as an electron shuttle for reduction of Fe(III) oxide, however further experiments are required to understand the exact shuttling mechanism of this protein. Purification of the PgcA protein and further biochemical analysis will likely provide future insights.

The third research project served to investigate the mechanism(s) for direct electron exchange from the reduced humic-analog anthrahydroquinone-2,6-disulfonate (AHQDS) to *G. sulfurreducens*. In this study *G. sulfurreducens* was cocultured with *G. metallireducens,* and the two species were required to exchange electrons via electron shuttling of the quinone moieties of AQDS/AHQDS in order to grow. This study showed that many of the currently known components that our involved in extracellular electron transfer form *G. sulfurreducens* onto extracellular electron acceptors are required for electron exchange in the reverse direction. This suggests that reverse electron exchange from extracellular electron donors into *G. sulfurreducens* happens via a novel mechanism. Transcriptomic analysis of the cocultures grown with the addition of AQDS compared with the cocultures without AQDS will provide some insights into potential candidate genes involved in this type of extracellular electron exchange. Future studies, including gene deletions and biochemical analysis will be required to identify components involved in this mechanism. Furthermore, studies on other extracellular electron donors other than AHQDS will be necessary in order to see if this mechanism is universal for all extracellular election donors to *G. sulfurreducens*, or specific to AHQDS.

All of the studies in this dissertation provide new insights into the mechanism(s) *Geobacter* species utilize for extracellular electron exchange. The extracellular electron exchange processes are extremely complex and diverse among *Geobacter* species, however their ability to undergo many types of extracellular electron exchange make them a valuable species both in the environment and for practical applications. Therefore, uncovering new components and further investigating the mechanisms they use for direct extracellular electron exchange is invaluable across many scientific fields.

APPENDIX A

OUTER CELL SURFACE COMPONENTS ESSENTIAL FOR FE(III) OXIDE REDUCTION BY *GEOBACTER METALLIREDUCENS*

Table A1: Genes that were up-regulated at least two-fold with growth on Fe(III) oxide compared with Fe(III) citrate as the electron acceptor (P-value cutoff ≤ 0.05)

Gene	Annotation	Fold change	P value	T value
Gmet_0442	flagellin fliC	94.509 up	0.000527	-11.408
Gmet_1044	molybdopterin biosynthesis sulfur carrier protein moaD	90.156 up	0.0473	-3.442
Gmet_0719	conserved hypothetical protein	77.044 up	0.0000544	-21.877
Gmet_1045	aldehyde ferredoxin oxidoreductase tungsten containing	76.354 up	0.024	-4.247
Gmet_1043	molybdopterin biosynthesis sulfur carrier protein sulfurylase; moeB	76.339 up	0.0328	-3.858
Gmet_1046	ethanol dehydrogenase, putative	75.546 up	0.0334	-3.841
Gmet_0438	flagellar hook-associated protein FlgK	56.927 up	4.68x10^-7	-89.469
Gmet_0430	flagellar basal body rod protein FlgF	55.842 up	0.0000413	-25.231
Gmet_0439	flagellar hook-filament junction protein FlgL	52.739 up	4.07x10^-7	-81.59
Gmet_0432	flagellar basal body P-ring formation protein FlgA	49.008 up	0.0000315	-32.008
Gmet_0431	flagellar basal body rod protein FlgG	43.844 up	0.000107	-17.966
Gmet_3115	flagellar basal-body rod protein FlgB	43.056 up	0.000238	-14.225
Gmet_3112	flagellar M-ring mounting plate protein FliF	42.517 up	0.0000408	-24.285
Gmet_0908	hypothetical protein	42.056 up	0.0027	-7.732
Gmet_3104	flagellar operon protein of unknown function DUF3766	39.524 up	0.0104	-5.415
Gmet_3098	flagellar biogenesis protein FliO	39.065 up	0.000232	-14.31
Gmet_0440	carbon storage regulator, CsrA/carbon storage regulator, CsrA	38.440 up	0.000198	-15.016
Gmet_0909	cytochrome c, 9 heme-binding sites	37.794 up	0.00226	-8.078
Gmet_0427	flagellar biogenesis protein FlhF	37.620 up	0.0000946	-18.375
Gmet_2043	repeat-containing protein	37.508 up	0.0000161	-39.331
Gmet_0910	lipoprotein cytochrome c, 10 heme-binding sites	32.723 up	0.00243	-7.926
Gmet_0444	flagellar filament cap protein FliD	32.146 up	0.00159	-8.84
Gmet_3101	flagellar basal body-associated protein FliL	31.002 up	0.000244	-13.945
Gmet_0433	flagellar L-ring lipoprotein FlgH	29.494 up	0.0000417	-23.53
Gmet_3589	lipoprotein, putative	29.302 up	0.000157	-15.917
Gmet_0441	flagellar assembly protein FliW	29.175 up	0.0000958	-18.385
Gmet_0434	flagellar P-ring protein FlgI	29.036 up	0.000742	-10.45
Gmet_0428	flagellar biogenesis protein FlhG (ATPase)	28.361 up	0.0002	-15.017

Gmet_3105	flagellar hook capping protein FlgD	27.424 up	0.00868	-5.662
Gmet_0437	flagellar biogenesis protein FlgN, putative	27.292 up	0.000326	-12.822
Gmet_3099	flagellar motor switch protein FliN	26.197 up	0.0000533	-21.859
Gmet_0429	RNA polymerase sigma-28 factor for flagellar operon fliA	25.445 up	0.00037	-12.479
Gmet_3266	chemotaxis sensor histidine kinase CheA-4	24.699 up	0.0003	-13.166
Gmet_3118	chemotaxis protein phosphatase CheX-1	23.733 up	6.77x10^-7	-70.028
Gmet_1042	phosphate-selective porin O and P	23.706 up	0.000288	-13.427
Gmet_3106	flagellar hook-length control protein FliK	23.315 up	0.00586	-6.304
Gmet_3100	flagellar motor switch protein FliM	21.723 up	0.000205	-14.78
Gmet_2042	conserved hypothetical protein	21.680 up	0.000247	-14.029
Gmet_2030	periplasmic polysaccharide biosynthesis/export protein	20.876 up	0.00014	-16.389
Gmet_0749	serine protease, subtilase family	20.766 up	0.000631	-10.841
Gmet_0445	flagellin export facilitator protein FliS	20.467 up	0.00253	-7.859
Gmet_0446	hypothetical protein	19.882 up	0.00206	-8.288
Gmet_3103	flagellar hook protein FlgE	18.710 up	0.00663	-6.099
Gmet_0557	cytochrome c, 4 heme-binding sites; omcP	18.539 up	0.00243	-7.935
Gmet_0531	rhodanese homology domain pair protein	18.433 up	0.000684	-10.644
Gmet_3113	flagellar hook-basal body complex protein FliE	18.384 up	0.0000306	-29.381
Gmet_2423	methyl-accepting chemotaxis sensory transducer; mcp018	18.368 up	0.0000311	-27.122
Gmet_0679	cytochrome c, 5 heme-binding sites; omcX	17.969 up	0.00373	-7.06
Gmet_0532	phosphate-selective porin O and P	17.862 up	0.000382	-12.357
Gmet_3092	hypothetical protein	17.526 up	0.00418	-6.882
Gmet_1041	tungstate ABC transporter, periplasmic tungstate-binding protein; tupA	17.518 up	0.000213	-14.541
Gmet_2428	chemotaxis protein CheY-3	17.494 up	0.000179	-15.475
Gmet_3267	chemotaxis protein-glutamate methyltransferase CheR-1	17.323 up	0.000056	-21.498
Gmet_0426	flagellar biogenesis protein FlhA	17.141 up	0.0000832	-19.461
Gmet_0558	cytochrome c, 23-27 heme-binding sites; omcO	17.057 up	0.00225	-8.107
Gmet_3586	conserved hypothetical protein	16.971 up	0.000559	-11.209
Gmet_3096	flagellar biosynthesis protein FliQ	16.693 up	0.000279	-13.552
Gmet_0571	cytochrome c, 26 heme-binding sites	16.506 up	0.00988	-5.472
Gmet_3109	flagellum-specific ATPase FliI	16.218 up	0.000473	-11.736
Gmet_2584	hypothetical protein	15.943 up	0.0152	-4.84
Gmet_1606	BioD and DRTGG domain protein	15.867 up	0.00038	-12.355
Gmet_3476	response regulator receiver modulated metal dependent phosphohydrolase	15.725 up	0.0000904	-18.62

Gmet_0461	chemotaxis MotA protein	15.705 up	0.000531	-11.38
Gmet_2424	methyl-accepting chemotaxis sensory transducer mcp005	15.425 up	0.0000556	-21.615
Gmet_2015	rhodanese homology domain superfamily selenoprotein, putative	15.355 up	0.000384	-12.293
Gmet_0556	NHL repeat domain protein	15.191 up	0.00786	-5.823
Gmet_1039	tungstate ABC transporter, ATP-binding protein; tupC	15.109 up	0.000146	-16.166
Gmet_3323	methyl viologen-reducing hydrogenase maturation protease; mvhP	14.574 up	0.000319	-12.963
Gmet_0748	hypothetical protein	14.418 up	0.000321	-12.903
Gmet_2029	polysaccharide chain length determinant protein, putative	14.281 up	0.0000316	-31.271
Gmet_3091	cytochrome c, 2 heme-binding sites macA	13.924 up	0.0499	-3.383
Gmet_0435	flagellar rod-binding protein FlgJ, putative	13.668 up	0.00294	-7.569
Gmet_3111	flagellar motor switch protein FliG	13.537 up	0.000247	-13.89
Gmet_3119	chemotaxis protein CheY-1	13.501 up	0.0000403	-24.975
Gmet_0716	hypothetical protein	12.919 up	0.000203	-15.088
Gmet_2825	methyl-accepting chemotaxis sensory transducer mcp001	12.457 up	0.0000387	-25.922
Gmet_2032	TPR domain lipoprotein	12.254 up	0.000112	-17.584
Gmet_2429	STAS domain protein	11.949 up	0.0000846	-19.538
Gmet_2028	protein tyrosine kinase, putative	11.823 up	0.0000324	-27.734
Gmet_3268	metal dependent phosphohydrolase	11.401 up	0.000245	-13.949
Gmet_3085	diguanylate cyclase/phosphodiesterase with PAS/PAC sensor(s)	11.265 up	0.000513	-11.539
Gmet_2653	hypothetical protein	11.224 up	0.000108	-17.743
Gmet_3477	sensor histidine kinase response regulator (HAMP, PAS, PAS, PAS, PAS, HATPase_c, REC, PAS)	11.213 up	0.0000423	-23.6
Gmet_1088	lipoprotein cytochrome c, 1 heme-binding site	11.119 up	0.000541	-11.322
Gmet_2723	peroxiredoxin, typical 2-Cys subfamily; prx-1	11.058 up	0.00136	-9.157
Gmet_1090	trehalose-phosphatase; otsB	10.534 up	0.000571	-11.135
Gmet_1040	tungstate ABC transporter, membrane protein; tupB	10.534 up	0.00313	-7.462
Gmet_1707	sensor histidine kinase response regulator (PAS, PAS, PAC, HisKA, HATPase_c, REC)	10.412 up	0.00047	-11.762
Gmet_0463	flagellar protein FlaG protein	10.240 up	0.000041	-25.074
Gmet_3472	response regulator receiver domain-containing protein	10.144 up	0.0000804	-19.778
Gmet_3097	fliP flagellar biosynthesis protein FliP	10.037 up	0.000839	-10.171
Gmet_3110	flagellar assembly protein fliH	9.854 up	0.000515	-11.518
Gmet_1089	Na+/H+ antiporter NhaA	9.843 up	0.000247	-14.055
Gmet_3095	flagellar biosynthesis protein FliR	9.741 up	0.0000332	-27.912
Gmet_3319	methyl viologen-reducing	9.737 up	0.00708	-5.99

	hydrogenase, small subunit, mvhS			
Gmet_2655	hypothetical protein	9.617 up	0.0000535	-22.036
Gmet_2016	aminotransferase, AHBA_syn family	9.415 up	0.0000733	-20.306
Gmet_3114	flagellar basal-body rod protein FlgC	9.232 up	0.00115	-9.527
Gmet_0460	chemotaxis MotB protein	9.221 up	0.0000314	-27.323
Gmet_2027	hypothetical protein	9.172 up	0.000247	-14.114
Gmet_2665	serine protease inhibitor, Kunitz family	8.945 up	0.000378	-12.352
Gmet_2701	phosphate ABC transporter, periplasmic phosphate-binding protein; pstS	8.796 up	0.000105	-17.931
Gmet_0534	cytochrome c, 5 heme-binding sites	8.710 up	0.0013	-9.268
Gmet_1037	pyranopterin monophosphate cyclase moaC	8.591 up	0.00221	-8.139
Gmet_2654	thioredoxin group II protein	8.558 up	0.000918	-9.981
Gmet_2021	acyl carrier protein; acpP-3	8.473 up	0.0000451	-22.884
Gmet_1095	conserved hypothetical protein	8.472 up	0.0172	-4.673
Gmet_0155	cytochrome c, 1 heme-binding site	8.443 up	0.0000727	-20.26
Gmet_2895	hypothetical protein	8.438 up	0.00128	-9.307
Gmet_1038	molybdopterin--molybdenum ligase; moeA-1	8.265 up	0.0086	-5.674
Gmet_0574	lipoprotein, putative	8.162 up	0.000428	-12.013
Gmet_3265	chemotaxis protein CheW-1	8.135 up	0.000378	-12.391
Gmet_2447	hypothetical protein	7.977 up	0.000133	-16.675
Gmet_2734	radical SAM family protein	7.930 up	0.031	-3.933
Gmet_3473	response receiver ATPase (REC, PulE)	7.905 up	0.0000428	-23.807
Gmet_2422	methyl-accepting chemotaxis sensory transducer with Pas/Pac sensor mcp036	7.893 up	0.000207	-14.725
Gmet_2031	glycosyltransferase domain protein	7.893 up	0.0000826	-19.239
Gmet_2425	diguanylate cyclase	7.849 up	0.000615	-10.909
Gmet_0529	methyl-accepting chemotaxis sensory transducer mcp032	7.833 up	0.0000291	-31.099
Gmet_3116	lipoprotein, putative	7.717 up	0.000193	-15.25
Gmet_2985	conserved hypothetical protein	7.680 up	0.00654	-6.128
Gmet_2512	hypothetical protein	7.661 up	0.00061	-10.94
Gmet_1908	cytochrome b1 (bacterioferritin)	7.653 up	0.0106	-5.374
Gmet_3321	methyl viologen-reducing hydrogenase-associated ferredoxin mvhF	7.645 up	0.00369	-7.099
Gmet_2656	hypothetical protein	7.587 up	0.000301	-13.127
Gmet_0573	ResC/HemX-like cytochrome c biogenesis membrane protein	7.578 up	0.0000915	-18.739
Gmet_1036	molybdopterin adenylyltransferase MoaB, putative	7.558 up	0.000626	-10.863
Gmet_1607	chemotaxis protein CheY-4	7.552 up	0.00467	-6.678
Gmet_2834	ron-sulfur-oxygen hybrid cluster protein (prismane); hcp	7.513 up	0.00336	-7.295
Gmet_2020	AMP-forming acyl-CoA synthetase	7.435 up	0.0000848	-19.465

Gmet_0169	nodulin 21-like transmembrane protein	7.303 up	0.000642	-10.79
Gmet_0462	flagellar protein FlbD	7.236 up	0.00961	-5.516
Gmet_2420	chemotaxis protein-glutamate methyltransferase CheR-2	7.152 up	0.0247	-4.213
Gmet_3320	methyl viologen-reducing hydrogenase, large subunit; mvhL	7.132 up	0.00161	-8.814
Gmet_0775	OmpA domain porin (beta-barrel, OmpA, OmpA)	7.076 up	0.0193	-4.531
Gmet_0158	hypothetical protein	7.052 up	0.000208	-14.646
Gmet_0705	membrane protein, putative	7.021 up	0.0125	-5.123
Gmet_0436	negative regulator of flagellin synthesis FlgM	6.968 up	0.0144	-4.925
Gmet_1618	protein of unknown function DUF327	6.964 up	0.00326	-7.364
Gmet_0704	conserved hypothetical protein	6.957 up	0.0465	-3.466
Gmet_0572	ResB-like family cytochrome c biogenesis protein	6.895 up	0.000111	-17.548
Gmet_2658	PDZ/DHR/GLGF:ankyrin	6.894 up	0.000298	-13.208
Gmet_3120	hypothetical protein	6.885 up	0.000117	-17.132
Gmet_2652	PDZ domain thioredoxin group II protein	6.832 up	0.0000584	-21.262
Gmet_0156	protein of unknown function DUF488	6.822 up	0.000199	-15.08
Gmet_2427	chemotaxis sensor histidine kinase CheA-1	6.790 up	0.00666	-6.092
Gmet_2470	cytochrome c, 27 heme-binding sites	6.767 up	0.000572	-11.104
Gmet_3646	conserved hypothetical protein	6.720 up	0.0000315	-28.844
Gmet_0244	hypothetical protein	6.660 up	0.0328	-3.864
Gmet_2024	asparagine synthetase;asnB-2	6.655 up	0.000469	-11.774
Gmet_2017	FemAB superfamily protein	6.631 up	0.00103	-9.745
Gmet_0241	lipoprotein, putative	6.571 up	0.0193	-4.533
Gmet_0168	NADH dehydrogenase I, L subunit; nuoL-2	6.539 up	0.00176	-8.61
Gmet_2409	ntracellular protease, PfpI family, putative	6.449 up	0.00143	-9.072
Gmet_2659	hypothetical protein	6.340 up	0.0000907	-18.715
Gmet_3475	GTPase, putative	6.275 up	0.000488	-11.647
Gmet_1092	polyphosphate-dependent ADP kinase	6.271 up	0.0139	-4.967
Gmet_2583	multicopper oxidase, putative	6.257 up	0.000638	-10.809
Gmet_0849	sensor cyclic diguanylate phosphodiesterase (HAMP, GAF, HD-GYP), putative heme-binding site	6.255 up	0.000316	-13.002
Gmet_1015	hypothetical protein	6.215 up	0.0468	-3.457
Gmet_2014	glycosyltransferase, family 2	6.127 up	0.000167	-15.707
Gmet_0565	hypothetical protein	6.063 up	0.000202	-14.858
Gmet_2025	Formyl transferase-like	6.029 up	0.0000415	-24.678
Gmet_2660	hypothetical protein	6.018 up	0.00044	-11.929
Gmet_1811	4Fe-4S ferredoxin, iron-sulfur binding protein	5.900 up	0.00369	-7.101
Gmet_3117	response regulator receiver	5.878 up	0.00939	-5.559

	domain-containing protein			
Gmet_0153	NADH dehydrogenase I, B/C/D subunits; nuoBCD	5.827 up	0.000115	-17.222
Gmet_3621	hypothetical protein	5.789 up	0.000329	-12.789
Gmet_2469	fibronectin type III-like repeat protein	5.783 up	0.00313	-7.458
Gmet_1812	polysulphide reductase, NrfD	5.709 up	0.000572	-11.122
Gmet_3546	pentapeptide repeat-containing protein	5.662 up	0.00106	-9.673
Gmet_3618	hypothetical protein	5.656 up	0.0036	-7.147
Gmet_0167	NADH dehydrogenase I, K subunit lipoprotein; nuok-2	5.648 up	0.00739	-5.91
Gmet_1833	integration host factor, beta subunit; ihfB-1	5.609 up	0.000208	-14.668
Gmet_1868	cytochrome c, 4 heme-binding sites	5.566 up	0.00159	-8.847
Gmet_2018	FemAB superfamily protein	5.556 up	0.000285	-13.411
Gmet_1813	hypothetical protein	5.529 up	0.000585	-11.029
Gmet_2448	major royal jelly-related protein	5.437 up	0.0165	-4.734
Gmet_3318	hypothetical protein; mvhR	5.435 up	0.00219	-8.162
Gmet_2622	conserved hypothetical protein	5.427 up	0.0323	-3.887
Gmet_0171	NADH dehydrogenase I, M subunit; nuoM-2	5.392 up	0.0000337	-29.812
Gmet_0717	hypothetical protein	5.370 up	0.0123	-5.155
Gmet_2033	conserved hypothetical protein	5.297 up	0.0144	-4.916
Gmet_3094	flagellar biogenesis protein FlhB	5.289 up	0.000825	-10.217
Gmet_3495	serine phosphatase, SpoIIE domain-containing	5.182 up	0.0367	-3.729
Gmet_1083	sensor histidine kinase (PAS, PAS, PAC, HisKA, HATPase_c)	5.173 up	0.000945	-9.908
Gmet_2026	type II secretion system ATPase ExeA	5.165 up	0.000289	-13.348
Gmet_0456	hypothetical protein	5.104 up	0.0242	-4.236
Gmet_2465	major facilitator transporter	5.099 up	0.000123	-16.963
Gmet_1706	response regulator receiver modulated diguanylate cyclase	5.096 up	0.0373	-3.709
Gmet_1022	respiratory nitrate reductase, gamma subunit; narI-2	5.080 up	0.00346	-7.241
Gmet_1851	pentapeptide repeat-containing protein	5.054 up	0.0007	-10.592
Gmet_1866	cytochrome c, 3-4 heme-binding sites	5.037 up	0.00795	-5.801
Gmet_2594	fatty acyltransferase-like lipase, putative	5.028 up	0.0115	-5.247
Gmet_3388	hypothetical protein	5.004 up	0.0000834	-19.267
Gmet_2498	heat shock protein Hsp90; htpG	4.994 up	0.00032	-12.895
Gmet_2446	dioxygenase, putative	4.988 up	0.00628	-6.19
Gmet_0170	cytochrome c, 8 heme-binding sites	4.950 up	0.0000406	-24.163
Gmet_3514	lipoprotein, putative	4.945 up	0.00174	-8.634
Gmet_0455	sialic acid synthase; neuB	4.930 up	0.00601	-6.264
Gmet_2661	ankyrin repeat protein	4.887 up	0.00128	-9.304
Gmet_0160	pyridoxamine 5'-phosphate oxidase-related FMN-binding	4.869 up	0.000371	-12.457

	protein			
Gmet_3322	conserved hypothetical protein; mvhU	4.848 up	0.0236	-4.272
Gmet_3324	HAMP domain-containing methyl-accepting chemotaxis sensory transducer; mvhV	4.848 up	0.0326	-3.876
Gmet_1928	ferritin-like domain protein	4.822 up	0.00367	-7.114
Gmet_1245	TonB-dependent receptor, putative	4.813 up	0.000031	-27.659
Gmet_2945	TPR domain protein	4.808 up	0.0336	-3.833
Gmet_2003	exopolysaccharide synthesis multitransmembrane protein H (exosortase), epsH	4.776 up	0.00649	-6.145
Gmet_0566	radical SAM domain iron-sulfur cluster-binding oxidoreductase	4.770 up	0.000926	-9.959
Gmet_1967	membrane protein, putative	4.768 up	0.00833	-5.721
Gmet_0568	ABC transporter, periplasmic substrate-binding lipoprotein	4.761 up	0.0023	-8.038
Gmet_0154	NADH dehydrogenase I, E subunit; nuoE-2	4.743 up	0.00832	-5.721
Gmet_2748	sensor histidine kinase (GAF, HisKA, HATPase_c)	4.738 up	0.00009	-18.685
Gmet_1966	lipoprotein, putative	4.719 up	0.00328	-7.347
Gmet_2023	polysaccharide deacetylase domain protein	4.704 up	0.000149	-16.083
Gmet_0907	conserved hypothetical protein	4.704 up	0.0217	-4.384
Gmet_1680	conserved hypothetical protein	4.694 up	0.00299	-7.543
Gmet_2666	hypothetical protein	4.681 up	0.00321	-7.411
Gmet_0157	NADH dehydrogenase I, F subunit, nuoF-2	4.670 up	0.00895	-5.625
Gmet_1831	conserved hypothetical protein	4.663 up	0.014	-4.974
Gmet_0967	type IV pilus tip-associated adhesin, pilY1-2	4.637 up	0.0000394	-25.638
Gmet_3121	hemerythrin family protein	4.607 up	0.000358	-12.576
Gmet_3187	DNA polymerase II, putative	4.592 up	0.00294	-7.572
Gmet_0789	aldehyde dehydrogenase family 11 protein	4.577 up	0.00797	-5.792
Gmet_1469	AMP-forming acyl-CoA synthetase	4.563 up	0.00327	-7.369
Gmet_0564	conserved hypothetical protein	4.519 up	0.00363	-7.13
Gmet_1702	deoxyguanosine triphosphate triphosphohydrolase, putative	4.461 up	0.0228	-4.313
Gmet_3269	chemotaxis protein-glutamate methylesterase CheB	4.439 up	0.000526	-11.421
Gmet_0561	lipoprotein, putative	4.425 up	0.00014	-16.343
Gmet_0793	conserved hypothetical protein	4.397 up	0.000113	-17.39
Gmet_3108	flagellar export protein FliJ	4.391 up	0.00485	-6.612
Gmet_2896	cytochrome c, 4 heme-binding sites	4.361 up	0.00963	-5.512
Gmet_2664	radical SAM domain iron-sulfur cluster-binding oxidoreductase, putative	4.306 up	0.00211	-8.237
Gmet_0152	NADH dehydrogenase I, A subunit; nuoA-2	4.254 up	0.0109	-5.333
Gmet_2618	6-phosphogluconolactonase; pgl	4.251 up	0.0225	-4.333

Gmet_0033	ATPase, AAA family	4.249 up	0.000245	-13.876
Gmet_0580	lipoprotein cytochrome c, 14 heme-binding sites	4.248 up	0.0071	-5.985
Gmet_1968	conserved hypothetical protein	4.231 up	0.0449	-3.503
Gmet_2703	phosphate ABC transporter, membrane protein PstA	4.213 up	0.000398	-12.2
Gmet_1470	conserved hypothetical protein	4.207 up	0.0000326	-29.493
Gmet_0029	chaperonin GroEL	4.204 up	0.00199	-8.353
Gmet_1082	sigma-54-dependent transcriptional response regulator (REC, sigma54 interaction, HTH8)	4.193 up	0.0037	-7.078
Gmet_0030	serine protein kinase, putative; prkA	4.121 up	0.00564	-6.359
Gmet_0560	conserved hypothetical protein	4.110 up	0.00534	-6.46
Gmet_1091	conserved hypothetical protein	4.071 up	0.036	-3.754
Gmet_2608	conserved hypothetical protein	4.062 up	0.00249	-7.881
Gmet_1867	cytochrome c, 7-8 heme-binding sites	4.053 up	0.0177	-4.63
Gmet_1468	alpha/beta hydrolase superfamily protein	4.052 up	0.000746	-10.432
Gmet_0889	LysM domain protein	4.050 up	0.000321	-12.915
Gmet_1923	cytochrome b/b6 complex, cytochrome b subunit	3.969 up	0.00214	-8.214
Gmet_1395	type IV pilus biogenesis protein PilC	3.962 up	0.0245	-4.224
Gmet_2702	phosphate ABC transporter, membrane protein PstC	3.946 up	0.0121	-5.18
Gmet_0457	aminotransferase, AHBA_syn family	3.928 up	0.00708	-5.993
Gmet_0821	methyl-accepting chemotaxis sensory transducer, mcp013	3.900 up	0.0125	-5.114
Gmet_0145	protein of unknown function DUF167	3.897 up	0.00417	-6.886
Gmet_2720	zinc protease TldD, putative modulator of DNA gyrase	3.895 up	0.00451	-6.741
Gmet_0166	lipoprotein, putative	3.888 up	0.00735	-5.919
Gmet_2006	selenocysteine lyase; sufS	3.883 up	0.00236	-7.987
Gmet_2002	conserved hypothetical protein	3.882 up	0.00498	-6.574
Gmet_3474	sensor histidine kinase (HATPase_c)	3.881 up	0.00604	-6.253
Gmet_2426	sensor histidine kinase response regulator (HAMP, HisKA, HATPase_c, REC), putative heme-binding site	3.853 up	0.00353	-7.194
Gmet_0299	HPP family protein	3.815 up	0.0249	-4.204
Gmet_2013	polysaccharide deacetylase, putative	3.812 up	0.000204	-14.862
Gmet_1552	ABC transporter, ATP-binding protein	3.812 up	0.00255	-7.833
Gmet_2419	chemotaxis protein-glutamine deamidase and protein-glutamate methylesterase CheD	3.776 up	0.00707	-5.985
Gmet_3210	chemotaxis protein phosphatase CheC	3.772 up	0.00724	-5.944

Gmet_1832	OmpA family outer membrane protein	3.728 up	0.0000503	-22.364
Gmet_1734	conserved hypothetical protein	3.722 up	0.0162	-4.754
Gmet_2044	hypothetical protein	3.680 up	0.0126	-5.104
Gmet_1998	porin lipoprotein, putative	3.671 up	0.000112	-17.55
Gmet_0159	NADH dehydrogenase I, G subunit,nuoG-2	3.656 up	0.00373	-7.063
Gmet_0454	sugar cytidylyltransferase and glycosyltransferase domain protein	3.644 up	0.0418	-3.592
Gmet_2019	ornithine/diaminopimelate/arginine decarboxylase 2	3.630 up	0.0165	-4.731
Gmet_0974	type IV pilus assembly lipoprotein PilP, putative; pilP	3.613 up	0.0173	-4.664
Gmet_0172	NADH dehydrogenase I, N subunit lipoprotein; nuoN-2	3.607 up	0.00161	-8.778
Gmet_3362	periplasmic trypsin-like serine protease lipoprotein	3.607 up	0.0294	-3.991
Gmet_0142	cytochrome c, 8 heme-binding sites	3.603 up	0.00515	-6.524
Gmet_2827	chemotaxis protein CheY-8	3.600 up	0.0016	-8.813
Gmet_0559	conserved hypothetical protein	3.599 up	0.0109	-5.328
Gmet_2431	chemotaxis protein CheY-2	3.569 up	0.00347	-7.231
Gmet_0563	membrane protein	3.568 up	0.00218	-8.183
Gmet_2022	hypothetical protein	3.561 up	0.0000471	-22.936
Gmet_3149	conserved hypothetical protein	3.549 up	0.000898	-10.036
Gmet_3147	protein of unknown function DUF1458	3.548 up	0.00801	-5.773
Gmet_2505	peptidoglycan L,D-transpeptidase, YkuD family	3.530 up	0.00287	-7.617
Gmet_0032	SpoVR-like family protein	3.522 up	0.00605	-6.245
Gmet_0031	conserved hypothetical protein	3.501 up	0.0179	-4.616
Gmet_0834	hemerythrin family protein	3.462 up	0.000517	-11.467
Gmet_1997	hypothetical protein	3.455 up	0.000428	-11.998
Gmet_2721	sensor diguanylate cyclase (GAF, GGDEF)	3.452 up	0.00302	-7.526
Gmet_1617	lipoprotein, putative	3.446 up	0.0144	-4.922
Gmet_1924	cytochrome c, 5 heme-binding sites	3.441 up	0.0000727	-20.413
Gmet_2004	glycosyltransferase	3.435 up	0.00144	-9.035
Gmet_2617	barnase inhibitor barstar	3.412 up	0.0228	-4.314
Gmet_2639	response receiver sensor histidine kinase (REC, HisKA, HATPase_c)	3.394 up	0.00371	-7.081
Gmet_3107	conserved hypothetical protein	3.386 up	0.0218	-4.381
Gmet_2435	potassium-transporting ATPase, C subunit;kdpC	3.386 up	0.0143	-4.934
Gmet_3400	twitching motility pilus retraction protein; pilT-3	3.368 up	0.0148	-4.875
Gmet_1970	membrane protein, putative	3.358 up	0.00725	-5.945
Gmet_0146	conserved hypothetical protein	3.352 up	0.000546	-11.272
Gmet_0695	ammonium transporter; amtB	3.339 up	0.00935	-5.57
Gmet_0183	peroxiredoxin, atypical 2-Cys subfamily	3.301 up	0.0000857	-19.061
Gmet_2811	sensor histidine kinase (Cache, HAMP, PAS, PAC, HisKA,	3.299 up	0.000247	-14.013

	HATPase_c)			
Gmet_0356	conserved hypothetical protein	3.294 up	0.000248	-14.062
Gmet_1189	magnesium transport protein CorA-1	3.272 up	0.0016	-8.813
Gmet_1999	lipoprotein, putative	3.267 up	0.000548	-11.286
Gmet_1996	lipoprotein, putative	3.266 up	0.00452	-6.742
Gmet_0911	conserved hypothetical protein	3.249 up	0.0237	-4.265
Gmet_0987	sensor diguanylate cyclase/phosphodiesterase (PAS, GGDEF, EAL)	3.245 up	0.0000295	-28.801
Gmet_2768	glucose-1-phosphate adenylyltransferase	3.238 up	0.0036	-7.153
Gmet_2894	conserved hypothetical protein	3.229 up	0.00333	-7.32
Gmet_0975	type IV pilus secretin lipoprotein PilQ	3.212 up	0.0213	-4.407
Gmet_0712	methyl-accepting chemotaxis sensory transducer, mcp011	3.206 up	0.0000459	-22.931
Gmet_3617	conserved hypothetical protein	3.189 up	0.000348	-12.65
Gmet_2410	superoxide dismutase, iron/manganese-containing, sodA	3.186 up	0.0108	-5.349
Gmet_0968	hypothetical protein	3.185 up	0.00057	-11.12
Gmet_3317	chemotaxis protein CheW-8 (MvhQ)	3.158 up	0.0354	-3.773
Gmet_0272	lipoprotein, putative	3.153 up	0.0467	-3.461
Gmet_2642	sensor histidine kinase response receiver domain protein (GAF, HATPase_c, REC, REC, REC)	3.134 up	0.00226	-8.071
Gmet_2418	response receiver chemotaxis protein-glutamate methylesterase CheB-2	3.129 up	0.00876	-5.65
Gmet_0913	cytochrome c, 9 heme-binding sites	3.120 up	0.00341	-7.261
Gmet_0355	histone-like protein; hup-1	3.115 up	0.00685	-6.048
Gmet_0452	hypothetical protein	3.106 up	0.0443	-3.523
Gmet_2007	coenzyme F390 synthetase superfamily protein	3.033 up	0.000722	-10.518
Gmet_1558	cysteine synthase A; cysK-2	3.032 up	0.0426	-3.569
Gmet_2468	conserved hypothetical protein	3.019 up	0.0128	-5.082
Gmet_2704	phosphate ABC transporter ATP-binding protein	2.992 up	0.011	-5.306
Gmet_2008	glycosyl transferase family protein	2.985 up	0.0276	-4.068
Gmet_2430	methyl-accepting chemotaxis sensory transducer	2.971 up	0.00134	-9.203
Gmet_2719	hypothetical protein	2.955 up	0.0257	-4.161
Gmet_0581	high-molecular-weight cytochrome c	2.940 up	0.000282	-13.487
Gmet_1005	multi-sensor signal transduction histidine kinase	2.918 up	0.0438	-3.535
Gmet_1384	cytochrome c biogenesis protein, transmembrane region	2.913 up	0.012	-5.189
Gmet_0912	cytochrome c family protein	2.908 up	0.0136	-5.007
Gmet_1733	O-methyltransferase family protein	2.889 up	0.0125	-5.134
Gmet_2061	Na+/solute symporter	2.888 up	0.027	-4.102
Gmet_1965	fibronectin, type III	2.887 up	0.0278	-4.06

Gmet_0725	hypothetical protein	2.864 up	0.00361	-7.142
Gmet_1922	Rieske (2Fe-2S) region	2.853 up	0.00794	-5.808
Gmet_1553	hypothetical protein	2.850 up	0.00938	-5.558
Gmet_1919	response regulator receiver (CheY-like) modulated metal dependent phosphohydrolase	2.844 up	0.00966	-5.502
Gmet_0425	hypothetical protein	2.843 up	0.000247	-13.956
Gmet_0035	metal dependent phosphohydrolase	2.820 up	0.000201	-15.082
Gmet_1963	signal peptide protein	2.793 up	0.00439	-6.785
Gmet_1079	CheW protein	2.775 up	0.0206	-4.449
Gmet_0034	metallophosphoesterase	2.767 up	0.000166	-15.699
Gmet_1559	peptidase M23B	2.737 up	0.0138	-4.992
Gmet_0833	Alpha amylase, catalytic region	2.733 up	0.00602	-6.265
Gmet_1918	PAS/PAC sensor hybrid histidine kinase	2.710 up	0.0444	-3.513
Gmet_3275	metal dependent phosphohydrolase	2.709 up	0.0169	-4.698
Gmet_1188	peptidoglycan binding domain-containing protein	2.694 up	0.0199	-4.495
Gmet_2641	MCP methyltransferase, CheR-type	2.690 up	0.000299	-13.183
Gmet_1371	hypothetical protein	2.666 up	0.00468	-6.68
Gmet_2826	CheB methylesterase	2.633 up	0.0187	-4.567
Gmet_3478	PAS/PAC sensor signal transduction histidine kinase	2.606 up	0.000041	-24.406
Gmet_1155	integral membrane protein TerC	2.604 up	0.0104	-5.417
Gmet_1551	response regulator receiver domain-containing protein	2.589 up	0.0428	-3.562
Gmet_2158	two component LuxR family transcriptional regulator	2.570 up	0.0157	-4.795
Gmet_1220	response regulator receiver domain-containing protein	2.569 up	0.00336	-7.297
Gmet_2938	methyl-accepting chemotaxis sensory transducer	2.560 up	0.000301	-13.141
Gmet_1373	hypothetical protein	2.555 up	0.00199	-8.357
Gmet_2440	cobalt ABC transporter CbiQ, permease subunit	2.548 up	0.00192	-8.462
Gmet_0298	PAS/PAC sensor protein	2.541 up	0.0216	-4.392
Gmet_1190	Outer membrane efflux protein	2.539 up	0.0272	-4.086
Gmet_0458	polysaccharide biosynthesis protein CapD	2.536 up	0.00312	-7.469
Gmet_3122	rhodanese-like protein	2.519 up	0.0107	-5.362
Gmet_2939	diguanylate cyclase/phosphodiesterase	2.507 up	0.0166	-4.723
Gmet_2157	two component AraC family transcriptional regulator	2.504 up	0.0327	-3.872
Gmet_1946	glyceraldehyde-3-phosphate dehydrogenase	2.497 up	0.00512	-6.533
Gmet_0583	spermine synthase	2.495 up	0.0311	-3.928
Gmet_1969	glycosyl transferase, group 1	2.483 up	0.0263	-4.137
Gmet_2011	hypothetical protein	2.483 up	0.00547	-6.412
Gmet_0598	PKD	2.482 up	0.0467	-3.46
Gmet_0825	cytochrome c family protein	2.482 up	0.00965	-5.507
Gmet_0835	hypothetical protein	2.473 up	0.049	-3.404
Gmet_1078	methyl-accepting chemotaxis	2.467 up	0.0113	-5.275

	sensory transducer			
Gmet_0736	hypothetical protein	2.452 up	0.0175	-4.644
Gmet_0930	cytochrome c family protein	2.450 up	0.00389	-6.994
Gmet_3455	PAS/PAC sensor signal transduction histidine kinase	2.433 up	0.00272	-7.72
Gmet_3152	glycine dehydrogenase subunit 2	2.430 up	0.0295	-3.985
Gmet_1230	serine phosphatase	2.430 up	0.00241	-7.956
Gmet_1153	hypothetical protein	2.427 up	0.00709	-5.985
Gmet_1429	Outer membrane lipoprotein Slp	2.422 up	0.0394	-3.654
Gmet_0533	hypothetical protein	2.417 up	0.0392	-3.661
Gmet_0342	thrombospondin type 3 repeat-containing OmpA/MotB protein	2.404 up	0.0328	-3.863
Gmet_0666	PAS/PAC sensor signal transduction histidine kinase	2.355 up	0.00535	-6.452
Gmet_0966	hypothetical protein	2.348 up	0.00349	-7.213
Gmet_0567	hypothetical protein	2.333 up	0.0295	-3.987
Gmet_1655	CoA-binding protein	2.325 up	0.0104	-5.413
Gmet_2506	rhomboid-like protein	2.320 up	0.000823	-10.215
Gmet_3504	cobalamin B12-binding/radical SAM family protein	2.314 up	0.00695	-6.026
Gmet_2010	glycosyl transferase family protein	2.312 up	0.0374	-3.708
Gmet_3310	lipoprotein	2.307 up	0.0121	-5.175
Gmet_2437	two component transcriptional regulato	2.305 up	0.014	-4.957
Gmet_1025	hypothetical protein	2.304 up	0.0319	-3.901
Gmet_0960	histidine kinase	2.295 up	0.00193	-8.43
Gmet_2009	O-antigen polymerase	2.295 up	0.0196	-4.514
Gmet_1218	PAS/PAC sensor signal transduction histidine kinas	2.283 up	0.000043	-23.664
Gmet_1909	pyridoxamine 5'-phosphate oxidase-related, FMN-binding	2.270 up	0.0418	-3.594
Gmet_0451	glucuronate isomerase	2.251 up	0.0406	-3.626
Gmet_0162	ankyrin	2.249 up	0.0196	-4.51
Gmet_1243	histidine kinase	2.241 up	0.00691	-6.034
Gmet_2001	glycosyl transferase, group 1	2.234 up	0.00562	-6.372
Gmet_1654	HhH-GPD	2.221 up	0.0037	-7.081
Gmet_0028	groES co-chaperonin GroES	2.210 up	0.00329	-7.348
Gmet_2760	dehydrogenase, E1 component	2.191 up	0.000984	-9.831
Gmet_2078	hypothetical protein	2.184 up	0.0427	-3.565
Gmet_2436	smosensitive K+ channel	2.182 up	0.0208	-4.435
Gmet_2156	hypothetical protein	2.178 up	0.00207	-8.274
Gmet_2897	NHL repeat-containing protein	2.173 up	0.0125	-5.118
Gmet_0972	fimbrial assembly	2.170 up	0.0266	-4.115
Gmet_3483	pseudo	2.167 up	0.0275	-4.074
Gmet_0815	PpiC-type peptidyl-prolyl cis-trans isomerase	2.166 up	0.0477	-3.432
Gmet_1023	pseudo	2.158 up	0.00329	-7.341
Gmet_1544	hypothetical protein	2.155 up	0.00796	-5.798
Gmet_1447	chromosome partitioning ATPase	2.155 up	0.000478	-11.701
Gmet_0173	hypothetical protein	2.153 up	0.0128	-5.082
Gmet_2305	MCP methyltransferase, CheR-typ	2.148 up	0.0257	-4.165
Gmet_2824	multi-sensor hybrid histidine kinase	2.132 up	0.00673	-6.071
Gmet_0151	pseudo	2.122 up	0.00604	-6.256

Gmet_0969	hypothetical protein	2.118 up	0.000615	-10.917
Gmet_0424	hypothetical protein	2.106 up	0.00156	-8.897
Gmet_1404	hypothetical protein	2.097 up	0.0239	-4.255
Gmet_2582	excinuclease ATPase subunit-like	2.093 up	0.0059	-6.293
Gmet_2663	hypothetical protein	2.090 up	0.0457	-3.485
Gmet_1543	YHS	2.077 up	0.0228	-4.31
Gmet_0138	hypothetical protein	2.073 up	0.0433	-3.549
Gmet_1614	cation transporter E1-E2 family ATPase	2.073 up	0.000134	-16.69
Gmet_2390	O-acetylhomoserine/O-acetylserine sulfhydrylase	2.068 up	0.0139	-4.978
Gmet_1545	hypothetical protein	2.064 up	0.00653	-6.128
Gmet_3213	thiamine-monophosphate kinase	2.057 up	0.002	-8.357
Gmet_3170	4Fe-4S ferredoxin, iron-sulfur binding protein	2.057 up	0.0437	-3.536
Gmet_2651	metallophosphoesterase	2.040 up	0.0201	-4.475
Gmet_1608	histone-like DNA-binding protein	2.017 up	0.00904	-5.612
Gmet_3031	Na+/solute symporter	2.012 up	0.0281	-4.048
Gmet_0959	type 4 prepilin peptidas	2.011 up	0.0273	-4.081

Table A2. Bacterial strains and plasmids used in this study

Strain or plasmid	Relevant characteristic(s)	Source or reference
Strains		
E. coli		
TOP10	*recA1 endA1 gyrA96 thi-1 hsdR17* (r_K^- m_K^+) *supE44 relA1 ΔlacU169*	Invitrogen, Carlsbad, CA
G. metallireducens		
GS-15 (ATCC 53774)	Wild type	(Lovley *et al*., 1993b)
2896	*ΔGmet 2896::Sp*^{r}	This work
0558	*ΔGmet 0558::Sp*^{r}	This work
0557	*ΔGmet 0557::Sp*^{r}	This work
1868	*ΔGmet 1868::Sp*^{r}	This work
1867	*ΔGmet 1867::Sp*^{r}	This work
0930	*ΔGmet 0930::Sp*^{r}	This work
0679	*ΔGmet 0679::Sp*^{r}	This work
0825	*ΔGmet 0825::Sp*^{r}	This work
2839	*ΔGmet 2839::Sp*^{r}	This work
0912	*ΔGmet 0912::Sp*^{r}	This work
0913	*ΔGmet 0913::Sp*^{r}	This work
0910	*ΔGmet 0910::Sp*^{r}	This work
0571	*ΔGmet 0571::Sp*^{r}	This work
0580	*ΔGmet 0580::Sp*^{r}	This work
2470	*ΔGmet 2470::Sp*^{r}	This work
0534	*ΔGmet 0534::Sp*^{r}	This work
0581	*ΔGmet 0581::Sp*^{r}	This work
1866	*ΔGmet 1866::Sp*^{r}	This work
0907	*ΔGmet 0907::Sp*^{r}	This work
0911	*ΔGmet 0911::Sp*^{r}	This work
0908	*ΔGmet 0908::Sp*^{r}	This work
0556	*ΔGmet 0556::Sp*^{r}	This work
Plasmids		
pCR2.1-TOPO	PCR cloning vector; Ap^r, Km^r	Invitrogen, Carlsbad, CA
pUC19-*Sp*^{r}*loxP*	pUC19 carrying *Sp*^{r}*loxP*; Ap^r, Sp^r	(Tremblay *et al*., 2012)
pCM66	Broad-host-range expression vector; Km^r	(Marx and Lidstrom, 2001)
pJS1	pCM66 carrying Gmet 2896	This work
pJS2	pCM66 carrying Gmet 0558	This work
pJS3	pCM66 carrying Gmet 0557	This work
pJS4	pCM66 carrying Gmet 1867	This work
pJS5	pCM66 carrying Gmet 1868	This work
pJS6	pCM66 carrying Gmet 0930	This work
pJS7	pCM66 carrying Gmet 0556	This work

TABLE A3. Primers used for mutant construction, complementation, and qRT-PCR

Primer name	Purpose	Sequence (5' to 3')	Source or reference
JsSpF	*Sp^r* cassette		This work
JsSpR	*Sp^r* cassette		This work
Gm2896comF	*2896* into pJS1	CAGGGATCCAACGAGGAGGAAGGAACAATG[b]	This work
Gm2896comR	*2896* into pJS1	TGCGGTACCCCATCGGCTCGTCACAACCTAC[c]	This work
Gmet2896up	*Δ2896::Sp^r*	CGGCCCTCCACCACGTTACTCTGG	This work
Gmet2896AvrIIup	*Δ2896::Sp^r*	CAGCCTAGGCATTGTTCCTTCCTCCTCGTTA[a]	This work
Gmet2896AvrIIdn	*Δ2896::Sp^r*	GTACCTAGGTCCACCATGGCGGGGAGCGC[a]	This work
Gmet2896dn	*Δ2896::Sp^r*	GGATCTTGCCGGCGCTCGTCG	This work
Gm0558comF	*0558* into pJS2	TATTCTAGATTGCTCAGGAGCTCGCCATGT[d]	This work
Gm0558comR	*0558* into pJS2	GCAGGATCCCCCTCCCCTCTTGATCGCT[b]	This work
Gmet0558up	*Δ0558::Sp^r*	GCCGGAATTGATGCTGGCGGTG	This work
Gmet0558AvrIIup	*Δ0558::Sp^r*	CAGCCTAGGCATGGCGAGCTCCTGAGCAAG[a]	This work
Gmet0558AvrIIdn	*Δ0558::Sp^r*	GTACCTAGGCTGCCACTTCCAGCCGACACCAC[a]	This work
Gmet0558dn	*Δ0558::Sp^r*	TCAGGGTGCCTCGCACGGTTA	This work
Gm0557comF	*0557* into pJS3	TATGCATGCACACGCAACGAGGTTTTCAAGATG[e]	This work
Gm0557comR	*0557* into pJS3	GCATCTAGAGCAAGGCAGACACGTCCTA[d]	This work
Gmet0557up	*Δ0557::Sp^r*	CGGCCCTTACGCTTGACCCGG	This work
Gmet0557AvrIIup	*Δ0557::Sp^r*	CAGCCTAGGCATCTTGAAAACCTCGTTGCGTG[a]	This work
Gmet0557AvrIIdn	*Δ0557::Sp^r*	GTACCTAGGTAATACCGGCAGCGCCATGTG[a]	This work
Gmet0557dn	*Δ0557::Sp^r*	CCAGGGTATGGTCAGTGGTGCTG	This work
Gm1867comF	*1867* into pJS4	GCGGCATGCAATAATCCATGAGTAAGCAACAATG[e]	This work
Gm1867comR	*1867* into pJS4	TATTCTAGAGGCACCTCTGTGGGTCTA[d]	This work
Gmet1867up	*Δ1867::Sp^r*	ACGATACCACCCAGACCTTCG	This work
Gmet1867AvrIIup	*Δ1867::Sp^r*	CAGCCTAGGCATTGTTGCTTACTCATGGAT[a]	This work
Gmet1867AvrIIdn	*Δ1867::Sp^r*	GTACCTAGGCTTTCCTGTCATGGTGTCG[a]	This work
Gmet1867dn	*Δ1867::Sp^r*	ACATTCCGTGGCATCAACTATTGCA	This work
Gm1868comF	*1868* into pJS5	TATGCATGCCCTGAGGCAAGGCACGCCATG[e]	This work
Gm1868comR	*1868* into pJS5	GCGTCTAGAATCGCCATTGTTGCTTACTCATG[d]	This work
Gmet1868up	*Δ1868::Sp^r*	GGTGATGTTTATGTGGTTGATGTG	This work
Gmet1868AvrIIup	*Δ1868::Sp^r*	CAGCCTAGGAAAAGGTTGTCTGTTTTAACC[a]	This work
Gmet1868AvrIIdn	*Δ1868::Sp^r*	GTACCTAGGGACTCGGTGTGCACTAACTGTCA[a]	This work
Gmet1868dn	*Δ1868::Sp^r*	GTTCATATTCCTTGTTTACGGACG	This work
Gmet0930comF	*0930* into pJS6	TATTCTAGACGAAAGGAGCAGAAAGG	This work

		GATG[d]	
Gmet0930comR	*0930* into pJS6	GCA<u>GGATCC</u>CCTATCCCGGAACATCAAAAATTA[b]	This work
Gmet0930up	*Δ0930::Sp^r*	GGTGGCTTAACGAGTGTTGCGTGG	This work
Gmet0930AvrIIup	*Δ0930::Sp^r*	CAG<u>CCTAGG</u>CATCCCTTTCTGCTCCTTTC[a]	This work
Gmet0930AvrIIdn	*Δ0930::Sp^r*	GTA<u>CCTAGG</u>TCGTTACCGGCGCAGGCA[a]	This work
Gmet0930dn	*Δ0930::Sp^r*	GGGAGGCGGCAACATTGGAGCCG	This work
Gm0556comF	*0556* into pJS7	TAT<u>GCATGC</u>GAATGCGGAGGCATTACCATG[e]	This work
Gm0556comR	*0556* into pJS7	GCA<u>TCTAGA</u>TCCACCCCGAGGGGTTCTA[d]	This work
Gmet0556up	*Δ0556::Sp^r*	CGTGGGGCTCACCACCTTCAAGC	This work
Gmet0556AvrIIup	*Δ0556::Sp^r*	CAG<u>CCTAGG</u>CATGGTAATGCCTCCGCATTC[a]	This work
Gmet0556AvrIIdn	*Δ0556::Sp^r*	GTA<u>CCTAGG</u>GGACGCAATACTGATCATGAG[a]	This work
Gmet0556dn	*Δ0556::Sp^r*	GTATATGATGATCCCACGGCC	This work
Gmet0679up	*Δ0679::Sp^r*	ACGATGACCTCCTGCAGCGCTGCG	This work
Gmet0679AvrIIup	*Δ0679::Sp^r*	CAG<u>CCTAGG</u>CATGATTGGTTCCTCCTTGACCAA[a]	This work
Gmet0679AvrIIdn	*Δ0679::Sp^r*	GTA<u>CCTAGG</u>GTTGATATGGCGGTGAAGCAGGTGA[a]	This work
Gmet0679dn	*Δ0679::Sp^r*	TGCGGCGTTGACGACAGGGTGGCGG	This work
Gmet0825up	*Δ0825::Sp^r*	GCGGATAACCTCCCGAACCGACAGCA	This work
Gmet0825AvrIIup	*Δ0825::Sp^r*	CAG<u>CCTAGG</u>CATCGGATACAGTCCCTTTCCG[a]	This work
Gmet0825AvrIIdn	*Δ0825::Sp^r*	GTA<u>CCTAGG</u>CCTCACCTGCCACCAGGATGCGC[a]	This work
Gmet0825dn	*Δ0825::Sp^r*	GCACCAGGTCGGTCTTGACGTAGA	This work
Gmet2839up	*Δ2839::Sp^r*	CTGCCTCCACGCCTTTCTTGTT	This work
Gmet2839AvrIIup	*Δ2839::Sp^r*	CAG<u>CCTAGG</u>CATCGTTCCTCCTCTGTG[a]	This work
Gmet2839AvrIIdn	*Δ2839::Sp^r*	GTA<u>CCTAGG</u>GCCAAAGCCGCTCCTGCGAAG[a]	This work
Gmet2839dn	*Δ2839::Sp^r*	ACCGCCTGAAGGAAGACAAGAAG	This work
Gmet0912up	*Δ0912::Sp^r*	GCGAGTGGTATCAGAGCTATCCGA	This work
Gmet0912AvrIIup	*Δ0912::Sp^r*	CAG<u>CCTAGG</u>CACGGATTCTCCCCCTTTCTAGAAG[a]	This work
Gmet0912AvrIIdn	*Δ0912::Sp^r*	GTA<u>CCTAGG</u>TGGCAACATCATCGATCGTA[a]	This work
Gmet0912dn	*Δ0912::Sp^r*	CATGGCCTGACTCAGCCCAGTC	This work
Gmet0913up	*Δ0913::Sp^r*	GGAGAGGGGGTTGCCCCGAAC	This work
Gmet0913AvrIIup	*Δ0913::Sp^r*	CAG<u>CCTAGG</u>CATGTGGCATACCTCCTTGTTG[a]	This work
Gmet0913AvrIIdn	*Δ0913::Sp^r*	GTA<u>CCTAGG</u>TTAGGGCCGACGCAACAACAG[a]	This work
Gmet0913dn	*Δ0913::Sp^r*	TGCCGTAGTCATCCCTTTGCTC	This work
Gmet0910up	*Δ0910::Sp^r*	CGTCCAACCAGACCTTCCGGCGCG	This work
Gmet0910AvrIIup	*Δ0910::Sp^r*	CAG<u>CCTAGG</u>CATACGCTACTCTCCTTTC[a]	This work
Gmet0910AvrIIdn	*Δ0910::Sp^r*	GTA<u>CCTAGG</u>ACTGCTTGTGGGGCCGGACT[a]	This work
Gmet0910dn	*Δ0910::Sp^r*	CGGTGTTCGCCCTCTTGAATCGA	This work

Gmet0571up	$\Delta 0571::Sp^r$	CCATCTGGAGCACCTCTGGAG	This work
Gmet0571AvrIIup	$\Delta 0571::Sp^r$	CAGCCTAGGCATATCATGCCTCCAGCAC[a]	This work
Gmet0571AvrIIdn	$\Delta 0571::Sp^r$	GAACCTAGGGGTATGCGGCAACCAGCAT[a]	This work
Gmet0571dn	$\Delta 0571::Sp^r$	CAAGATTGAGAAGCCCACGATGC	This work
Gmet0580up	$\Delta 0580::Sp^r$	CCTGGCTCACCATTGCGGCACTTC	This work
Gmet0580AvrIIup	$\Delta 0580::Sp^r$	CAGCCTAGGCATGACTTCCCCCACGTCAA[a]	This work
Gmet0580AvrIIdn	$\Delta 0580::Sp^r$	GTACCTAGGCGCGACAACGTGTGTCAATTG[a]	This work
Gmet0580dn	$\Delta 0580::Sp^r$	AATCTCGCGTTATTGGCGGCACCG	This work
Gmet2470up	$\Delta 2470::Sp^r$	GCTGGAGAACCCCGGCAAGATCC	This work
Gmet2470AvrIIup	$\Delta 2470::Sp^r$	CAGCCTAGGCACGCCACCCCTCCCCCATT[a]	This work
Gmet2470AvrIIdn	$\Delta 2470::Sp^r$	GTACCTAGGACCCGACTGGCGTGTGGCCC[a]	This work
Gmet2470dn	$\Delta 2470::Sp^r$	GTGGCCGATGTCGTTGCCGCCGG	This work
Gmet0534up	$\Delta 0534::Sp^r$	GGTGGCGAGCGGCATCCAGGGA	This work
Gmet0534AvrIIup	$\Delta 0534::Sp^r$	CAGCCTAGGCATTCACCTCTCCTTTACC[a]	This work
Gmet0534AvrIIdn	$\Delta 0534::Sp^r$	GTACCTAGGGGTGGAGATGGTGAACCGTGC[a]	This work
Gmet0534dn	$\Delta 0534::Sp^r$	GAAAGCAGCAGGGCGAGCGGAAGCAGC	This work
Gmet0581up	$\Delta 0581::Sp^r$	GCACCGGCAATGACAGCAGCCA	This work
Gmet0581AvrIIup	$\Delta 0581::Sp^r$	CAGCCTAGGCATACCTTACCGGTTACATGGC[a]	This work
Gmet0581AvrIIdn	$\Delta 0581::Sp^r$	GTACCTAGGCACCAACTACACGACGCAGCAC[a]	This work
Gmet0581dn	$\Delta 0581::Sp^r$	CGATGGTCACCTTTTTCGTGCCGCC	This work
Gmet1866up	$\Delta 1866::Sp^r$	GGGAGGCAAGTAAACAAACGGATG	This work
Gmet1866AvrIIup	$\Delta 1866::Sp^r$	CAGCCTAGGCATCGCCTGGCACCTCTGT[a]	This work
Gmet1866AvrIIdn	$\Delta 1866::Sp^r$	GTACCTAGGTTCCCCTGTCGAAAATCTGT[a]	This work
Gmet1866dn	$\Delta 1866::Sp^r$	CGATGGATAGACGAGGGCTGAG	This work
Gmet0907up	$\Delta 0907::Sp^r$	GCCGGCGAACTGGGTGTCACC	This work
Gmet0907AvrIIup	$\Delta 0907::Sp^r$	CAGCCTAGGCATTGAAAATCCCTTCCGTTT[a]	This work
Gmet0907AvrIIdn	$\Delta 0907::Sp^r$	GTACCTAGGTACGCGGATGAGCCTTCTACGG[a]	This work
Gmet0907dn	$\Delta 0907::Sp^r$	CCGTAACCGTAGAGGGAGAACT	This work
Gmet0911up	$\Delta 0911::Sp^r$	AGCCTCATATCTCCCCTCGCA	This work
Gmet0911AvrIIup	$\Delta 0911::Sp^r$	CAGCCTAGGCATTCAGTGGACCTCCTTTCTC[a]	This work
Gmet0911AvrIIdn	$\Delta 0911::Sp^r$	GTACCTAGGCGACACGCAAGGACGCTTCG[a]	This work
Gmet0911dn	$\Delta 0911::Sp^r$	CGGTGGCATGCTCGCTGTTCCAGA	This work
Gmet0908up	$\Delta 0908::Sp^r$	GGAAAAGGTTGTCCACCGGG	This work
Gmet0908AvrIIup	$\Delta 0908::Sp^r$	CAGCCTAGGCATTCAGTGGACCTCCTTTCTCA[a]	This work
Gmet0908AvrIIdn	$\Delta 0908::Sp^r$	GTACCTAGGATCAACGGCCGCTTCGTTCTG[a]	This work

Gmet0908dn	*Δ0908::Sp*^{r}	GCTCTGGCACTGGGTCGCCGAGA	This work
0557QF	qRT-PCR	CCATTAATCCGATTGCCACT	This work
0557QR	qRT-PCR	AAATCCATGCCGTAATCCAC	This work
2896QF	qRT-PCR	GCATCCGGTCAACTTCGTAT	This work
2896QR	qRT-PCR	ACTCCAGGTTATTGGCAACG	This work
0909QF	qRT-PCR	ATTGCAACGACTGTCACGAT	This work
0909QR	qRT-PCR	GGGATTATCCATTGCCTTGA	This work
0930QF	qRT-PCR	GTCGCTCCACAACATTGAGA	This work
0930QR	qRT-PCR	GACGGATCGGTTGCATACTT	This work
1868QF	qRT-PCR	ATCCAACACTCTTGCCATCC	This work
1868QR	qRT-PCR	ACCATTGGGCTCAGACTTGT	This work
2029QF	qRT-PCR	GAGTATCATCGCATCGCTCA	This work
2029QR	qRT-PCR	CCGTGCTGAATTCCTCTTTC	This work

[a] *AvrII* restriction site is underlined
[b] *BamH* I restriction site is underlined
[c] *Kpn* I restriction site is underlined
[d] *XbaI* restriction site underlined
[e] *Sph* I restriction site is underlined

APPENDIX B

GOING WIRELESS: FE(III) OXIDE REDUCTION WITHOUT PILI BY *GEOBACTER SULFURREDUCENS* STRAIN JS-1

Table B1. Bacterial strains and plasmids used in this study

Strain or plasmid	Relevant characteristic(s)	Source or reference
Strains		
E. coli		
TOP10	*recA1 endA1 gyrA96 thi-1 hsdR17* ($r_K^- m_K^+$) *supE44 relA1* Δ*lacU169*	Invitrogen, Carlsbad, CA
G. sulfurreducens		
KN400	Wild type	(Yi *et al*,, 2009)
KN400 unadapted *pilA*	Δ*pilA::*Km^r	(Richter *et al*., 2012)
JS-1	Δ*pilA::*Km^r Adapted for Fe(III) oxide reduction	This work
JS-1 *omcZ*	Δ*omcZ::*Sp^r	This work
KN400 *omcZ*	Δ*omcZ::*Sp^r	This work
JS-1 *pgcA*	Δ*pgcA::*Gm^r	This work
KN400 *pgcA*	Δ*pgcA::*Gm^r	This work
Plasmids		
pCR2.1-TOPO	PCR cloning vector; Ap^r, Km^r	Invitrogen, Carlsbad, CA
pUC19-*Sp^{r}loxP*	pUC19 carrying *Sp^{r}loxP*; Ap^r, Sp^r	(Marx and Lidstrom, 2001)
pUC19-*Gm^r loxP*	pUC19 carrying *Gm^r loxP*; Ap^r Gm^r	(Aklujkar and Lovley 2010)

Table B2. Primers used for mutant construction, and quantitative PCR

Primer name	Purpose	Sequence (5’ to 3’)	Source or reference
pgcAup	*pgcA::Gm*^{r}	AAGGATTACGCCCACAAGACCTGCA	This work
pgcAAvrIIup	*pgcA::Gm*^{r}	CAGCCTAGGCATTAAGTTTCCTCCCTGAGCGCG[a]	This work
pgcAAvrIIdn	*pgcA::Gm*^{r}	GTACCTAGGCCGCGGATCTTGCAAATCTTAAGAC[a]	This work
pgcAdn	*pgcA::Gm*^{r}	TCACGCCGGATATCAGGGCAACTTTG	This work
omcZup	*omcZ::Sp*^{r}	CCGGTCAGATAGGTGCTGCTCG	This work
omcZdn	*omcZ::Sp*^{r}	GCCATGGCTGAGGGAGTATGCG	This work
Pilaf	qPCR	AACACAAGCAGCAAAAAGAAGA	This work
pilAR	qPCR	TTTCCTGTTTCTGAGTTTCTGAAG	This work
kmF	qPCR	TGAATGAACTGCAGGACGAG	This work
kmR	qPCR	CAATAGCAGCCAGTCCCTTC	This work
1784QF	qRT-PCR	GGCAGTGGCTCCTACTCCTA	This work
1784QR	qRT-PCR	GTCTGGATGTCGGAATTCGT	This work
1319QF	qRT-PCR	ATCGCGGCCAAGAACTACTA	This work
1319QR	qRT-PCR	GGTCCGTAGATCTGGTCGAA	This work
2603QF	qRT-PCR	TCTGCAATGTGGAAGACAGC	This work
2603QR	qRT-PCR	AATCCCCCTCTATGGTGAGC	This work
2641QF	qRT-PCR	AGCAGAGCAACAGAGCAACA	This work
2641QR	qRT-PCR	GCAACAGAGAAAGGCTTTGG	This work
2978QF	qRT-PCR	ACGTGATCTCCGTCTCCATC	This work
2978QR	qRT-PCR	GATGCTCGACACGTTCTTGA	This work
1523QF	qRT-PCR	AGTTCTCGGCGTATCGTGTC	This work
1523QR	qRT-PCR	AATGCGGACTCAAGAGCAGT	This work
proCF	qRT-PCR	ACCGATGACGATCTGTTCTTT	This work
proCR	qRT-PCR	ATGAGCTTTTCCTCCACCAC	This work

[a] *AvrII* restriction site is underlined

Table B3. Genes encoding for proteins involved in sulfate assimilation up-regulated at least two-fold in JS-1 compared with KN400 (p-value <0.05)

Gene	Annotation	Fold Change
KN400_1319	sulfate ABC transporter, periplasmic sulfate-binding protein	17.4
KN400_1320	sulfate ABC transporter, membrane protein CysU	3.6
KN400_1321	sulfate ABC transporter, membrane protein CysW	4.5
KN400_1736	sulfate adenylyltransferase, subunit 2	7.1
KN400_1737	sulfate adenylyltransferase, subunit 1	4.2
KN400_1735	adenosine-5'-phosphosulfate reductase, glutathione-dependent	7.2
KN400_2472	nitrite/sulfite reductase domain protein	4.5
KN400_0524	cysteine synthase A	3.1

Table B4. Genes differentially expressed at least two-fold in JS-1 compared with KN400 (P-value cutoff ≤ 0.05)

Gene	Annotation	Fold change	P value	T value
KN400_1784	lipoprotein cytochrome c, 3 heme-binding sites	57.185 up	1.96E-05	-37.613
KN400_0540	protein of unknown function of ISGsu7	20.955 up	2.93E-05	-44.332
KN400_1319	sulfate ABC transporter, periplasmic sulfate-binding protein	17.356 up	0.00149	-8.728
KN400_2603	conserved hypothetical protein	13.492 up	0.000096	-20.529
KN400_1318	winged helix-turn-helix transcriptional regulator, Rrf2 family	11.075 up	9.15E-05	-21.979
KN400_2690	hypothetical protein	10.495 up	9.85E-05	-21.225
KN400_3415	hypothetical protein	10.075 up	0.00142	-8.881
KN400_2691	anaerobic C4-dicarboxylate antiporter, Dcu family	9.904 up	0.000115	-19.51
KN400_1211	iron-sulfur cluster-binding oxidoreductase	9.900 up	0.000347	-13.23
KN400_1038	conserved hypothetical protein	9.842 up	3.98E-05	-29.731
KN400_2687	conserved hypothetical protein	9.483 up	0.000542	-11.724
KN400_1785	TPR domain lipoprotein	9.133 up	0.000414	-12.473
KN400_1693	conserved hypothetical protein	9.028 up	0.00905	-5.231
KN400_2641	efflux pump, RND family, outer membrane protein	8.727 up	0.000294	-14.289
KN400_0541	transposase of ISGsu7	8.147 up	1.53E-05	-36.641
KN400_1289	response regulator sensor (REC, GAF)	7.936 up	0.000193	-16.57
KN400_1086	nucleoside diphosphate kinase	7.666 up	0.00728	-5.547
KN400_2463	rhodanese homology domain superfamily protein	7.642 up	6.45E-05	-24.155
KN400_2644	transcriptional regulator, TetR family	7.167 up	0.00636	-5.787
KN400_1735	adenosine-5'-phosphosulfate reductase, glutathione-dependent	7.167 up	0.0199	-4.139
KN400_1736	sulfate adenylyltransferase, subunit 2	7.113 up	0.0121	-4.79
KN400_3504	hypothetical protein	6.924 up	0.00196	-7.985
KN400_1694	lipoprotein, putative	6.756 up	0.0237	-3.921
KN400_2418	antitoxin, AbrB family	6.685 up	0.00116	-9.361
KN400_0061	conserved hypothetical protein	6.493 up	0.000109	-19.327
KN400_2619	ATP-independent chaperone, alpha-crystallin/Hsp20 family	6.427 up	0.000612	-11.209
KN400_0478	ATP-dependent RNA helicase RhlE	6.316 up	0.000211	-16.123
KN400_0146	conserved hypothetical protein	6.077 up	0.00274	-7.294
KN400_1212	glutamate synthase, FMN-Fe(II)-binding domain protein	5.977 up	0.000192	-16.749
KN400_1986	conserved hypothetical protein	5.888 up	0.00219	-7.737
KN400_1210	FAD-dependent pyridine nucleotide-disulfide oxidoreductase family protein	5.788 up	0.000293	-14.415
KN400_0246	cytochrome c, 9 heme-binding sites, and cytochrome b	5.615 up	3.66E-05	-29.566
KN400_1510	winged helix-turn-helix transcriptional regulator, MarR family	5.549 up	0.000345	-13.375
KN400_0749	hypothetical protein	5.414 up	0.000789	-10.385
KN400_1292	conserved hypothetical protein	5.385 up	0.00216	-7.788
KN400_2464	hydroxyacyl/enoyl-CoA dehydratase/reductase YjiM, putative	5.101 up	0.000803	-10.308
KN400_2467	DsrE domain protein	5.040 up	0.00177	-8.269

KN400_1987	polysaccharide ABC transporter, ATP-binding/membrane protein, putative	5.004 up	0.00271	-7.314
KN400_2247	conserved hypothetical protein	4.952 up	0.00514	-6.141
KN400_0523	helix-turn-helix iron-sulfur cluster-binding transcriptional regulator IscR	4.910 up	0.0008	-10.306
KN400_0060	heterodisulfide oxidoreductase, NAD(P)H oxidoreductase subunit	4.892 up	0.000656	-10.92
KN400_2818	ribosomal protein S9	4.865 up	0.00408	-6.541
KN400_1509	efflux pump, RND family, outer membrane protein	4.832 up	0.000133	-18.232
KN400_0083	ATP synthase F0, B' subunit	4.765 up	0.00496	-6.202
KN400_0705	protein glutamine deamidase and protein glutamate methylesterase CheD associated with MCPs of classes 40H and 40+24H	4.686 up	0.00408	-6.556
KN400_1252	protein of unknown function DUF1858	4.628 up	0.0207	-4.096
KN400_2140	ferritin-like domain protein	4.623 up	0.0105	-4.991
KN400_0161	protein of unknown function DUF1579	4.611 up	0.00432	-6.441
KN400_1607	protein of unknown function DUF150	4.541 up	0.00109	-9.505
KN400_0238	helix-turn-helix transcriptional regulator, LysR family	4.530 up	0.00504	-6.171
KN400_1321	sulfate ABC transporter, membrane protein CysW	4.484 up	0.0549	-3.006
KN400_2472	nitrite/sulfite reductase domain protein	4.480 up	0.00154	-8.638
KN400_1278	glutamate dehydrogenase, NADP-dependent	4.475 up	0.000218	-15.938
KN400_2000	glycosyltransferase, CESA-like subfamily	4.354 up	0.000838	-10.161
KN400_0442	phage regulatory protein, AlpA family	4.348 up	0.00183	-8.19
KN400_1644	protein of unknown function, DUF162-containing	4.331 up	0.00352	-6.8
KN400_3059	disulfide bond formation oxidoreductase DsbA	4.303 up	0.0492	-3.117
KN400_0700	conserved hypothetical protein	4.285 up	0.000915	-9.941
KN400_2640	response regulator (REC), putative	4.250 up	0.000377	-12.781
KN400_1076	protein of unknown function DUF2495	4.203 up	0.00546	-6.03
KN400_0706	lipoprotein, putative	4.194 up	0.000102	-20.824
KN400_3443	glycosyltransferase	4.194 up	0.0105	-4.988
KN400_2337	conserved hypothetical protein	4.188 up	0.0064	-5.777
KN400_1737	sulfate adenylyltransferase, subunit 1	4.152 up	0.00503	-6.18
KN400_1608	transcription elongation factor NusA	4.129 up	0.00301	-7.085
KN400_1330	conserved hypothetical protein	4.106 up	0.00513	-6.139
KN400_0900	conserved hypothetical protein	4.026 up	0.0208	-4.084
KN400_1645	D-lactate/L-lactate/glycolate transporter, putative	4.010 up	0.000463	-12.112
KN400_0062	heterodisulfide reductase, iron-sulfur cluster-binding subunit, putative	3.992 up	6.96E-05	-24.64
KN400_0067	heterodisulfide reductase, subunit C	3.978 up	0.000113	-19.481
KN400_3463	glycosyltransferase	3.956 up	9.57E-05	-21.483
KN400_0332	cytochrome c, 3 heme-binding sites	3.941 up	0.00148	-8.727
KN400_2011	conserved hypothetical protein	3.917 up	0.0362	-3.443
KN400_0165	hypothetical protein	3.909 up	0.00804	-5.406
KN400_0014	winged helix-turn-helix transcriptional regulator, MarR family	3.889 up	0.00433	-6.435
KN400_1997	aminotransferase, AHBA_syn family	3.870 up	0.000287	-14.697

KN400_1620	protein of unknown function DUF177	3.812 up	0.00438	-6.416
KN400_2642	efflux pump, RND family, inner membrane protein	3.770 up	0.00556	-5.986
KN400_1988	polysaccharide pyruvyl transferase-related domain	3.756 up	0.000349	-13.39
KN400_0844	regulatory protein, CxxC_CxxC_SSSS domain-containing, putative	3.754 up	0.00914	-5.209
KN400_2357	ATP-independent chaperone, alpha-crystallin/Hsp20 family	3.738 up	0.00398	-6.595
KN400_1662	winged helix-turn-helix transcriptional regulator, Rrf2 family	3.737 up	0.0194	-4.181
KN400_2299	helix-turn-helix transcriptional regulator, IclR family	3.709 up	0.000362	-12.959
KN400_0010	sensor histidine kinase of FgrL (PAS, HisKA, HATPase_c)	3.674 up	0.00055	-11.598
KN400_2002	exopolysaccharide synthesis multitransmembrane protein H (exosortase)	3.661 up	0.000198	-16.342
KN400_3481	hypothetical protein	3.635 up	0.00849	-5.326
KN400_2128	glycerol dehydratase-activating enzyme, putative	3.619 up	0.0398	-3.339
KN400_1320	sulfate ABC transporter, membrane protein CysU	3.595 up	0.0457	-3.197
KN400_3421	conserved hypothetical protein	3.590 up	0.0423	-3.277
KN400_0504	universal stress protein Usp	3.543 up	0.00186	-8.13
KN400_1980	O-antigen polymerase, putative	3.533 up	0.000344	-13.469
KN400_2515	tRNA (5-carboxymethylaminomethyl-2-thio-U34)-thioltransferase	3.529 up	0.000296	-14.3
KN400_0559	cold shock DNA/RNA-binding protein	3.511 up	0.0197	-4.152
KN400_3471	hypothetical protein	3.493 up	0.00908	-5.222
KN400_0040	tRNA (adenosine-34) deaminase	3.457 up	0.000807	-10.272
KN400_2604	efflux pump, RND family, inner and outer membrane proteins	3.449 up	0.00186	-8.122
KN400_1663	cytochrome bd menaquinol oxidase, subunit I	3.444 up	0.000118	-18.812
KN400_0497	protein of unknown function YceG	3.405 up	0.00438	-6.415
KN400_1738	conserved hypothetical protein	3.403 up	0.000554	-11.559
KN400_1508	multidrug resistance efflux pump, RND family, membrane fusion protein EmrA	3.388 up	0.0122	-4.781
KN400_0084	ATP synthase F0, B subunit	3.378 up	0.00253	-7.432
KN400_0239	helix-turn-helix transcriptional regulator, UTRA domain-containing, GntR family	3.372 up	0.00691	-5.651
KN400_1526	conserved hypothetical protein	3.354 up	0.000198	-16.393
KN400_1734	SsrA-binding protein	3.329 up	0.000345	-13.489
KN400_0183	cold shock DNA/RNA-binding protein	3.319 up	0.0469	-3.171
KN400_2356	ATP-independent chaperone, alpha-crystallin/Hsp20 family	3.308 up	0.0283	-3.707
KN400_0064	methyl viologen-reducing hydrogenase, iron-sulfur cluster-containing subunit, MvhD	3.296 up	0.00373	-6.705
KN400_1533	ADP-heptose--lipopolysaccharide heptosyltransferase, putative	3.295 up	0.0181	-4.262
KN400_1135	superoxide dismutase, iron/manganese-containing	3.285 up	0.0232	-3.95

KN400_2643	efflux pump, RND family, membrane fusion lipoprotein	3.282 up	0.00747	-5.505
KN400_0735	conserved hypothetical protein	3.279 up	0.00608	-5.847
KN400_1535	glycosyltransferase	3.259 up	0.0427	-3.262
KN400_1943	undecaprenyl diphosphate synthase	3.247 up	0.00154	-8.627
KN400_2004	conserved hypothetical protein	3.245 up	0.000334	-13.759
KN400_0047	conserved hypothetical protein	3.243 up	0.000558	-11.504
KN400_0143	ABC transporter, ATP-binding protein	3.218 up	0.00139	-8.943
KN400_3085	pyranopterin triphosphate synthase	3.207 up	0.00222	-7.707
KN400_3411	protein of unknown function DUF37	3.199 up	0.0171	-4.332
KN400_1880	acetyltransferase, GNAT family	3.199 up	0.0314	-3.59
KN400_0890	cold shock DNA/RNA-binding protein	3.197 up	0.0085	-5.318
KN400_1315	amidohydrolase, YcaC-related	3.192 up	0.000294	-14.604
KN400_1527	ABC transporter, ATP-binding protein	3.187 up	0.00115	-9.381
KN400_1232	NosL family protein	3.179 up	0.00355	-6.781
KN400_0065	heterodisulfide reductase, subunit A	3.174 up	0.00681	-5.68
KN400_1160	O-acetyl-L-homoserine sulfhydrylase	3.173 up	0.00148	-8.714
KN400_3017	cell division protein MraZ	3.165 up	0.000451	-12.21
KN400_0454	conserved hypothetical protein	3.154 up	0.000291	-14.4
KN400_3490	uracil-DNA glycosylase superfamily protein	3.154 up	0.027	-3.761
KN400_2654	ferredoxin	3.149 up	0.0148	-4.504
KN400_2680	transcriptional regulator, TetR family	3.137 up	0.0135	-4.632
KN400_1113	2',3'-cyclic nucleotide 2'-phosphodiesterase	3.135 up	0.0192	-4.193
KN400_1209	glutamine amidotransferase, class II	3.128 up	0.00035	-13.151
KN400_3440	very short patch repair endonuclease	3.123 up	0.00679	-5.693
KN400_0668	sensor histidine kinase (PAS, PAS, PAS, HisKA, HATPase_c)	3.106 up	0.00145	-8.826
KN400_1978	glycosyltransferase, putative	3.096 up	0.00148	-8.721
KN400_0524	cysteine synthase A	3.079 up	0.000305	-14.142
KN400_2003	polysaccharide deacetylase and DUF3473 domain protein	3.070 up	0.000117	-18.759
KN400_1643	iron-sulfur cluster-binding DUF162/cysteine-rich domain protein	3.065 up	0.000561	-11.505
KN400_3405	acyl-CoA thioesterase	3.059 up	0.0106	-4.979
KN400_2417	toxin, PIN family	3.048 up	0.0034	-6.862
KN400_1812	GDP-mannose--undecaprenyl-phosphate mannosyltransferase	3.046 up	0.0133	-4.662
KN400_3307	iron-sulfur cluster-binding sigma-54-dependent transcriptional regulator (FehydlgC, FeS, sigma54 interaction, HTH8)	3.025 up	0.00146	-8.785
KN400_0701	protein of unknown function DUF3106	3.018 up	0.000293	-14.583
KN400_1554	sensor histidine kinase response regulator (PAS, HisKA, HATPase_c, REC)	3.007 up	0.00275	-7.279
KN400_2689	NOL1/NOP2/Sun (tRNA and rRNA cytosine-C5-methyltransferase) family protein	2.979 up	0.00293	-7.141
KN400_2899	membrane protein DUF318	2.971 up	0.0123	-4.771
KN400_1507	multidrug resistance efflux pump, RND family, inner membrane protein EmrB	2.969 up	0.00295	-7.123
KN400_1529	glycosyltransferase	2.969 up	0.0215	-4.049
KN400_2001	exopolysaccharide synthesis periplasmic	2.961 up	9.84E-05	-20.812

	protein I			
KN400_3014	peptidoglycan transglycosylase and transpeptidase FtsI	2.960 up	0.000178	-17.141
KN400_2828	NHL repeat domain protein	2.947 up	0.0033	-6.918
KN400_2355	ATP-independent chaperone, alpha-crystallin/Hsp20 family	2.945 up	0.000258	-15.195
KN400_2711	transposase, Y1_Tnp domain-containing	2.936 up	0.00219	-7.753
KN400_3177	peroxiredoxin, typical 2-Cys subfamily	2.929 up	0.00492	-6.22
KN400_3482	hypothetical protein	2.919 up	0.0408	-3.312
KN400_2518	serine O-acetyltransferase	2.909 up	0.022	-4.021
KN400_0716	antitoxin	2.902 up	0.00964	-5.127
KN400_2235	response regulator (REC), putative	2.883 up	0.00452	-6.362
KN400_1990	membrane protein, putative	2.874 up	0.00085	-10.112
KN400_3308	hydrogen-dependent growth transcriptional repressor	2.871 up	0.00432	-6.445
KN400_2010	TPR domain lipoprotein	2.845 up	0.000371	-12.833
KN400_3181	protein of unknown function, DUF523 and DUF1722	2.838 up	0.00148	-8.723
KN400_1327	DNA cytosine methyltransferase family protein	2.817 up	0.00131	-9.063
KN400_0573	conserved hypothetical protein	2.782 up	0.00158	-8.547
KN400_1112	endoribonuclease Y	2.780 up	0.00075	-10.536
KN400_2007	polysaccharide chain length determinant protein	2.776 up	0.00173	-8.319
KN400_0316	NADH dehydrogenase I, K subunit	2.774 up	0.00591	-5.889
KN400_3467	glycosyltransferase	2.770 up	0.0356	-3.461
KN400_3009	cell division protein FtsW	2.758 up	0.0118	-4.827
KN400_0066	heterodisulfide reductase, subunit B	2.754 up	0.00631	-5.8
KN400_0614	SAM-dependent methyltransferase	2.734 up	0.0127	-4.722
KN400_1114	tyrosyl-tRNA synthetase	2.731 up	0.00727	-5.562
KN400_1328	hypothetical protein	2.726 up	0.0025	-7.454
KN400_1021	sensor histidine kinase (PAS, HisKA, HATPase_c)	2.718 up	0.0012	-9.26
KN400_1525	membrane protein, putative	2.714 up	0.00571	-5.942
KN400_0631	RNA polymerase sigma-32 factor RpoH	2.711 up	0.00475	-6.277
KN400_0946	conserved hypothetical protein	2.710 up	0.00458	-6.334
KN400_0741	conserved hypothetical protein	2.710 up	0.0314	-3.593
KN400_1553	ABC transporter, periplasmic substrate-binding protein	2.709 up	0.0021	-7.865
KN400_0002	DNA polymerase III, beta subunit	2.694 up	0.00147	-8.757
KN400_0503	helix-turn-helix transcriptional regulator, IclR family	2.688 up	0.00212	-7.845
KN400_1995	N-acetylneuraminate cytidylyltransferase	2.686 up	0.00105	-9.635
KN400_1282	conserved hypothetical protein	2.669 up	0.000348	-13.245
KN400_3058	disulfide bond formation oxidoreductase DsbB	2.668 up	0.0136	-4.628
KN400_1755	branched-chain amino acid ABC transporter, ATP-binding protein	2.668 up	0.000785	-10.377
KN400_0933	cystathionine gamma-synthase/beta-lyase	2.659 up	0.0172	-4.327
KN400_0591	cytochrome c, 3 heme-binding sites	2.658 up	0.0446	-3.22
KN400_1317	amidohydrolase, YtcJ-related	2.642 up	0.000718	-10.718
KN400_1903	oxidoreductase, 2-nitropropane dioxygenase family	2.641 up	0.000797	-10.34
KN400_0810	efflux pump, RND family, outer	2.632 up	0.00232	-7.601

	membrane protein			
KN400_2652	phosphate acetyltransferase	2.630 up	0.00888	-5.258
KN400_1999	glycosyltransferase, YqgM-like family	2.628 up	0.00118	-9.319
KN400_0351	peptidylprolyl cis-trans isomerase, FKBP-type	2.619 up	0.0104	-5.009
KN400_1536	glycosyltransferase	2.614 up	0.0193	-4.18
KN400_1528	phosphoglycosyl-diphosphate--polyprenyl-phosphate phosphoglycosyltransferase, putative	2.604 up	0.00909	-5.22
KN400_1979	asparagine synthetase	2.602 up	0.00661	-5.735
KN400_2918	membrane protein DedA	2.589 up	0.0158	-4.432
KN400_2710	lipoprotein, putative	2.581 up	0.00232	-7.595
KN400_2309	dTDP-glucose 4,6-dehydratase	2.579 up	0.00759	-5.484
KN400_3500	conserved hypothetical protein	2.577 up	0.00819	-5.382
KN400_1882	polysaccharide chain length determinant protein	2.569 up	0.00513	-6.139
KN400_1532	SAM-dependent methyltransferase, FkbM family	2.568 up	0.00972	-5.11
KN400_2778	adenylate kinase	2.564 up	0.000522	-11.819
KN400_2336	integrase domain protein, N-terminal fragment	2.562 up	0.021	-4.075
KN400_2774	ribosomal protein S11	2.561 up	0.00449	-6.372
KN400_0939	transcriptional regulator, TetR family	2.547 up	0.00145	-8.831
KN400_2880	conserved hypothetical protein	2.536 up	0.00101	-9.721
KN400_3479	conserved hypothetical protein	2.535 up	0.0219	-4.028
KN400_1621	ribosomal protein L32	2.534 up	0.0345	-3.494
KN400_2416	ATPase, AAA family	2.501 up	0.00456	-6.343
KN400_1947	ribosomal protein S2	2.496 up	0.0047	-6.291
KN400_0411	DNA cytosine methyltransferase	2.471 up	0.00683	-5.673
KN400_1646	D-lactate/glycolate dehydrogenase, FAD-binding protein, putative	2.469 up	0.000271	-14.991
KN400_0621	16S rRNA processing protein RimM	2.465 up	0.0043	-6.457
KN400_0982	hypothetical protein	2.461 up	0.00213	-7.814
KN400_1144	conserved hypothetical protein	2.455 up	0.0057	-5.951
KN400_0928	nitrogen fixation transcript antitermination sensor histidine kinase (HisKA, HATPase_c)	2.448 up	0.00825	-5.37
KN400_0263	conserved hypothetical protein	2.446 up	0.0068	-5.696
KN400_1293	sensor histidine kinase (HisKA, HATPase_c)	2.436 up	0.0104	-5.004
KN400_2606	transcriptional regulator, TetR family	2.433 up	0.05	-3.101
KN400_0748	RarD protein, DMT superfamily transporter	2.426 up	0.011	-4.916
KN400_0071	protein of unknown function DUF149	2.426 up	0.0229	-3.965
KN400_1110	cell division protein ZapA	2.421 up	0.00279	-7.244
KN400_0617	protein of unknown function DUF3343	2.420 up	0.0414	-3.297
KN400_2217	lysyl-tRNA synthetase	2.420 up	0.000173	-17.106
KN400_2036	conserved hypothetical protein	2.416 up	0.027	-3.761
KN400_0167	conserved hypothetical protein	2.412 up	0.0224	-3.991
KN400_2115	ABC transporter, ATP-binding protein	2.401 up	0.000453	-12.17
KN400_1136	intracellular protease, PfpI family, putative	2.396 up	0.00374	-6.696
KN400_3203	conserved hypothetical protein	2.396 up	0.021	-4.074
KN400_0901	methyl-accepting chemotaxis sensory	2.394 up	0.00952	-5.146

	transducer, class 40H			
KN400_3019	conserved hypothetical protein	2.392 up	0.00475	-6.275
KN400_2486	helix-turn-helix transcriptional regulator PuuR (HTH_XRE, cupin)	2.391 up	0.00187	-8.091
KN400_2875	cytochrome b/b6 complex, cytochrome b subunit	2.389 up	0.00264	-7.362
KN400_0184	conserved hypothetical protein	2.385 up	0.0499	-3.103
KN400_0699	RNA polymerase sigma-24 factor, putative	2.378 up	0.000889	-10.016
KN400_0358	protein of unknown function DUF2062	2.375 up	0.0228	-3.971
KN400_3150	ribosome biogenesis GTPase ObgE	2.371 up	0.00156	-8.599
KN400_1647	D-lactate/glycolate dehydrogenase, iron-sulfur cluster-binding protein, putative	2.370 up	0.00395	-6.605
KN400_1989	conserved hypothetical protein	2.370 up	0.00185	-8.158
KN400_1482	hypothetical protein	2.369 up	0.0055	-6.006
KN400_0330	conserved hypothetical protein	2.367 up	0.00379	-6.674
KN400_1479	RNA methyltransferase, TrmA family	2.367 up	0.0116	-4.845
KN400_3175	conserved hypothetical protein	2.365 up	0.0129	-4.703
KN400_2485	carboxynorspermidine/carboxyspermidine dehydrogenase	2.364 up	0.0116	-4.844
KN400_1803	type II secretion system protein PulO, putative	2.357 up	0.0184	-4.238
KN400_1942	phosphatidate cytidylyltransferase	2.356 up	0.0109	-4.938
KN400_1195	ammonium transporter, putative	2.351 up	0.0263	-3.794
KN400_3232	transcriptional regulator, Fur family	2.340 up	0.0123	-4.77
KN400_2009	undecaprenyl-phosphate glycosylphosphotransferase	2.338 up	0.000536	-11.705
KN400_1984	glycosyltransferase	2.332 up	0.00526	-6.099
KN400_0356	conserved hypothetical protein	2.323 up	0.0068	-5.697
KN400_0087	ATP synthase F1, gamma subunit	2.321 up	0.0101	-5.051
KN400_3060	arylsulfotransferase	2.318 up	0.0269	-3.766
KN400_0634	ATP-dependent chaperone ClpB	2.317 up	0.00115	-9.403
KN400_0001	chromosomal replication initiator protein DnaA	2.315 up	0.0496	-3.11
KN400_3007	UDP-N-acetylmuramate--alanine ligase	2.312 up	0.00823	-5.373
KN400_1816	ribosome-associated peptidylprolyl cis-trans isomerase, FKBP-type (trigger factor)	2.301 up	0.0167	-4.359
KN400_2372	conserved hypothetical protein	2.296 up	0.00927	-5.183
KN400_1841	phosphoglycerate mutase family protein	2.295 up	0.00158	-8.522
KN400_0983	amidohydrolase, YcaC-related	2.294 up	0.0264	-3.794
KN400_3456	cytochrome c, 3 heme-binding sites	2.292 up	0.0057	-5.947
KN400_3445	SAM-dependent methyltransferase, type 11	2.291 up	0.00525	-6.106
KN400_1878	membrane protein, putative	2.288 up	0.0174	-4.31
KN400_0203	peptidylprolyl cis-trans isomerase, FKBP-type, putative	2.279 up	0.0244	-3.888
KN400_0715	toxin, MazF family	2.277 up	0.00183	-8.197
KN400_3018	conserved hypothetical protein	2.275 up	0.00147	-8.713
KN400_3341	helix-turn-helix transcriptional regulator, GntR family	2.274 up	0.0134	-4.644
KN400_2049	chorismate synthase	2.268 up	0.0417	-3.29
KN400_3061	sensor histidine kinase (HATPase_c)	2.263 up	0.00188	-8.097
KN400_2462	iron-sulfur cluster-binding	2.262 up	0.000604	-11.272

	oxidoreductase, putative, rhodanese homology domain pair-containing			
KN400_1951	cytidylate kinase domain phospholipid-binding protein, putative	2.261 up	0.00726	-5.558
KN400_2803	ribosomal protein S7	2.261 up	0.00307	-7.055
KN400_1796	zinc metalloendopeptidase M23 domain protein	2.258 up	0.0033	-6.907
KN400_2785	ribosomal protein S8	2.250 up	0.0112	-4.892
KN400_3444	glycosyltransferase	2.250 up	0.00198	-7.965
KN400_1781	ribosomal protein S18 alanine N-acetyltransferase	2.245 up	0.00957	-5.135
KN400_1991	nucleotidyltransferase, CBS domain pair and CBS domain pair-containing	2.240 up	0.000618	-11.133
KN400_2804	ribosomal protein S12	2.234 up	0.00433	-6.432
KN400_0455	hypothetical protein	2.233 up	0.0095	-5.153
KN400_0891	ribosomal protein S21	2.231 up	0.0426	-3.268
KN400_0670	conserved hypothetical protein	2.227 up	0.00192	-8.033
KN400_1706	protein of unknown function UPF0027	2.220 up	0.00073	-10.634
KN400_1877	hypothetical protein	2.218 up	0.00273	-7.293
KN400_0489	translation-regulating membrane GTPase TypA	2.210 up	0.00127	-9.128
KN400_3505	metal-dependent hydrolase, beta-lactamase superfamily	2.208 up	0.0111	-4.902
KN400_0814	lipoprotein, putative	2.194 up	0.0234	-3.944
KN400_1129	membrane protein, putative	2.188 up	0.0187	-4.221
KN400_1985	glycosyltransferase	2.175 up	0.0133	-4.666
KN400_1101	conserved hypothetical protein	2.171 up	0.0221	-4.006
KN400_3478	hypothetical protein	2.171 up	0.0161	-4.403
KN400_2901	thioredoxin family protein	2.167 up	0.00986	-5.085
KN400_0531	diguanylate cyclase (GGDEF)	2.163 up	0.00295	-7.122
KN400_2605	efflux pump, RND family, membrane fusion lipoprotein	2.146 up	0.0299	-3.649
KN400_2183	DNA-directed RNA polymerase, omega subunit	2.144 up	0.0142	-4.561
KN400_0164	ATP-dependent RNA helicase DbpA	2.144 up	0.0074	-5.526
KN400_1078	winged-helix phosphate transcriptional response regulator (REC, trans_reg_C)	2.143 up	0.00282	-7.219
KN400_0730	lipoprotein, putative	2.138 up	0.0129	-4.705
KN400_1611	ribosome-binding factor A	2.135 up	3.02E-05	-39.285
KN400_2925	hypothetical protein	2.133 up	0.00106	-9.606
KN400_1437	NifU-like domain protein	2.133 up	0.0497	-3.106
KN400_0753	membrane protein, major facilitator superfamily	2.131 up	0.00134	-9.015
KN400_0942	conserved hypothetical protein	2.116 up	0.022	-4.017
KN400_3410	preprotein translocase subunit YidC	2.112 up	0.033	-3.543
KN400_3217	LysM domain protein	2.110 up	0.014	-4.574
KN400_3497	conserved hypothetical protein	2.109 up	0.0029	-7.164
KN400_1197	conserved hypothetical protein	2.105 up	0.00973	-5.106
KN400_2034	nitrogen fixation iron-sulfur cluster assembly protein NifU	2.097 up	0.0131	-4.688
KN400_3045	thymidylate synthase, FAD-dependent	2.089 up	0.00859	-5.305
KN400_1251	transcription elongation factor GreA	2.088 up	0.00143	-8.862
KN400_1932	2-isopropylmalate synthase	2.087 up	0.0225	-3.985
KN400_2055	helix-turn-helix transcriptional regulator,	2.081 up	0.00635	-5.792

	XRE family			
KN400_1776	translation elongation factor P	2.079 up	0.0184	-4.238
KN400_1534	conserved hypothetical protein	2.078 up	0.0135	-4.641
KN400_0155	peptidoglycan L,D-transpeptidase lipoprotein, YkuD family, TPR domain-containing	2.074 up	0.0364	-3.436
KN400_0090	4-hydroxythreonine-4-phosphate dehydrogenase	2.067 up	0.0097	-5.113
KN400_1881	glycosyltransferase, putative	2.064 up	0.0013	-9.083
KN400_3472	conserved hypothetical protein	2.063 up	0.00907	-5.217
KN400_1793	conserved hypothetical protein	2.059 up	0.0112	-4.887
KN400_0702	hypothetical protein	2.055 up	6.24E-05	-24.061
KN400_2310	lipopolysaccharide biogenesis outer membrane protein LptD, putative	2.055 up	0.00637	-5.784
KN400_2072	preprotein translocase, SecA subunit	2.054 up	0.000621	-11.16
KN400_0240	membrane protein, putative	2.050 up	0.0438	-3.24
KN400_2608	hypothetical protein	2.049 up	0.0254	-3.838
KN400_3425	hypothetical protein	2.048 up	0.00889	-5.259
KN400_3460	SAM-dependent methyltransferase, type 11	2.045 up	0.0018	-8.24
KN400_3399	radical SAM domain iron-sulfur cluster-binding oxidoreductase	2.043 up	0.00163	-8.452
KN400_2802	translation elongation factor G	2.041 up	0.00308	-7.041
KN400_1982	glycosyltransferase, WbnK-like family	2.040 up	0.0108	-4.946
KN400_0006	conserved hypothetical protein	2.038 up	0.00548	-6.023
KN400_0152	helix-turn-helix transcriptional regulator HxlR	2.037 up	0.00355	-6.78
KN400_2754	sensor histidine kinase (PAS, PAS, PAS, PAS, HisKA, HATPase_c)	2.034 up	0.00466	-6.308
KN400_1992	hypothetical protein	2.033 up	0.000411	-12.471
KN400_3172	radical SAM domain iron-sulfur cluster-binding oxidoreductase, DUF2344-containing	2.031 up	0.00707	-5.61
KN400_2248	HAD superfamily hydrolase	2.027 up	0.0225	-3.985
KN400_1938	dihydroxy-acid dehydratase	2.022 up	0.00035	-13.115
KN400_1497	2-oxoglutarate:ferredoxin oxidoreductase, gamma subunit	2.022 up	0.0106	-4.982
KN400_1613	tRNA pseudouridine 55 synthase	2.018 up	0.0023	-7.623
KN400_3437	transport protein, Tim44-like domain, putative	2.013 up	0.0173	-4.315
KN400_1522	sigma-54-dependent transcriptional response regulator PilR (REC, sigma54 interaction, HTH8)	2.003 up	0.0122	-4.778
KN400_0582	4-amino-5-hydroxymethyl-2-methylpyrimidine-phosphate synthase	2.002 up	0.00186	-8.144
KN400_2493	tRNA (5-methyl-U54)-methylenetransferase/reductase	2.002 up	0.0132	-4.68
KN400_3366	DTW domain protein	2.002 up	0.00542	-6.045
KN400_1046	sodium/solute symporter family protein	2.000 up	0.00194	-8.003
KN400_0817	RNA polymerase-binding protein Rnk	2.000 down	0.0294	3.666
KN400_2719	efflux pump, RND family, inner membrane protein, AcrB/AcrD/AcrF family	2.001 down	0.0369	3.422
KN400_1066	iron-sulfur cluster-binding oxidoreductase	2.004 down	0.014	4.581

KN400_2095	dystroglycan-type cadherin-like domain repeat protein	2.005 down	0.00109	9.537
KN400_1084	aldehyde dehydrogenase	2.009 down	0.00355	6.777
KN400_1357	toxin, Fic family	2.012 down	0.0261	3.808
KN400_1641	protein phosphoaspartate phosphatase CheX	2.017 down	0.0413	3.299
KN400_2146	protein of unknown function DUF3373	2.020 down	0.00741	5.522
KN400_2745	protein of unknown function YcbK	2.027 down	0.00656	5.747
KN400_2284	sodium/proton antiporter complex Mrp, protein G	2.034 down	0.00952	5.149
KN400_0048	outer membrane protein, putative	2.035 down	0.00116	9.365
KN400_1027	ribonuclease Z-related hydrolase	2.037 down	0.0078	5.451
KN400_0099	amidophosphoribosyltransferase, putative	2.044 down	0.00121	9.229
KN400_2981	flagellar hook-filament junction protein FlgL	2.051 down	0.00551	6.011
KN400_0884	conserved hypothetical protein	2.051 down	0.0034	6.861
KN400_2260	sensor histidine kinase response regulator (DUF3365, PAS, PAS, HisKA, HATPase_c, REC, Hpt), heme-binding	2.052 down	0.00146	8.778
KN400_2571	diguanylate cyclase (GGDEF)	2.054 down	0.00526	6.102
KN400_1704	lipoprotein, putative	2.055 down	0.00219	7.747
KN400_0460	sensor diguanylate cyclase/phosphodiesterase (PAS, PAS, GGDEF, EAL)	2.056 down	0.00185	8.149
KN400_1634	phosphoglycerate mutase 1	2.057 down	0.0139	4.585
KN400_0887	sensor histidine kinase (HisKA, HATPase_c)	2.061 down	0.00969	5.119
KN400_1731	pantoate--beta-alanine ligase	2.074 down	0.00862	5.297
KN400_1103	conserved hypothetical protein	2.077 down	0.0194	4.178
KN400_1448	rRNA methyltransferase, YqxC-related, putative	2.084 down	0.0153	4.465
KN400_0149	transcriptional regulator, TetR family	2.084 down	0.0277	3.731
KN400_0561	methyl-accepting chemotaxis sensory transducer, class 40+24H	2.085 down	0.000412	12.449
KN400_1014	methyl-accepting chemotaxis sensory transducer, class 40H	2.086 down	0.0011	9.51
KN400_3274	radical SAM domain iron-sulfur cluster-binding oxidoreductase	2.086 down	0.0046	6.327
KN400_0764	periplasmically oriented, membrane-bound [NiFe]-hydrogenase integral membrane subunit	2.094 down	0.0124	4.752
KN400_2750	glutaredoxin family protein	2.094 down	0.00487	6.238
KN400_2856	cytochrome c, 4 heme-binding sites	2.095 down	0.000566	11.465
KN400_2391	pyruvate dehydrogenase complex, E1 protein, alpha subunit	2.096 down	0.000752	10.541
KN400_0404	PilB/PulE/GspE family ATPase	2.097 down	0.00551	6.007
KN400_1201	lipoprotein cytochrome c, 10 heme-binding sites	2.101 down	0.00841	5.338
KN400_0649	iron-sulfur-oxygen hybrid cluster protein (prismane)	2.105 down	0.00158	8.561
KN400_3159	conserved hypothetical protein	2.114 down	0.0134	4.643
KN400_0686	conserved hypothetical protein	2.116 down	0.00686	5.665
KN400_2928	periplasmic divalent manganese/zinc-binding lipoprotein	2.137 down	0.0439	3.236

KN400_2455	undecaprenyl-phosphate glycosyltransferase, putative	2.153 down	0.0261	3.808
KN400_2562	peptide ABC transporter, ATP-binding protein	2.161 down	0.0489	3.126
KN400_3375	NADH dehydrogenase I, L subunit	2.165 down	0.000357	12.954
KN400_3290	Kup system potassium transporter	2.171 down	0.00357	6.765
KN400_0684	quaternary ammonium compound resistance transporter SugE	2.178 down	0.00729	5.548
KN400_3469	hypothetical protein	2.180 down	0.00392	6.622
KN400_0889	conserved hypothetical protein	2.181 down	0.00412	6.524
KN400_0387	flagellar hook protein FlgE	2.183 down	0.000374	12.835
KN400_2982	flagellar hook-associated protein FlgK	2.192 down	0.000346	13.2
KN400_2991	flagellar basal body rod protein FlgF	2.194 down	0.000666	10.934
KN400_2620	membrane protein of unknown function DUF606	2.200 down	0.003	7.092
KN400_0405	twitching motility pilus retraction protein	2.210 down	0.000062	23.664
KN400_3300	diguanylate cyclase (HAMP, GGDEF)	2.215 down	0.00141	8.904
KN400_0690	hypothetical protein	2.222 down	0.00171	8.355
KN400_0514	D-aminoacyl-tRNA deacylase	2.224 down	0.00743	5.514
KN400_3294	cyclase/hydrolase, putative	2.227 down	0.00247	7.49
KN400_0886	response receiver	2.228 down	0.00227	7.649
KN400_1125	sensor histidine kinase (HAMP, HisKA, HATPase_c)	2.230 down	0.00331	6.918
KN400_0205	twitching motility pilus retraction protein	2.233 down	0.00259	7.391
KN400_0543	SAM-dependent methyltransferase, FkbM family	2.246 down	0.00223	7.696
KN400_2820	tRNA pseudouridines 38,39,40 synthase	2.249 down	0.0301	3.642
KN400_1810	cytochrome c, 4 heme-binding sites	2.253 down	0.000859	10.086
KN400_3186	UDP-glucose--galactose-1-phosphate uridylyltransferase	2.256 down	0.00394	6.616
KN400_2840	lipoprotein cytochrome c, 34 heme-binding sites	2.266 down	0.000119	18.867
KN400_2973	PilZ domain protein	2.268 down	0.00246	7.488
KN400_0679	lipoprotein cytochrome c, 35 heme-binding sites	2.272 down	0.00694	5.639
KN400_2148	cytochrome c, 8 heme-binding sites	2.279 down	0.000734	10.646
KN400_3185	glycoside hydrolase, family 57	2.280 down	0.00678	5.693
KN400_2908	molybdate transport regulatory protein ModE	2.286 down	0.00918	5.201
KN400_3466	hypothetical protein	2.295 down	0.0208	4.086
KN400_2704	hypothetical protein	2.299 down	0.0119	4.805
KN400_1060	flotillin band_7_5 domain protein	2.301 down	0.000808	10.263
KN400_2136	sensor histidine kinase (HATPase_c)	2.302 down	0.00114	9.403
KN400_2993	flagellar biogenesis ATPase FlhG	2.305 down	0.00219	7.744
KN400_2768	conserved hypothetical protein	2.305 down	0.00456	6.35
KN400_1505	protein of unknown function DUF477	2.308 down	0.0179	4.275
KN400_3160	NHL repeat domain lipoprotein	2.309 down	0.023	3.962
KN400_0971	glycosyltransferase, ExpC-like family	2.310 down	0.0184	4.238
KN400_1124	conserved hypothetical protein	2.310 down	0.00677	5.691
KN400_3094	methyl-accepting chemotaxis sensory transducer, class 30H	2.312 down	0.00788	5.434
KN400_0783	phosphoenolpyruvate synthase	2.315 down	0.0118	4.822
KN400_0366	rhodanese homology domain superfamily protein	2.326 down	0.0146	4.518

KN400_1642	response receiver CheY	2.329 down	0.0326	3.553
KN400_1576	conserved hypothetical protein	2.330 down	0.0092	5.193
KN400_2727	conserved hypothetical protein	2.333 down	0.00719	5.577
KN400_0897	conserved hypothetical protein	2.333 down	0.00743	5.515
KN400_2272	cation-translocating P-type ATPase	2.337 down	0.00672	5.714
KN400_1057	PEP motif-containing protein, putative exosortase substrate	2.342 down	0.00433	6.442
KN400_2989	flagellar basal body P-ring formation protein FlgA	2.343 down	0.0102	5.032
KN400_0962	phage protein D, putative	2.346 down	0.0184	4.242
KN400_2027	branched-chain amino acid ABC transporter, periplasmic amino acid-binding protein, putative	2.352 down	0.00538	6.062
KN400_0125	motility response receiver histidine kinase (REC, HisKA, HATPase_c)	2.353 down	0.00242	7.518
KN400_2276	cyclopropane-fatty-acyl-phospholipid synthase	2.354 down	0.00695	5.635
KN400_0380	flagellar assembly protein FliH	2.354 down	0.0106	4.975
KN400_0656	helix-turn-helix transcriptional response regulator, LuxR family (REC, HTH_LuxR)	2.356 down	5.95E-05	24.03
KN400_3131	thiamin monophosphate kinase	2.359 down	0.014	4.576
KN400_1061	conserved hypothetical protein	2.362 down	0.00202	7.933
KN400_0097	periplasmically oriented, membrane-bound [NiFe]-hydrogenase large subunit	2.365 down	0.00158	8.546
KN400_2425	potassium-transporting ATPase, C subunit	2.376 down	0.0471	3.165
KN400_0956	phage tail sheath protein, putative	2.377 down	0.00503	6.174
KN400_0095	periplasmically oriented, membrane-bound [NiFe]-hydrogenase maturation protease	2.383 down	0.000658	10.922
KN400_0501	protein of unknown function DUF342	2.386 down	0.000344	13.357
KN400_2983	flagellar biogenesis protein FlgN, putative	2.390 down	0.00556	5.988
KN400_2262	small-conductance mechanosensitive ion channel	2.393 down	0.00186	8.126
KN400_2149	helix-turn-helix transcriptional regulator, LysR family	2.398 down	0.000335	13.73
KN400_2259	response receiver-modulated diguanylate cyclase (REC, GGDEF)	2.398 down	0.00239	7.551
KN400_0816	conserved hypothetical protein	2.399 down	0.00807	5.401
KN400_0392	flagellar biogenesis protein FliP	2.401 down	0.0107	4.964
KN400_0053	PilZ domain protein	2.408 down	0.00144	8.818
KN400_0079	response regulator (REC), putative	2.413 down	0.0354	3.468
KN400_0050	conserved hypothetical protein	2.420 down	0.00121	9.215
KN400_2726	sensor histidine kinase (PAS , PAS, PAS, HisKA, HATPase_c)	2.421 down	0.00174	8.294
KN400_0326	iron-sulfur cluster-binding oxidoreductase	2.433 down	0.00187	8.113
KN400_0100	protein of unknown function DUF162	2.433 down	0.00166	8.418
KN400_0683	membrane protein, major facilitator superfamily	2.436 down	0.0274	3.744
KN400_2561	sensor cyclic diguanylate phosphodiesterase (HAMP, GAF, HD-GYP), putative heme-binding site	2.438 down	0.00976	5.1
KN400_2686	conserved hypothetical protein	2.454 down	0.0105	4.992

KN400_0350	conserved hypothetical protein	2.463 down	0.00121	9.229
KN400_0098	periplasmically oriented, membrane-bound [NiFe]-hydrogenase small subunit	2.468 down	0.00181	8.215
KN400_0549	dihydrofolate reductase	2.477 down	0.0033	6.916
KN400_0361	conserved hypothetical protein	2.488 down	0.0398	3.34
KN400_3133	methyl-accepting chemotaxis sensory transducer, class 44H	2.491 down	0.000194	16.5
KN400_2741	nitrogenase-associated ferredoxin	2.498 down	0.0222	4.003
KN400_0766	periplasmically oriented, membrane-bound [NiFe]-hydrogenase maturation protease	2.503 down	0.0102	5.043
KN400_1428	sensor diguanylate cyclase (PAS, GGDEF)	2.504 down	0.000312	14.004
KN400_0949	hypothetical protein	2.506 down	0.00352	6.804
KN400_0379	flagellar motor switch protein FliG	2.507 down	0.0302	3.636
KN400_2274	conserved hypothetical protein	2.510 down	0.000242	15.523
KN400_3067	lipoprotein, putative	2.511 down	0.00953	5.141
KN400_0385	flagellar hook capping protein FlgD	2.516 down	0.0135	4.635
KN400_2995	flagellar biogenesis protein FlhA	2.519 down	0.000577	11.399
KN400_2598	multicopper oxidase, manganese oxidase family	2.522 down	0.00317	6.997
KN400_1575	HAMP and SpoIIE domain protein	2.537 down	0.00288	7.179
KN400_1733	metal-dependent hydrolase, subgroup D	2.540 down	0.000661	10.925
KN400_0767	twin-arginine translocation pathway protein, TatA/TatE family	2.541 down	0.0029	7.161
KN400_2992	RNA polymerase sigma-28 factor for flagellar operon	2.547 down	0.0386	3.371
KN400_1581	mechanosensitive ion channel family protein	2.557 down	0.000242	15.488
KN400_2751	cytochrome c peroxidase, 2 heme-binding sites	2.565 down	0.000104	20.169
KN400_0426	futalosine hydrolase, putative	2.578 down	0.00194	8.009
KN400_0912	ABC transporter, periplasmic substrate-binding protein, MCE domain-containing	2.584 down	0.0168	4.354
KN400_2256	YeeE/YedE family lipoprotein	2.591 down	0.00576	5.929
KN400_0698	desulfoferrodoxin, putative	2.599 down	0.00972	5.109
KN400_2749	cytochrome c, 2 heme-binding sites	2.605 down	0.000834	10.18
KN400_1358	CRISPR-associated endodeoxyribonuclease Cas1	2.620 down	0.0339	3.513
KN400_2285	sodium/proton antiporter complex Mrp, protein F	2.624 down	0.0104	5.01
KN400_0675	cyclic diguanylate phosphodiesterase (HD-GYP)	2.624 down	0.00719	5.575
KN400_0581	conserved hypothetical protein	2.627 down	0.00163	8.457
KN400_0179	MobA-related glycosyltransferase, putative	2.627 down	0.0376	3.4
KN400_0948	membrane protein, putative	2.654 down	0.000342	13.626
KN400_3164	helix-turn-helix transcriptional response regulator, LuxR family (REC, HTH_LuxR)	2.655 down	0.0116	4.849
KN400_1955	MgtC family protein	2.663 down	0.026	3.81
KN400_1730	3-methyl-2-oxobutanoate hydroxymethyltransferase	2.664 down	0.00542	6.043
KN400_0370	hemerythrin family protein	2.675 down	0.00073	10.666

KN400_2568	8-amino-7-oxononanoate synthase	2.679 down	0.0444	3.225
KN400_2593	methyl-accepting chemotaxis sensory transducer, class 40H	2.685 down	0.00274	7.289
KN400_0560	methyl-accepting chemotaxis sensory transducer, class 40H, putative dimer with helix-swapped heme-binding site-containing PAS domain	2.713 down	0.0122	4.783
KN400_3287	SpoVR-like family protein	2.721 down	0.00307	7.057
KN400_1121	protein glutamine deamidase and protein glutamate methylesterase CheD associated with MCPs of class 34H	2.722 down	0.00187	8.109
KN400_0895	aldehyde:ferredoxin oxidoreductase, tungsten-containing	2.722 down	0.000663	10.93
KN400_1276	methyl-accepting chemotaxis sensory transducer, class 34H	2.730 down	0.00222	7.706
KN400_0878	zinc protease TldD, putative modulator of DNA gyrase	2.731 down	0.00359	6.756
KN400_3511	conserved hypothetical protein	2.733 down	0.00151	8.667
KN400_0877	sensor diguanylate cyclase (GAF, GGDEF)	2.771 down	0.00158	8.525
KN400_2275	protein of unknown function DUF1365	2.771 down	0.0019	8.058
KN400_3271	protein of unknown function DUF1847	2.786 down	0.0236	3.924
KN400_3227	magnesium-dependent deoxyribonuclease, TatD family	2.793 down	0.000647	11.01
KN400_2839	ankyrin repeat protein	2.812 down	0.00851	5.32
KN400_0657	methyl-accepting chemotaxis sensory transducer, class 34H	2.832 down	0.0108	4.941
KN400_2748	catalase	2.835 down	0.000349	13.414
KN400_0818	response regulator (REC)	2.841 down	0.000377	12.742
KN400_2296	cation-translocating P-type ATPase	2.853 down	0.000292	14.46
KN400_0373	response regulator (REC)	2.854 down	0.00171	8.367
KN400_1771	integration host factor, beta subunit	2.870 down	0.0136	4.619
KN400_1770	OmpA family outer membrane protein	2.881 down	0.000301	14.114
KN400_2393	aconitate hydratase, putative	2.888 down	0.000766	10.486
KN400_2096	peptidylprolyl cis-trans isomerase, PpiC-type	2.891 down	0.000787	10.399
KN400_1260	response receiver CheY associated with MCPs of class 34H	2.893 down	0.00157	8.579
KN400_2958	glucose-1-phosphate cytidylyltransferase	2.910 down	0.0159	4.422
KN400_0799	hypothetical protein	2.934 down	0.016	4.413
KN400_2097	serine protease, subtilase family	2.939 down	0.000806	10.285
KN400_0547	nicotinamidase-related cysteine hydrolase	2.951 down	0.0255	3.834
KN400_2447	spermine/spermidine synthase-related protein	2.951 down	0.00527	6.094
KN400_2855	cytochrome c, 27 heme-binding sites	2.954 down	8.79E-05	21.957
KN400_3273	conserved hypothetical protein	2.954 down	0.00204	7.916
KN400_2984	negative regulator of flagellin synthesis FlgM	2.959 down	0.000413	12.511
KN400_2602	membrane protein, putative	2.966 down	0.0139	4.588
KN400_2857	NHL repeat domain protein	2.969 down	0.000215	16.016
KN400_3157	NHL repeat domain lipoprotein	2.975 down	0.00173	8.327
KN400_3359	radical SAM domain iron-sulfur cluster-binding oxidoreductase with cobalamin-binding-like domain	3.012 down	0.000354	13.046

KN400_2977	flagellar filament cap protein FliD	3.017 down	0.00276	7.264
KN400_0709	iron-sulfur cluster-binding oxidoreductase	3.036 down	0.0129	4.705
KN400_1309	lipoprotein, putative	3.047 down	0.00973	5.105
KN400_1229	SCO family protein	3.051 down	0.0043	6.46
KN400_0825	aconitate hydratase 1	3.053 down	0.00109	9.543
KN400_3286	VWFA superfamily protein	3.054 down	0.00186	8.137
KN400_0378	flagellar M-ring mounting plate protein FliF	3.070 down	0.0167	4.366
KN400_0265	metal-dependent phosphohydrolase (HDOD)	3.136 down	0.000779	10.438
KN400_3302	conserved hypothetical protein	3.151 down	0.0016	8.501
KN400_0324	sensor histidine kinase (DUF3365, HisKA, HATPase_c), heme-binding	3.165 down	0.00918	5.198
KN400_0697	conserved hypothetical protein	3.165 down	0.0202	4.122
KN400_2830	lipoprotein cytochrome c, 27 heme-binding sites	3.176 down	0.000697	10.783
KN400_2362	SGNH-hydrolase lipoprotein, lysophospholipase L1-like subgroup, frameshifted	3.185 down	0.0278	3.728
KN400_1592	transcriptional repressor, HgtR-related	3.190 down	0.0196	4.158
KN400_0768	conserved hypothetical protein	3.201 down	0.00011	19.851
KN400_3289	hypothetical protein	3.201 down	0.00409	6.541
KN400_0249	efflux pump, RND family, outer membrane protein	3.202 down	0.000607	11.239
KN400_1122	protein glutamate methylesterase CheB associated with MCPs of class 34H, response receiver domain-containing	3.204 down	0.00871	5.283
KN400_2364	scaffold protein CheW associated with MCPs of classes 40H and 40+24H	3.242 down	0.00686	5.663
KN400_0597	cytochrome c, 4 heme-binding sites	3.255 down	0.00105	9.632
KN400_0546	conserved hypothetical protein	3.264 down	0.0265	3.785
KN400_1010	methyl-accepting chemotaxis sensory transducer, class 40H, Cache_2 domain-containing	3.291 down	0.00212	7.843
KN400_2457	sensor diguanylate cyclase/phosphodiesterase (CHASE4, PAS, GGDEF, EAL)	3.309 down	0.000194	16.663
KN400_0054	helix-turn-helix transcriptional regulator with cupin domain	3.358 down	0.00158	8.538
KN400_2762	nitrogen fixation transcript antitermination response regulator (REC, ANTAR)	3.365 down	0.0314	3.593
KN400_2975	conserved hypothetical protein	3.385 down	6.26E-05	24.526
KN400_0427	1,4-dihydroxy-6-naphthoate synthase	3.395 down	0.00226	7.663
KN400_0794	efflux pump, RND family, outer membrane protein	3.439 down	0.0139	4.591
KN400_0343	glycine cleavage system T protein	3.465 down	0.000247	15.383
KN400_0096	periplasmically oriented, membrane-bound [NiFe]-hydrogenase b-type cytochrome subunit	3.490 down	0.000999	9.751
KN400_2476	sensor histidine kinase (HAMP, PAS, PAS, HisKA, HATPase_c)	3.507 down	0.00045	12.201
KN400_0765	periplasmically oriented, membrane-bound [NiFe]-hydrogenase large subunit	3.511 down	0.000343	13.549

KN400_2847	conserved hypothetical protein	3.511 down	0.0237	3.919
KN400_0345	glycine cleavage system P protein, subunit 1	3.558 down	0.00171	8.366
KN400_3288	ATPase, AAA family	3.577 down	0.000345	13.226
KN400_1563	cytochrome c, 2 heme-binding sites	3.589 down	0.000268	14.977
KN400_0400	type VI secretion system protein of unknown function DUF879	3.629 down	0.00279	7.242
KN400_0141	transposase, Y1_Tnp domain-containing	3.671 down	0.000342	13.535
KN400_2955	metal-dependent phosphohydrolase (HDOD)	3.696 down	0.000344	13.294
KN400_1186	protein of unknown function DUF2950	3.703 down	0.00782	5.445
KN400_3089	conserved hypothetical protein	3.707 down	0.00157	8.573
KN400_2522	sensor histidine kinase response regulator (HisKA, HATPase_c, REC, Hpt)	3.725 down	0.00158	8.534
KN400_0391	flagellar biogenesis protein FliO	3.739 down	0.0359	3.45
KN400_0893	MoaD family protein	3.802 down	0.0115	4.854
KN400_3088	HPP family protein	3.844 down	0.0109	4.937
KN400_0784	NAD(P)H:quinone oxidoreductase flavoprotein WrbA	3.846 down	0.0439	3.236
KN400_2523	metal-dependent phosphohydrolase (HDOD)	3.875 down	0.00239	7.544
KN400_2371	methyl-accepting chemotaxis sensory transducer	3.877 down	0.00148	8.741
KN400_3360	[lipopolysaccharide]-lipid A 3-O-deacylase outer membrane protein, PagL family	3.884 down	0.0026	7.393
KN400_0746	AzlC family protein	3.912 down	0.0368	3.425
KN400_2572	lipoprotein, putative	3.924 down	0.00331	6.923
KN400_0401	type VI secretion system protein of unknown function DUF1305	3.952 down	0.000278	14.851
KN400_1241	signal peptidase I	3.953 down	0.000265	15.087
KN400_3369	conserved hypothetical protein	3.972 down	0.0126	4.733
KN400_2729	SAM-dependent methyltransferase, putative	3.984 down	0.0156	4.448
KN400_2911	conserved hypothetical protein	4.011 down	0.000347	13.387
KN400_0763	periplasmically oriented, membrane-bound [NiFe]-hydrogenase iron-sulfur cluster-binding subunit	4.025 down	0.000348	13.565
KN400_2147	conserved hypothetical protein	4.029 down	0.00118	9.309
KN400_2967	flagellar basal body stator protein MotA	4.043 down	0.00455	6.349
KN400_1117	methyl-accepting chemotaxis sensory transducer, class 34H	4.060 down	0.00102	9.707
KN400_2450	conserved hypothetical protein	4.082 down	0.00456	6.341
KN400_2738	cytochrome c, 5 heme-binding sites	4.118 down	9.52E-05	20.797
KN400_1013	nitrate/nitrite-sensing methyl-accepting chemotaxis sensory transducer, class 40H, NIT domain-containing	4.124 down	0.000548	11.619
KN400_2886	methyl-accepting chemotaxis sensory transducer, class 40H	4.174 down	0.000772	10.463
KN400_0544	NrdH-like redox domain protein, YruB family	4.200 down	0.0373	3.409
KN400_2968	flagellar basal body stator protein MotB	4.231 down	0.0042	6.495
KN400_2477	periplasmic solute-binding protein	4.243 down	0.00059	11.344
KN400_1011	methyl-accepting chemotaxis sensory	4.263 down	0.00322	6.959

	transducer, class 40H			
KN400_1239	sensor histidine kinase response regulator (HisKA, HATPase_c, REC)	4.265 down	6.52E-05	24.625
KN400_2370	methyl viologen-reducing hydrogenase maturation protease	4.297 down	0.015	4.487
KN400_0195	cytochrome c oxidase, caa3-type, subunit III	4.310 down	0.00618	5.825
KN400_0325	cytochrome c nitrite reductase, 8 heme-binding sites	4.326 down	0.000346	13.303
KN400_2580	PATAN domain GTPase-activating protein, putative	4.357 down	0.00054	11.718
KN400_2725	OsmC family protein	4.365 down	0.000295	14.343
KN400_1264	sensor histidine kinase CheA associated with MCPs of class 34H	4.387 down	0.000122	18.873
KN400_1262	STAS domain protein	4.392 down	0.000604	11.283
KN400_1116	methyl-accepting chemotaxis sensory transducer, class 34H	4.402 down	0.00046	12.11
KN400_1263	response receiver CheY associated with MCPs of class 34H	4.517 down	0.00036	12.956
KN400_3362	sigma-54-dependent transcriptional response regulator (REC, sigma54 interaction, HTH8)	4.547 down	0.000249	15.322
KN400_1261	methyl-accepting chemotaxis sensory transducer, class 34H-related	4.647 down	0.000302	14.133
KN400_3361	dioxygenase, putative	4.648 down	0.0008	10.325
KN400_0250	cadherin domain/calx-beta domain protein	4.696 down	0.000349	13.307
KN400_3200	conserved hypothetical protein	4.764 down	0.00931	5.176
KN400_0372	protein phosphoaspartate phosphatase CheX associated with MCPs of classes 40H and 40+24H	4.906 down	0.000123	18.541
KN400_3151	cytochrome c, 3 heme-binding sites	4.932 down	0.00289	7.175
KN400_0371	response receiver CheY associated with MCPs of classes 40H and 40+24H	4.942 down	0.000612	11.2
KN400_3502	hypothetical protein	4.972 down	0.00713	5.591
KN400_0598	conserved hypothetical protein	4.994 down	0.0017	8.365
KN400_0653	SAM-dependent methyltransferase	5.041 down	0.00695	5.637
KN400_0859	response receiver scaffold protein CheV (CheW, REC)	5.063 down	0.00308	7.037
KN400_3522	thioredoxin family protein, selenocysteine-containing	5.129 down	0.0137	4.613
KN400_1839	UDP-glucose 6-dehydrogenase	5.135 down	0.00281	7.224
KN400_3436	hypothetical protein	5.142 down	2.43E-05	38.064
KN400_1243	hypothetical protein	5.164 down	6.85E-05	25.356
KN400_2368	methyl viologen-reducing hydrogenase-associated ferredoxin	5.201 down	0.000522	11.831
KN400_2163	response receiver CheY associated with MCPs of class 40H	5.309 down	0.00229	7.629
KN400_2611	hypothetical protein	5.422 down	0.000959	9.828
KN400_2837	SEL1 repeat-containing protein	5.433 down	0.000239	15.599
KN400_3158	cytochrome c, 5 heme-binding sites	5.471 down	0.00378	6.678
KN400_0572	cytochrome c, 7 heme-binding sites	5.515 down	0.000415	12.484
KN400_2841	lipoprotein cytochrome c, 23 heme-binding sites	5.560 down	0.00118	9.299
KN400_2976	flagellin export facilitator protein FliS	5.661 down	0.00408	6.55

KN400_0571	cytochrome b, putative	5.796 down	0.000621	11.146
KN400_1119	protein glutamate methyltransferase CheR associated with MCPs of class 34H	5.826 down	0.000397	12.613
KN400_0268	scaffold protein CheW associated with MCPs of classes 40H and 40+24H	5.939 down	0.00185	8.162
KN400_2579	conserved hypothetical protein	5.983 down	0.00139	8.942
KN400_0267	sensor histidine kinase CheA associated with MCPs of classes 40H and 40+24H	6.048 down	0.000571	11.434
KN400_1766	pppGpp 5'-phosphohydrolase and exopolyphosphatase, putative	6.079 down	0.00679	5.687
KN400_0266	protein glutamate methyltransferase CheR associated with MCPs of classes 40H and 40+24H	6.095 down	0.000101	21.02
KN400_2521	response receiver-modulated cyclic diguanylate phosphodiesterase (REC, HD-GYP)	6.106 down	0.0018	8.232
KN400_1238	histidine phosphotransfer domain protein	6.205 down	0.000789	10.405
KN400_2956	flagellar protein FlaG	6.213 down	0.0134	4.653
KN400_0885	response receiver (REC)	6.234 down	0.0059	5.892
KN400_0397	lipoprotein, putative	6.252 down	0.00035	13.135
KN400_2526	methyl-accepting chemotaxis sensory transducer, class 40H	6.370 down	6.98E-05	25.646
KN400_0892	ThiF family protein	6.379 down	0.00187	8.091
KN400_3357	lipoprotein, putative	6.542 down	0.000107	19.842
KN400_0822	rubredoxin reductase	6.622 down	0.022	4.015
KN400_0733	methyl-accepting chemotaxis sensory transducer, class 40H	6.692 down	0.00378	6.681
KN400_3201	conserved hypothetical protein	6.748 down	0.00546	6.031
KN400_2957	metalloprotease domain protein	6.824 down	0.000377	12.764
KN400_1118	scaffold protein CheW associated with MCPs of class 34H	6.903 down	0.000277	14.822
KN400_0398	type VI secretion system protein of unknown function DUF876	7.166 down	0.00114	9.423
KN400_2978	flagellin	7.474 down	0.000812	10.245
KN400_1269	periplasmic solute-binding protein	7.601 down	0.00145	8.832
KN400_1242	helix-turn-helix transcriptional regulator, LysR family	7.674 down	0.000327	13.835
KN400_2829	cytochrome c, 7 heme-binding sites	7.689 down	0.000354	13.027
KN400_0011	flagellar biogenesis master response receiver sensor histidine kinase (REC, PAS, GAF, HisKA, HATPase_c)	7.801 down	0.000098	20.575
KN400_1016	response receiver-modulated diguanylate cyclase/phosphodiesterase (REC, GGDEF, EAL)	7.832 down	0.000289	14.58
KN400_0419	conserved hypothetical protein	7.935 down	0.00409	6.544
KN400_2527	conserved hypothetical protein	8.129 down	0.00014	17.929
KN400_2838	hypothetical protein	8.528 down	0.000746	10.565
KN400_2367	methyl viologen-reducing hydrogenase, large subunit	8.648 down	0.000346	13.628
KN400_1965	sensor histidine kinase cyclic nucleotide phosphodiesterase (GAF, HisKA, HATPase_c, GAF, HD-GYP-related)	8.952 down	0.000319	13.925
KN400_1583	radical SAM domain iron-sulfur cluster-binding oxidoreductase	9.133 down	0.00139	8.933

KN400_0399	type VI secretion system lysozyme-related protein of unknown function DUF1316	9.294 down	0.000289	14.511
KN400_2016	PEP motif-containing protein, putative exosortase substrate	9.338 down	0.000895	9.996
KN400_2524	conserved hypothetical protein	10.626 down	0.00174	8.308
KN400_2481	dienelactone hydrolase family protein	10.963 down	0.0311	3.604
KN400_1969	PEP motif-containing protein, putative exosortase substrate	11.184 down	2.58E-05	32.709
KN400_0677	cytochrome c, 6 heme-binding sites	12.287 down	0.000838	10.154
KN400_3363	sensor histidine kinase (HisKA, HATPase_c)	12.529 down	5.61E-05	27.037
KN400_3358	hypothetical protein	13.073 down	0.000285	14.579
KN400_0388	flagellar basal body-associated protein FliL	14.686 down	0.000954	9.845
KN400_1009	methyl-accepting chemotaxis sensory transducer, class 40H	15.444 down	0.000656	10.973
KN400_2525	scaffold protein CheW associated with MCPs of classes 40H and 40+24H	16.711 down	0.00193	8.022
KN400_1582	#N/A	18.590 down	0.00284	7.2
KN400_3449	hypothetical protein	19.115 down	0.0289	3.684
KN400_1970	PEP motif-containing protein, putative exosortase substrate	21.020 down	0.000194	16.605
KN400_3090	PAS domain protein	26.255 down	0.0105	4.994
KN400_1523	geopilin	1834.866 down	0.000112	19.399

REFERENCES

Afkar, E., Reguera, G., Schiffer, M., and Lovley, D.R. (2005). A novel *Geobacteraceae*-specific outer membrane protein J (OmpJ) is essential for electron transport to Fe(III) and Mn(IV) oxides in *Geobacter sulfurreducens*. *BMC Microbiol* **5,** 41. doi: 10.1186/1471-2180-5-41.

Aklujkar, M., Coppi, M.V., Leang, C., Kim, B.C., Chavan, M.A., Perpetua, L.A., Giloteaux, L., Liu, A., and Holmes, D.E. (2013). Proteins involved in electron transfer to Fe(III) and Mn(IV) oxides by *Geobacter sulfurreducens* and *Geobacter uraniireducens*. *Microbiology* **159,** 515-535. doi: 10.1099/mic.0.064089-0.

Aklujkar, M., Haveman, S.A., Didonato, R., Jr., Chertkov, O., Han, C.S., Land, M.L., Brown, P., and Lovley, D.R. (2012). The genome of *Pelobacter carbinolicus* reveals surprising metabolic capabilities and physiological features. *BMC Genomics* **13,** 690. doi: 10.1186/1471-2164-13-690.

Aklujkar, M., Krushkal, J., Dibartolo, G., Lapidus, A., Land, M.L., and Lovley, D.R. (2009). The genome sequence of *Geobacter metallireducens*: features of metabolism, physiology and regulation common and dissimilar to *Geobacter sulfurreducens*. *BMC Microbiol* **9,** 109. doi: 10.1186/1471-2180-9-109.

Aklujkar, M., and Lovley, D.R. (2010). Interference with histidyl-tRNA synthetase by a CRISPR spacer sequence as a factor in the evolution of *Pelobacter carbinolicus*. *BMC Evol Biol* **10,** 230. doi: 1471-2148-10-230 [pii] 10.1186/1471-2148-10-230.

Aklujkar, M., Risso, C., Smith, J., Beaulieu, D., Dubay, R., Giloteaux, L., Diburro, K., and Holmes, D. (2014). Anaerobic degradation of aromatic amino acids by the hyperthermophilic archaeon, *Ferroglobus placidus*. *Microbiology*. doi: 10.1099/mic.0.083261-0.

Aktas, O., and Cecen, F. (2007). Adsorption reversibility and bioregeneration of activated carbon in the treatment of phenol. *Water Sci Technol* **55,** 237-244.

Aller, R.C., Mackin, J.E., and Cox, R.T. (1986). Diagenesis of Fe and S in Amazon inner shelf muds - apparent dominance of Fe reduction and implications for the genesis of ironstones. *Continental Shelf Research* **6,** 263-289. doi: Doi 10.1016/0278-4343(86)90064-6.

Anderson, I., Risso, C., Holmes, D., Lucas, S., Copeland, A., Lapidus, A., Cheng, J.F., Bruce, D., Goodwin, L., Pitluck, S., Saunders, E., Brettin, T., Detter, J.C., Han, C., Tapia, R., Larimer, F., Land, M., Hauser, L., Woyke, T., Lovley, D., Kyrpides, N., and Ivanova, N. (2011). Complete genome sequence of *Ferroglobus placidus* AEDII12DO. *Stand Genomic Sci* **5,** 50-60. doi: 10.4056/sigs.2225018.

Anderson, R.T., and Lovley, D.R. (1999). Naphthalene and benzene degradation under Fe(III)-reducing conditions in petroleum-contaminated aquifers. *Bioremediation Journal* **3,** 121-135. doi: 10.1080/10889869991219271.

Anderson, R.T., Vrionis, H.A., Ortiz-Bernad, I., Resch, C.T., Long, P.E., Dayvault, R., Karp, K., Marutzky, S., Metzler, D.R., Peacock, A., White, D.C., Lowe, M., and Lovley, D.R. (2003). Stimulating the in situ activity of *Geobacter* species to remove uranium from the groundwater of a uranium-contaminated aquifer. *Appl Environ Microbiol* **69,** 5884-5891.

Arnold, J.W., and Shimkets, L.J. (1988). Cell surface properties correlated with cohesion in *Myxococcus xanthus*. *J Bacteriol* **170,** 5771-5777.

Aziz, S.Q., Aziz, H.A., Yusoff, M.S., and Bashir, M.J. (2011). Landfill leachate treatment using powdered activated carbon augmented sequencing batch reactor (SBR) process: optimization by response surface methodology. *J Hazard Mater* **189,** 404-413. doi: 10.1016/j.jhazmat.2011.02.052.

Balch, W.E., Fox, G.E., Magrum, L.J., Woese, C.R., and Wolfe, R.S. (1979). Methanogens: reevaluation of a unique biological group. *Microbiol Rev* **43,** 260-296.

Bond, D.R., Holmes, D.E., Tender, L.M., and Lovley, D.R. (2002a). Electrode-reducing microorganisms that harvest energy from marine sediments. *Science* **295,** 483-485. doi: 10.1126/science.1066771.

Bond, D.R., and Lovley, D.R. (2002b). Reduction of Fe(III) oxide by methanogens in the presence and absence of extracellular quinones. *Environ Microbiol* **4,** 115-124.

Bond, D.R., and Lovley, D.R. (2003). Electricity production by *Geobacter sulfurreducens* attached to electrodes. *Appl Environ Microbiol* **69,** 1548-1555.

Bork, P., Holm, L., and Sander, C. (1994). The immunoglobulin fold. Structural classification, sequence patterns and common core. *J Mol Biol* **242,** 309-320. doi: 10.1006/jmbi.1994.1582.

Bucking, C., Piepenbrock, A., Kappler, A., and Gescher, J. (2012). Outer-membrane cytochrome-independent reduction of extracellular electron acceptors in *Shewanella oneidensis*. *Microbiology* **158,** 2144-2157. doi: 10.1099/mic.0.058404-0.

Burrows, L.L., Charter, D.F., and Lam, J.S. (1996). Molecular characterization of the *Pseudomonas aeruginosa* serotype O5 (PAO1) B-band lipopolysaccharide gene cluster. *Mol Microbiol* **22,** 481-495.

Butler, J.E., Glaven, R.H., Esteve-Nunez, A., Nunez, C., Shelobolina, E.S., Bond, D.R., and Lovley, D.R. (2006). Genetic characterization of a single bifunctional enzyme for fumarate reduction and succinate oxidation in *Geobacter sulfurreducens* and engineering of fumarate reduction in *Geobacter metallireducens*. *J Bacteriol* **188,** 450-455. doi: 10.1128/JB.188.2.450-455.2006.

Butler, J.E., He, Q., Nevin, K.P., He, Z., Zhou, J., and Lovley, D.R. (2007). Genomic and microarray analysis of aromatics degradation in *Geobacter metallireducens* and comparison to a *Geobacter* isolate from a contaminated field site. *BMC Genomics* **8,** 180. doi: 10.1186/1471-2164-8-180.

Butler, J.E., Kaufmann, F., Coppi, M.V., Nunez, C., and Lovley, D.R. (2004). MacA, a diheme *c*-type cytochrome involved in Fe(III) reduction by *Geobacter sulfurreducens*. *J Bacteriol* **186,** 4042-4045. doi: 10.1128/JB.186.12.4042-4045.2004.

Butler, J.E., Young, N.D., Aklujkar, M., and Lovley, D.R. (2012). Comparative genomic analysis of *Geobacter sulfurreducens* KN400, a strain with enhanced capacity for extracellular electron transfer and electricity production. *BMC Genomics* **13,** 471. doi: 10.1186/1471-2164-13-471.

Butler, J.E., Young, N.D., and Lovley, D.R. (2010). Evolution of electron transfer out of the cell: comparative genomics of six *Geobacter* genomes. *BMC Genomics* **11,** 40. doi: 10.1186/1471-2164-11-40.

Caccavo, F., Jr., Lonergan, D.J., Lovley, D.R., Davis, M., Stolz, J.F., and Mcinerney, M.J. (1994). *Geobacter sulfurreducens* sp. nov., a hydrogen- and acetate-oxidizing dissimilatory metal-reducing microorganism. *Appl Environ Microbiol* **60,** 3752-3759.

Canfield, D.E., Thamdrup, B., and Hansen, J.W. (1993). The anaerobic degradation of organic matter in Danish coastal sediments: iron reduction, manganese reduction, and sulfate reduction. *Geochim Cosmochim Acta* **57,** 3867-3883.

Chen, S., Rotaru, A.E., Liu, F., Philips, J., Woodard, T.L., Nevin, K.P., and Lovley, D.R. (2014a). Carbon cloth stimulates direct interspecies electron transfer in syntrophic co-cultures. *Bioresour. Technol.* **173C,** 82-86. doi: 10.1016/j.biortech.2014.09.009.

Chen, S., Rotaru, A.E., Shrestha, P.M., Malvankar, N.S., Liu, F., Fan, W., Nevin, K.P., and Lovley, D.R. (2014b). Promoting interspecies electron transfer with biochar. *Sci. Rep.* **4,** 5019. doi: 10.1038/srep05019.

Childers, S.E., Ciufo, S., and Lovley, D.R. (2002). *Geobacter metallireducens* accesses insoluble Fe(III) oxide by chemotaxis. *Nature* **416,** 767-769. doi: 10.1038/416767a.

Coates, J.D., Lonergan, D.J., Philips, E.J., Jenter, H., and Lovley, D.R. (1995). *Desulfuromonas palmitatis* sp. nov., a marine dissimilatory Fe(III) reducer that can oxidize long-chain fatty acids. *Arch Microbiol* **164,** 406-413.

Coppi, M.V., Leang, C., Sandler, S.J., and Lovley, D.R. (2001). Development of a genetic system for *Geobacter sulfurreducens*. *Appl Environ Microbiol* **67,** 3180-3187. doi: 10.1128/AEM.67.7.3180-3187.2001.

Coppi, M.V., O'neil, R.A., and Lovley, D.R. (2004). Identification of an uptake hydrogenase required for hydrogen-dependent reduction of Fe(III) and other electron acceptors by *Geobacter sulfurreducens*. *J Bacteriol* **186,** 3022-3028.

Cord-Ruwisch, R., Lovley, D.R., and Schink, B. (1998). Growth of *Geobacter sulfurreducens* with acetate in syntrophic cooperation with hydrogen-oxidizing anaerobic partners. *Appl Environ Microbiol* **64,** 2232-2236.

Coursolle, D., Baron, D.B., Bond, D.R., and Gralnick, J.A. (2010). The Mtr respiratory pathway is essential for reducing flavins and electrodes in *Shewanella oneidensis*. *J Bacteriol* **192,** 467-474. doi: 10.1128/JB.00925-09.

Daltrop, O., Allen, J.W., Willis, A.C., and Ferguson, S.J. (2002). In vitro formation of a *c*-type cytochrome. *Proc Natl Acad Sci U S A* **99,** 7872-7876. doi: 10.1073/pnas.132259099.

Daniels, C., and Morona, R. (1999). Analysis of *Shigella flexneri wzz* (Rol) function by mutagenesis and cross-linking: wzz is able to oligomerize. *Mol Microbiol* **34,** 181-194.

Ding, Y.H., Hixson, K.K., Aklujkar, M.A., Lipton, M.S., Smith, R.D., Lovley, D.R., and Mester, T. (2008). Proteome of *Geobacter sulfurreducens* grown with Fe(III) oxide or Fe(III) citrate as the electron acceptor. *Biochim Biophys Acta* **1784,** 1935-1941. doi: 10.1016/j.bbapap.2008.06.011.

Ding, Y.H., Hixson, K.K., Giometti, C.S., Stanley, A., Esteve-Nunez, A., Khare, T., Tollaksen, S.L., Zhu, W., Adkins, J.N., Lipton, M.S., Smith, R.D., Mester, T., and Lovley, D.R. (2006). The proteome of dissimilatory metal-reducing microorganism *Geobacter sulfurreducens* under various growth conditions. *Biochim Biophys Acta* **1764,** 1198-1206. doi: 10.1016/j.bbapap.2006.04.017.

Doran, J.W., and Alexander, M. (1977). Microbial Formation of Volatile Selenium-Compounds in Soil. *Soil Science Society of America Journal* **41,** 70-73.

Dumas, C., Basseguy, R., and Bergel, A. (2008). Microbial electrocatalysis with *Geobacter sulfurreducens* biofilm on stainless steel cathodes. *Electrochimica Acta* **53,** 2494-2500. doi: DOI 10.1016/j.electacta.2007.10.018.

El-Naggar, M.Y., Wanger, G., Leung, K.M., Yuzvinsky, T.D., Southam, G., Yang, J., Lau, W.M., Nealson, K.H., and Gorby, Y.A. (2010). Electrical transport along bacterial nanowires from *Shewanella oneidensis* MR-1. *Proc Natl Acad Sci U S A* **107,** 18127-18131. doi: 10.1073/pnas.1004880107.

Faridmoayer, A., Fentabil, M.A., Mills, D.C., Klassen, J.S., and Feldman, M.F. (2007). Functional characterization of bacterial oligosaccharyltransferases involved in O-linked protein glycosylation. *J Bacteriol* **189,** 8088-8098. doi: 10.1128/JB.01318-07.

Finneran, K.T., Housewright, M.E., and Lovley, D.R. (2002). Multiple influences of nitrate on uranium solubility during bioremediation of uranium-contaminated subsurface sediments. *Environ Microbiol* **4,** 510-516.

Giloteaux, L., Holmes, D.E., Williams, K.H., Wrighton, K.C., Wilkins, M.J., Montgomery, A.P., Smith, J.A., Orellana, R., Thompson, C.A., Roper, T.J., Long, P.E., and Lovley, D.R. (2013). Characterization and transcription of arsenic respiration and resistance genes during in situ uranium bioremediation. *ISME J* **7,** 370-383. doi: 10.1038/ismej.2012.109.

Gorby, Y.A., and Lovley, D.R. (1991). Electron transport in the dissimilatory iron reducer, GS-15. *Appl Environ Microbiol* **57,** 867-870.

Gorby, Y.A., and Lovley, D.R. (1992). Enzymatic uranium precipitation. *Environ Sci Technol* **26,** 205-207. doi: Doi 10.1021/Es00025a026.

Gralnick, J.A., and Newman, D.K. (2007). Extracellular respiration. *Mol Microbiol* **65,** 1-11. doi: 10.1111/j.1365-2958.2007.05778.x.

Gregory, K.B., Bond, D.R., and Lovley, D.R. (2004). Graphite electrodes as electron donors for anaerobic respiration. *Environ Microbiol* **6,** 596-604. doi: 10.1111/j.1462-2920.2004.00593.x.

Gregory, K.B., and Lovley, D.R. (2005). Remediation and recovery of uranium from contaminated subsurface environments with electrodes. *Environ Sci Technol* **39,** 8943-8947.

Gregory, K.B., Mason, M.G., Picken, H.D., Weathers, L.J., and Parkin, G.F. (2000). Bioaugmentation of Fe(0) for the remediation of chlorinated aliphatic hydrocarbons. *Environmental Engineering Science* **17,** 169-181. doi: DOI 10.1089/ees.2000.17.169.

Guo, H., Kong, Q., Cheng, J., Wang, L., and Feng, L. (2005a). Characterization of the *Escherichia coli* O59 and O155 O-antigen gene clusters: the atypical *wzx* genes are evolutionary related. *FEMS Microbiol Lett* **248,** 153-161. doi: 10.1016/j.femsle.2005.05.036.

Guo, H., Yi, W., Shao, J., Lu, Y., Zhang, W., Song, J., and Wang, P.G. (2005b). Molecular analysis of the O-antigen gene cluster of *Escherichia coli* O86:B7 and characterization of the chain length determinant gene (*wzz*). *Appl Environ Microbiol* **71,** 7995-8001. doi: 10.1128/AEM.71.12.7995-8001.2005.

Hafenbradl, D., Keller, M., Dirmeier, R., Rachel, R., Rossnagel, P., Burggraf, S., Huber, H., and Stetter, K.O. (1996). *Ferroglobus placidus* gen. nov., sp. nov., A novel hyperthermophilic archaeum that oxidizes Fe2+ at neutral pH under anoxic conditions. *Arch Microbiol* **166,** 308-314.

Hartshorne, R.S., Reardon, C.L., Ross, D., Nuester, J., Clarke, T.A., Gates, A.J., Mills, P.C., Fredrickson, J.K., Zachara, J.M., Shi, L., Beliaev, A.S., Marshall, M.J., Tien, M., Brantley, S., Butt, J.N., and Richardson, D.J. (2009). Characterization of an electron conduit between bacteria and the extracellular environment. *Proc Natl Acad Sci U S A* **106,** 22169-22174. doi: 10.1073/pnas.0900086106.

Holm, N.G., Cairns-Smith, A.G., Daniel, R.M., Ferris, J.P., Hennet, R.J., Shock, E.L., Simoneit, B.R., and Yanagawa, H. (1992). Marine hydrothermal systems and the origin of life: future research. *Orig Life Evol Biosph* **22,** 181-242.

Holmes, D.E., Chaudhuri, S.K., Nevin, K.P., Mehta, T., Methe, B.A., Liu, A., Ward, J.E., Woodard, T.L., Webster, J., and Lovley, D.R. (2006). Microarray and genetic analysis of electron transfer to electrodes in *Geobacter sulfurreducens*. *Environ Microbiol* **8,** 1805-1815. doi: 10.1111/j.1462-2920.2006.01065.x.

Holmes, D.E., Finneran, K.T., O'neil, R.A., and Lovley, D.R. (2002). Enrichment of members of the family *Geobacteraceae* associated with stimulation of dissimilatory metal reduction in uranium-contaminated aquifer sediments. *Appl Environ Microbiol* **68,** 2300-2306.

Holmes, D.E., Mester, T., O'neil, R.A., Perpetua, L.A., Larrahondo, M.J., Glaven, R., Sharma, M.L., Ward, J.E., Nevin, K.P., and Lovley, D.R. (2008). Genes for two multicopper proteins required for Fe(III) oxide reduction in *Geobacter sulfurreducens* have different expression patterns both in the subsurface and on energy-harvesting electrodes. *Microbiology-Sgm* **154,** 1422-1435. doi: DOI 10.1099/mic.0.2007/014365-0.

Holmes, D.E., Nevin, K.P., O'neil, R.A., Ward, J.E., Adams, L.A., Woodard, T.L., Vrionis, H.A., and Lovley, D.R. (2005). Potential for quantifying expression of the *Geobacteraceae* citrate synthase gene to assess the activity of *Geobacteraceae* in the subsurface and on current-harvesting electrodes. *Appl Environ Microbiol* **71,** 6870-6877. doi: 10.1128/AEM.71.11.6870-6877.2005.

Holmes, D.E., O'neil, R.A., Chavan, M.A., N'guessan, L.A., Vrionis, H.A., Perpetua, L.A., Larrahondo, M.J., Didonato, R., Liu, A., and Lovley, D.R. (2009). Transcriptome of *Geobacter uraniireducens* growing in uranium-contaminated subsurface sediments. *ISME J* **3,** 216-230. doi: 10.1038/ismej.2008.89.

Holmes, D.E., O'neil, R.A., Vrionis, H.A., N'guessan L, A., Ortiz-Bernad, I., Larrahondo, M.J., Adams, L.A., Ward, J.A., Nicoll, J.S., Nevin, K.P., Chavan, M.A., Johnson, J.P., Long, P.E., and Lovley, D.R. (2007). Subsurface clade of *Geobacteraceae* that predominates in a diversity of Fe(III)-reducing subsurface environments. *ISME J* **1,** 663-677. doi: 10.1038/ismej.2007.85.

Holmes, D.E., Risso, C., Smith, J.A., and Lovley, D.R. (2011). Anaerobic oxidation of benzene by the hyperthermophilic archaeon *Ferroglobus placidus*. *Appl Environ Microbiol* **77,** 5926-5933. doi: 10.1128/AEM.05452-11.

Holmes, D.E., Risso, C., Smith, J.A., and Lovley, D.R. (2012). Genome-scale analysis of anaerobic benzoate and phenol metabolism in the hyperthermophilic archaeon *Ferroglobus placidus*. *ISME J* **6,** 146-157. doi: 10.1038/ismej.2011.88.

Horzempa, J., Dean, C.R., Goldberg, J.B., and Castric, P. (2006). *Pseudomonas aeruginosa* 1244 pilin glycosylation: glycan substrate recognition. *J Bacteriol* **188,** 4244-4252. doi: 10.1128/JB.00273-06.

Inoue, K., Leang, C., Franks, A.E., Woodard, T.L., Nevin, K.P., and Lovley, D.R. (2011). Specific localization of the *c*-type cytochrome OmcZ at the anode surface in current-producing biofilms of *Geobacter sulfurreducens*. *Environmental Microbiology Reports* **3,** 211-217. doi: 10.1111/j.1758-2229.2010.00210.x.

Inoue, K., Qian, X., Morgado, L., Kim, B.C., Mester, T., Izallalen, M., Salgueiro, C.A., and Lovley, D.R. (2010). Purification and characterization of OmcZ, an outer-surface, octaheme *c*-type cytochrome essential for optimal current production by *Geobacter sulfurreducens*. *Appl Environ Microbiol* **76,** 3999-4007. doi: 10.1128/AEM.00027-10.

Karri, S., Sierra-Alvarez, R., and Field, J.A. (2005). Zero valent iron as an electron-donor for methanogenesis and sulfate reduction in anaerobic sludge. *Biotechnol Bioeng* **92,** 810-819. doi: Doi 10.1002/Bit.20623.

Kashefi, K., Holmes, D.E., Lovley, D.R., and Tor, J.M. (2004). Potential importance of dissimilatory Fe(III)-reducing microorganisms in hot sedimentary environments. *Subseafloor Biosphere at Mid-Ocean Ranges* 144**,** 199-211. doi: Doi 10.1029/144gm13.

Kashefi, K., Tor, J.M., Nevin, K.P., and Lovley, D.R. (2001). Reductive precipitation of gold by dissimilatory Fe(III)-reducing bacteria and archaea. *Appl Environ Microbiol* **67,** 3275-3279. doi: 10.1128/AEM.67.7.3275-3279.2001.

Kastening, B., Hahn, M., Rabanus, B., Heins, M., and Zumfelde, U. (1997). Electronic properties and double layer of activated carbon. *Electrochimica Acta* **42,** 2789-2799. doi: Doi 10.1016/S0013-4686(97)00082-0.

Kato, S., Hashimoto, K., and Watanabe, K. (2012). Microbial interspecies electron transfer via electric currents through conductive minerals. *Proc. Natl. Acad. Sci. U.S.A.* **109,** 10042-10046. doi: 10.1073/pnas.1117592109.

Kim, B.C., Leang, C., Ding, Y.H.R., Glaven, R.H., Coppi, M.V., and Lovley, D.R. (2005). OmcF, a putative *c*-type monoheme outer membrane cytochrome required for the expression of other outer membrane cytochromes in *Geobacter sulfurreducens*. *J Bacteriol* **187,** 4505-4513. doi: Doi 10.1128/Jb.187.134505-4513.2005.

Kim, B.C., Qian, X.L., Ching, L.A., Coppi, M.V., and Lovley, D.R. (2006). Two putative *c*-type multiheme cytochromes required for the expression of OmcB, an outer membrane protein essential for optimal Fe(III) reduction in *Geobacter sulfurreducens*. *J Bacteriol* **188,** 3138-3142. doi: Doi 10.1128/Jb.188.8.3138-3142.2006.

Kostka, J.E., and Nealson, K.H. (1995). Dissolution and reduction of magnetite by bacteria. *Environ Sci Technol* **29,** 2535-2540.

Kotloski, N.J., and Gralnick, J.A. (2013). Flavin Electron Shuttles Dominate Extracellular Electron Transfer by *Shewanella oneidensis*. *MBio* **4**. doi: ARTN e00553 DOI 10.1128/mBio.00553-12.

Lampron, K.J., Chiu, P.C., and Cha, D.K. (2001). Reductive dehalogenation of chlorinated ethenes with elemental iron: The role of microorganisms. *Water Res* **35,** 3077-3084. doi: Doi 10.1016/S0043-1354(01)00017-3.

Law, N., Ansari, S., Livens, F.R., Renshaw, J.C., and Lloyd, J.R. (2008). Formation of nanoscale elemental silver particles via enzymatic reduction by *Geobacter sulfurreducens*. *Applied and Environmental Microbiology* **74,** 7090-7093. doi: Doi 10.1128/Aem.01069-08.

Leang, C., Coppi, M.V., and Lovley, D.R. (2003). OmcB, a *c*-type polyheme cytochrome, involved in Fe(III) reduction in *Geobacter sulfurreducens*. *J Bacteriol* **185,** 2096-2103.

Leang, C., Malvankar, N.S., Franks, A.E., Nevin, K.P., and Lovley, D.R. (2013). Engineering *Geobacter sulfurreducens* to produce a highly cohesive conductive matrix with enhanced capacity for current production. *Energy & Environmental Science* **6,** 1901-1908. doi: Doi 10.1039/C3ee40441b.

Leang, C., Qian, X.L., Mester, T., and Lovley, D.R. (2010). Alignment of the *c*-type cytochrome OmcS along pili of *Geobacter sulfurreducens*. *Appl Environ Microbiol* **76,** 4080-4084. doi: Doi 10.1128/Aem.00023-10.

Leung, K.M., Wanger, G., El-Naggar, M.Y., Gorby, Y., Southam, G., Lau, W.M., and Yang, J. (2013). *Shewanella oneidensis* MR-1 bacterial nanowires exhibit *p*-type, tunable electronic behavior. *Nano Lett* **13,** 2407-2411. doi: 10.1021/nl400237p.

Li, X.Q., Elliott, D.W., and Zhang, W.X. (2006). Zero-valent iron nanoparticles for abatement of environmental pollutants: Materials and engineering aspects. *Critical Reviews in Solid State and Materials Sciences* **31,** 111-122. doi: Doi 10.1080/10408430601057611.

Liang, L.Y., Korte, N., Gu, B.H., Puls, R., and Reeter, C. (2000). Geochemical and microbial reactions affecting the long-term performance of in situ 'iron barriers'. *Advances in Environmental Research* **4,** 273-286. doi: Doi 10.1016/S1093-0191(00)00026-5.

Lies, D.P., Hernandez, M.E., Kappler, A., Mielke, R.E., Gralnick, J.A., and Newman, D.K. (2005). *Shewanella oneidensis* MR-1 uses overlapping pathways for iron reduction at a distance and by direct contact under conditions relevant for biofilms. *Appl Environ Microbiol* **71,** 4414-4426. doi: 10.1128/AEM.71.8.4414-4426.2005.

Lin TJ, Breves EA, Dyar MD, Ver Eecke HC, Jamieson JW, Holden JF. 2014. Magnetite formation from ferrihydrite by hyperthermophilic archaea from Endeavour Segment, Juan de Fuca Ridge hydrothermal vent chimneys. Geobiology **12:**200-211.

Liu, F.H., Rotaru, A.E., Shrestha, P.M., Malvankar, N.S., Nevin, K.P., and Lovley, D.R. (2012). Promoting direct interspecies electron transfer with activated carbon. *Energy & Environmental Science* **5,** 8982-8989. doi: Doi 10.1039/C2ee22459c.

Liu, F., Rotaru, A.E., Shrestha, P.M., Malvankar, N.S., Nevin, K.P., and Lovley, D.R. (2014). Magnetite compensates for the lack of a pilin-associated *c*-type cytochrome in extracellular electron exchange. *Environ. Microbiol*. **doi**: 10.1111/1462-2920.12485.

Livak, K.J., and Schmittgen, T.D. (2001). Analysis of relative gene expression data using real-time quantitative PCR and the 2(-Delta Delta C(T)) Method. *Methods* **25,** 402-408. doi: 10.1006/meth.2001.1262.

Lloyd, J.R., Blunt-Harris, E.L., and Lovley, D.R. (1999). The periplasmic 9.6-kilodalton *c*-type cytochrome of *Geobacter sulfurreducens* is not an electron shuttle to Fe(III). *J Bacteriol* **181,** 7647-7649.

Lloyd, J.R., Leang, C., Myerson, A.L.H., Coppi, M.V., Cuifo, S., Methe, B., Sandler, S.J., and Lovley, D.R. (2003). Biochemical and genetic characterization of PpcA, a periplasmic *c*-type cytochrome in *Geobacter sulfurreducens*. *Biochemical Journal* **369,** 153-161. doi: Doi 10.1042/Bj20020597.

Lloyd, J.R., and Macaskie, L.E. (1996). A novel phosphorImager-based technique for monitoring the microbial reduction of technetium. *Appl Environ Microbiol* **62,** 578-582.

Lloyd, J.R., Sole, V.A., Van Praagh, C.V., and Lovley, D.R. (2000). Direct and Fe(II)-mediated reduction of technetium by Fe(III)-reducing bacteria. *Appl Environ Microbiol* **66,** 3743-3749.

Lovley, D.R. (1991a). Dissimilatory Fe(III) and Mn(IV) reduction. *Microbiol Rev* **55,** 259-287.

Lovley, D.R. (1993a). Dissimilatory metal reduction. *Annu Rev Microbiol* **47,** 263-290. doi: 10.1146/annurev.mi.47.100193.001403.

Lovley, D.R. (1995). Microbial reduction of iron, manganese, and other metals. *Advances in Agronomy, Vol 54* **54,** 175-231. doi: Doi 10.1016/S0065-2113(08)60900-1.

Lovley, D.R. (2006a). Bug juice: harvesting electricity with microorganisms. *Nat Rev Microbiol* **4,** 497-508. doi: 10.1038/nrmicro1442.

Lovley, D.R. (2006b). Microbial fuel cells: novel microbial physiologies and engineering approaches. *Curr Opin Biotechnol* **17,** 327-332. doi: 10.1016/j.copbio.2006.04.006.

Lovley, D.R. (2008). The microbe electric: conversion of organic matter to electricity. *Curr Opin Biotechnol* **19,** 564-571. doi: 10.1016/j.copbio.2008.10.005.

Lovley, D.R. (2011a). Live wires: direct extracellular electron exchange for bioenergy and the bioremediation of energy-related contamination. *Energy & Environmental Science* **4,** 4896-4906. doi: Doi 10.1039/C1ee02229f.

Lovley, D.R. (2011b). Reach out and touch someone: potential impact of DIET (direct interspecies energy transfer) on anaerobic biogeochemistry, bioremediation, and bioenergy. *Reviews in Environmental Science and Bio-Technology* **10,** 101-105. doi: DOI 10.1007/s11157-011-9236-9.

Lovley, D.R. (2011e). Powering microbes with electricity: direct electron transfer from electrodes to microbes. *Environ. Microbiol. Rep.* 3**,** 27-35. **doi**: 10.1111/j.1758-2229.2010.00211.x.

Lovley, D.R. (2012a). Electromicrobiology. *Annu Rev Microbiol* **66,** 391-409. doi: 10.1146/annurev-micro-092611-150104.

Lovley, D.R. (2012b). Long-range electron transport to Fe(III) oxide via pili with metallic-like conductivity. *Biochem Soc Trans* **40,** 1186-1190. doi: Doi 10.1042/Bst20120131.

Lovley, D.R., Coates, J.D., Bluntharris, E.L., Phillips, E.J.P., and Woodward, J.C. (1996a). Humic substances as electron acceptors for microbial respiration. *Nature* **382,** 445-448. doi: Doi 10.1038/382445a0.

Lovley, D.R., Fraga, J.L., Blunt-Harris, E.L., Hayes, L.A., Phillips, E.J.P., and Coates, J.D. (1998). Humic substances as a mediator for microbially catalyzed metal reduction. *Acta Hydrochimica Et Hydrobiologica* **26,** 152-157. doi: Doi 10.1002/(Sici)1521-401x(199805)26:3<152::Aid-Aheh152>3.0.Co;2-D.

Lovley, D.R., Fraga, J.L., Coates, J.D., and Blunt-Harris, E.L. (1999). Humics as an electron donor for anaerobic respiration. *Environ Microbiol* **1,** 89-98.

Lovley, D.R., Giovannoni, S.J., White, D.C., Champine, J.E., Phillips, E.J., Gorby, Y.A., and Goodwin, S. (1993b). *Geobacter metallireducens* gen. nov. sp. nov., a microorganism capable of coupling the complete oxidation of organic compounds to the reduction of iron and other metals. *Arch Microbiol* **159,** 336-344.

Lovley, D.R., Holmes, D.E., and Nevin, K.P. (2004). Dissimilatory Fe(III) and Mn(IV) reduction. *Adv Microb Physiol* **49,** 219-286. doi: 10.1016/S0065-2911(04)49005-5.

Lovley, D.R., and Nevin, K.P. (2011c). A shift in the current: new applications and concepts for microbe-electrode electron exchange. *Curr Opin Biotechnol* **22,** 441-448. doi: 10.1016/j.copbio.2011.01.009.

Lovley, D.R., and Nevin, K.P. (2013). Electrobiocommodities: powering microbial production of fuels and commodity chemicals from carbon dioxide with electricity. *Curr Opin Biotechnol* **24,** 385-390. doi: 10.1016/j.copbio.2013.02.012.

Lovley, D.R., and Phillips, E.J. (1986a). Availability of ferric iron for microbial reduction in bottom sediments of the freshwater tidal potomac river. *Appl Environ Microbiol* **52,** 751-757.

Lovley, D.R., and Phillips, E.J. (1986b). Organic matter mineralization with reduction of ferric iron in anaerobic sediments. *Appl Environ Microbiol* **51,** 683-689.

Lovley, D.R., and Phillips, E.J. (1988). Novel mode of microbial energy metabolism: organic carbon oxidation coupled to dissimilatory reduction of iron or manganese. *Appl Environ Microbiol* **54,** 1472-1480.

Lovley, D.R., and Phillips, E.J. (1989). Requirement for a microbial consortium to completely oxidize glucose in Fe(III)-reducing sediments. *Appl Environ Microbiol* **55,** 3234-3236.

Lovley, D.R., and Phillips, E.J. (1992a). Reduction of uranium by *Desulfovibrio desulfuricans*. *Appl Environ Microbiol* **58,** 850-856.

Lovley, D.R., and Phillips, E.J.P. (1992b). Bioremediation of uranium contamination with enzymatic uranium reduction. *Environ Sci Technol* **26,** 2228-2234. doi: Doi 10.1021/Es00035a023.

Lovley, D.R., Phillips, E.J.P., and Lonergan, D.J. (1991b). Enzymatic versus nonenzymatic mechanisms for Fe(III) reduction in aquatic sediments. *Environ Sci Technol* **25,** 1062-1067. doi: Doi 10.1021/Es00018a007.

Lovley, D.R., Roden, E.E., Phillips, E.J.P., and Woodward, J.C. (1993c). Enzymatic iron and uranium reduction by sulfate-reducing bacteria. *Marine Geology* **113,** 41-53. doi: Doi 10.1016/0025-3227(93)90148-O.

Lovley, D.R., Ueki, T., Zhang, T., Malvankar, N.S., Shrestha, P.M., Flanagan, K.A., Aklujkar, M., Butler, J.E., Giloteaux, L., Rotaru, A.E., Holmes, D.E., Franks, A.E., Orellana, R., Risso, C., and Nevin, K.P. (2011d). *Geobacter*: the microbe electric's physiology, ecology, and practical applications. *Adv Microb Physiol* **59,** 1-100. doi: 10.1016/B978-0-12-387661-4.00004-5.

Lovley, D.R., Woodward, J.C., and Chapelle, F.H. (1994). Stimulated anoxic biodegradation of aromatic hydrocarbons using Fe(III) ligands. *Nature* **370,** 128-131. doi: 10.1038/370128a0.

Lovley, D.R., Woodward, J.C., and Chapelle, F.H. (1996b). Rapid anaerobic benzene oxidation with a variety of chelated Fe(III) forms. *Appl Environ Microbiol* **62,** 288-291.

Mahadevan, R., Yan, B., Postier, B., Nevin, K.P., Woodard, T.L., O'neil, R., Coppi, M.V., Methe, B.A., and Krushkal, J. (2008). Characterizing regulation of metabolism in *Geobacter sulfurreducens* through genome-wide expression data and sequence analysis. *OMICS* **12,** 33-59. doi: 10.1089/omi.2007.0043.

Maiers, D.T., Wichlacz, P.L., Thompson, D.L., and Bruhn, D.F. (1988). Selenate reduction by bacteria from a selenium-rich environment. *Applied and Environmental Microbiology* **54,** 2591-2593.

Malvankar, N.S., Lau, J., Nevin, K.P., Franks, A.E., Tuominen, M.T., and Lovley, D.R. (2012a). Electrical conductivity in a mixed-species biofilm. *Appl Environ Microbiol* **78,** 5967-5971. doi: 10.1128/AEM.01803-12.

Malvankar, N.S., and Lovley, D.R. (2012b). Microbial nanowires: a new paradigm for biological electron transfer and bioelectronics. *ChemSusChem* **5,** 1039-1046. doi: 10.1002/cssc.201100733.

Malvankar, N.S., Mester, T., Tuominen, M.T., and Lovley, D.R. (2012c). Supercapacitors based on *c*-type cytochromes using conductive nanostructured networks of living bacteria. *Chemphyschem* **13,** 463-468. doi: 10.1002/cphc.201100865.

Malvankar, N.S., Tuominen, M.T., and Lovley, D.R. (2012d). Biofilm conductivity is a decisive variable for high-current-density *Geobacter sulfurreducens* microbial fuel cells. *Energy & Environmental Science* **5,** 5790-5797. doi: Doi 10.1039/C2ee03388g.

Malvankar, N.S., Vargas, M., Nevin, K.P., Franks, A.E., Leang, C., Kim, B.C., Inoue, K., Mester, T., Covalla, S.F., Johnson, J.P., Rotello, V.M., Tuominen, M.T., and Lovley, D.R. (2011). Tunable metallic-like conductivity in microbial nanowire networks. *Nat Nanotechnol* **6,** 573-579. doi: 10.1038/nnano.2011.119.

Manzella, M.P., Reguera, G., and Kashefi, K. (2013). Extracellular electron transfer to Fe(III) oxides by the hyperthermophilic archaeon *Geoglobus ahangari* via a direct contact mechanism. *Appl Environ Microbiol* **79,** 4694-4700. doi: 10.1128/AEM.01566-13.

Marsili, E., Baron, D.B., Shikhare, I.D., Coursolle, D., Gralnick, J.A., and Bond, D.R. (2008). *Shewanella* secretes flavins that mediate extracellular electron transfer. *Proc Natl Acad Sci U S A* **105,** 3968-3973. doi: 10.1073/pnas.0710525105.

Marx, C.J., and Lidstrom, M.E. (2001). Development of improved versatile broad-host-range vectors for use in methylotrophs and other Gram-negative bacteria. *Microbiology* **147,** 2065-2075.

Mcinerney, M.J., Sieber, J.R., and Gunsalus, R.P. (2009). Syntrophy in anaerobic global carbon cycles. *Curr Opin Biotechnol* **20,** 623-632. doi: 10.1016/j.copbio.2009.10.001.

Mckay, D.S., Gibson, E.K., Jr., Thomas-Keprta, K.L., Vali, H., Romanek, C.S., Clemett, S.J., Chillier, X.D., Maechling, C.R., and Zare, R.N. (1996). Search for past life on Mars: possible relic biogenic activity in martian meteorite ALH84001. *Science* **273,** 924-930.

Mehta-Kolte, M.G., and Bond, D.R. (2012). *Geothrix fermentans* secretes two different redox-active compounds to utilize electron acceptors across a wide range of redox potentials. *Appl Environ Microbiol* **78,** 6987-6995. doi: 10.1128/AEM.01460-12.

Mehta, T., Childers, S.E., Glaven, R., Lovley, D.R., and Mester, T. (2006). A putative multicopper protein secreted by an atypical type II secretion system involved in the reduction of insoluble electron acceptors in *Geobacter sulfurreducens*. *Microbiology* **152,** 2257-2264. doi: 10.1099/mic.0.28864-0.

Mehta, T., Coppi, M.V., Childers, S.E., and Lovley, D.R. (2005). Outer membrane *c*-type cytochromes required for Fe(III) and Mn(IV) oxide reduction in *Geobacter sulfurreducens*. *Appl Environ Microbiol* **71,** 8634-8641. doi: 10.1128/AEM.71.12.8634-8641.2005.

Methe, B.A., Nelson, K.E., Eisen, J.A., Paulsen, I.T., Nelson, W., Heidelberg, J.F., Wu, D., Wu, M., Ward, N., Beanan, M.J., Dodson, R.J., Madupu, R., Brinkac, L.M., Daugherty, S.C., Deboy, R.T., Durkin, A.S., Gwinn, M., Kolonay, J.F., Sullivan, S.A., Haft, D.H., Selengut, J., Davidsen, T.M., Zafar, N., White, O., Tran, B., Romero, C., Forberger, H.A., Weidman, J., Khouri, H., Feldblyum, T.V., Utterback, T.R., Van Aken, S.E., Lovley, D.R., and Fraser, C.M. (2003). Genome of *Geobacter sulfurreducens*: metal reduction in subsurface environments. *Science* **302,** 1967-1969. doi: 10.1126/science.1088727.

Morgado, L., Saraiva, I.H., Louro, R.O., and Salgueiro, C.A. (2010). Orientation of the axial ligands and magnetic properties of the hemes in the triheme ferricytochrome PpcA from *G. sulfurreducens* determined by paramagnetic NMR. *FEBS Letters* **584,** 3442-3445.

Morita, M., Malvankar, N.S., Franks, A.E., Summers, Z.M., Giloteaux, L., Rotaru, A.E., Rotaru, C., and Lovley, D.R. (2011). Potential for direct interspecies electron transfer in methanogenic wastewater digester aggregates. *mBio* **2,** e00159-00111. doi: 10.1128/mBio.00159-11.

Mowat, C.G., and Chapman, S.K. (2005). Multi-heme cytochromes—new structures, new chemistry. *Dalton Transactions* **2005,** 3381-3389.

Myers, C.R., and Nealson, K.H. (1988). Bacterial manganese reduction and growth with manganese oxide as the sole electron-acceptor. *Science* **240,** 1319-1321. doi: DOI 10.1126/science.240.4857.1319.

Nevin, K.P., Kim, B.C., Glaven, R.H., Johnson, J.P., Woodard, T.L., Methe, B.A., Didonato, R.J., Covalla, S.F., Franks, A.E., Liu, A., and Lovley, D.R. (2009). Anode biofilm transcriptomics reveals outer surface components essential for high density current production in *Geobacter sulfurreducens* fuel cells. *PLoS One* **4,** e5628. doi: 10.1371/journal.pone.0005628.

Nevin, K.P., and Lovley, D.R. (2000). Lack of production of electron-shuttling compounds or solubilization of Fe(III) during reduction of insoluble Fe(III) oxide by *Geobacter metallireducens*. *Appl Environ Microbiol* **66,** 2248-2251.

Nevin, K.P., and Lovley, D.R. (2002a). Mechanisms for accessing insoluble Fe(III) oxide during dissimilatory Fe(III) reduction by *Geothrix fermentans*. *Appl Environ Microbiol* **68,** 2294-2299.

Nevin, K.P., and Lovley, D.R. (2002b). Mechanisms for Fe(III) oxide reduction in sedimentary environments. *Geomicrobiology Journal* **19,** 141-159.

Nevin, K.P., Richter, H., Covalla, S.F., Johnson, J.P., Woodard, T.L., Orloff, A.L., Jia, H., Zhang, M., and Lovley, D.R. (2008). Power output and columbic efficiencies from biofilms of *Geobacter sulfurreducens* comparable to mixed community microbial fuel cells. *Environ Microbiol* **10,** 2505-2514. doi: 10.1111/j.1462-2920.2008.01675.x.

Nevin, K.P., Woodard, T.L., Franks, A.E., Summers, Z.M., and Lovley, D.R. (2010). Microbial electrosynthesis: feeding microbes electricity to convert carbon dioxide and water to multicarbon extracellular organic compounds. *MBio* **1**. doi: 10.1128/mBio.00103-10.

Newman, D.K., and Kolter, R. (2000). A role for excreted quinones in extracellular electron transfer. *Nature* **405,** 94-97. doi: 10.1038/35011098.

Novak, P.J., Daniels, L., and Parkin, G.F. (1998). Enhanced dechlorination of carbon tetrachloride and chloroform in the presence of elemental iron and *Methanosarcina barkeri*, *Methanosarcina thermophila*, or *Methanosaeta concillii*. *Environ Sci Technol* **32,** 1438-1443. doi: Doi 10.1021/Es970785h.

O'Carroll, D., Sleep, B., Krol, M., Boparai, H., and Kocur, C. (2013). Nanoscale zero valent iron and bimetallic particles for contaminated site remediation. *Advances in Water Resources* **51,** 104-122. doi: http://dx.doi.org/10.1016/j.advwatres.2012.02.005.

Orellana, R., Leavitt, J.J., Comolli, L.R., Csencsits, R., Janot, N., Flanagan, K.A., Gray, A.S., Leang, C., Izallalen, M., Mester, T., and Lovley, D.R. (2013). U(VI) reduction by diverse outer surface *c*-type cytochromes of *Geobacter sulfurreducens*. *Appl Environ Microbiol* **79,** 6369-6374. doi: 10.1128/AEM.02551-13.

Ortiz-Bernad, I., Anderson, R.T., Vrionis, H.A., and Lovley, D.R. (2004). Vanadium respiration by *Geobacter metallireducens*: novel strategy for in situ removal of vanadium from groundwater. *Appl Environ Microbiol* **70,** 3091-3095.

Park, I., and Kim, B.C. (2011). Homologous overexpression of *omcZ*, a gene for an outer surface *c*-type cytochrome of *Geobacter sulfurreducens* by single-step gene replacement. *Biotechnol Lett*. doi: **10**.1007/s10529-011-0668-7.

Phillips, E.J.P., Landa, E.R., and Lovley, D.R. (1995). Remediation of uranium contaminated soils with bicarbonate extraction and microbial U(VI) reduction. *J Ind Microbiol* **14,** 203-207. doi: Doi 10.1007/Bf01569928.

Pirbadian, S., Barchinger, S.E., Leung, K.M., Byun, H.S., Jangir, Y., Bouhenni, R.A., Reed, S.B., Romine, M.F., Saffarini, D.A., Shi, L., Gorby, Y.A., Golbeck, J.H., and El-Naggar, M.Y. (2014). *Shewanella oneidensis* MR-1 nanowires are outer membrane and periplasmic extensions of the extracellular electron transport components. *Proc Natl Acad Sci U S A* **111,** 12883-12888. doi: 10.1073/pnas.1410551111.

Qian, X., Mester, T., Morgado, L., Arakawa, T., Sharma, M.L., Inoue, K., Joseph, C., Salgueiro, C.A., Maroney, M.J., and Lovley, D.R. (2011). Biochemical characterization of purified OmcS, a *c*-type cytochrome required for insoluble Fe(III) reduction in *Geobacter sulfurreducens*. *Biochim Biophys Acta* **1807,** 404-412. doi: 10.1016/j.bbabio.2011.01.003.

Qian, X.L., Reguera, G., Mester, T., and Lovley, D.R. (2007). Evidence that OmcB and OmpB of *Geobacter sulfurreducens* are outer membrane surface proteins. *FEMS Microbiol Lett* **277,** 21-27. doi: DOI 10.1111/j.1574-6968.2007.00915.x.

Reguera, G., Mccarthy, K.D., Mehta, T., Nicoll, J.S., Tuominen, M.T., and Lovley, D.R. (2005). Extracellular electron transfer via microbial nanowires. *Nature* **435,** 1098-1101. doi: 10.1038/nature03661.

Reguera, G., Nevin, K.P., Nicoll, J.S., Covalla, S.F., Woodard, T.L., and Lovley, D.R. (2006). Biofilm and nanowire production leads to increased current in *Geobacter sulfurreducens* fuel cells. *Appl Environ Microbiol* **72,** 7345-7348. doi: 10.1128/AEM.01444-06.

Richter, H., Nevin, K.P., Jia, H.F., Lowy, D.A., Lovley, D.R., and Tender, L.M. (2009). Cyclic voltammetry of biofilms of wild type and mutant *Geobacter sulfurreducens* on fuel cell anodes indicates possible roles of OmcB, OmcZ, type IV pili, and protons in extracellular electron transfer. *Energy & Environmental Science* **2,** 506-516. doi: Doi 10.1039/B816647a.

Richter, L.V., Sandler, S.J., and Weis, R.M. (2012). Two isoforms of *Geobacter sulfurreducens* PilA have distinct roles in pilus biogenesis, cytochrome localization, extracellular electron transfer, and biofilm formation. *J Bacteriol* **194,** 2551-2563. doi: 10.1128/JB.06366-11.

Roden, E.E., Kappler, A., Bauer, I., Jiang, J., Paul, A., Stoesser, R., Konishi, H., and Xu, H.F. (2010). Extracellular electron transfer through microbial reduction of solid-phase humic substances. *Nature Geoscience* **3,** 417-421. doi: Doi 10.1038/Ngeo870.

Roling, W.F., Head, I.M., and Larter, S.R. (2003). The microbiology of hydrocarbon degradation in subsurface petroleum reservoirs: perspectives and prospects. *Res Microbiol* **154,** 321-328. doi: 10.1016/S0923-2508(03)00086-X.

Rollefson, J.B., Levar, C.E., and Bond, D.R. (2009). Identification of genes involved in biofilm formation and respiration via mini-Himar transposon mutagenesis of *Geobacter sulfurreducens*. *J Bacteriol* **191,** 4207-4217. doi: 10.1128/JB.00057-09.

Rollefson, J.B., Stephen, C.S., Tien, M., and Bond, D.R. (2011). Identification of an extracellular polysaccharide network essential for cytochrome anchoring and biofilm formation in *Geobacter sulfurreducens*. *J Bacteriol* **193,** 1023-1033. doi: 10.1128/JB.01092-10.

Ross, D.E., Flynn, J.M., Baron, D.B., Gralnick, J.A., and Bond, D.R. (2011). Towards electrosynthesis in *Shewanella*: energetics of reversing the Mtr pathway for reductive metabolism. *PLoS One* **6,** e16649. doi: 10.1371/journal.pone.0016649.

Ross, D.E., Ruebush, S.S., Brantley, S.L., Hartshorne, R.S., Clarke, T.A., Richardson, D.J., and Tien, M. (2007). Characterization of protein-protein interactions involved in iron reduction by *Shewanella oneidensis* MR-1. *Appl Environ Microbiol* **73,** 5797-5808. doi: 10.1128/AEM.00146-07.

Rotaru, A.E., Shrestha, P.M., Liu, F., Markovaite, B., Chen, S., Nevin, K.P., and Lovley, D.R. (2014a). Direct interspecies electron transfer between *Geobacter metallireducens* and *Methanosarcina barkeri*. *Appl Environ Microbiol* **80,** 4599-4605. doi: 10.1128/AEM.00895-14.

Rotaru, A.E., Shrestha, P.M., Liu, F., Ueki, T., Nevin, K., Summers, Z.M., and Lovley, D.R. (2012). Interspecies electron transfer via hydrogen and formate rather than direct electrical connections in cocultures of *Pelobacter carbinolicus* and *Geobacter sulfurreducens*. *Appl Environ Microbiol* **78,** 7645-7651. doi: 10.1128/AEM.01946-12.

Rotaru, A.E., Shrestha, P.M., Liu, F.H., Shrestha, M., Shrestha, D., Embree, M., Zengler, K., Wardman, C., Nevin, K.P., and Lovley, D.R. (2014b). A new model for electron flow during anaerobic digestion: direct interspecies electron transfer to *Methanosaeta* for the reduction of carbon dioxide to methane. *Energy & Environmental Science* **7,** 408-415. doi: Doi 10.1039/C3ee42189a.

Sambrook, J., Fritsch, E.F., and Maniatis, T. (1989). *Molecular cloning : a laboratory manual.* Cold Spring Harbor, N.Y.: Cold Spring Harbor Laboratory Press.

Schicklberger, M., Sturm, G., and Gescher, J. (2013). Genomic plasticity enables a secondary electron transport pathway in *Shewanella oneidensis*. *Appl Environ Microbiol* **79,** 1150-1159. doi: 10.1128/AEM.03556-12.

Scott, D.T., Mcknight, D.M., Blunt-Harris, E.L., Lovley, D.R., and Kolesar, S.E. (1998). Quinone grows in humic substances as electron acceptors by humic-reducing microorganisms. *Abstracts of Papers of the American Chemical Society* 216**,** U781-U781.

Seeliger, S., Cord-Ruwisch, R., and Schink, B. (1998). A periplasmic and extracellular *c*-type cytochrome of *Geobacter sulfurreducens* acts as a ferric iron reductase and as an electron carrier to other acceptors or to partner bacteria. *J Bacteriol* **180,** 3686-3691.

Shelobolina, E.S., Coppi, M.V., Korenevsky, A.A., Didonato, L.N., Sullivan, S.A., Konishi, H., Xu, H., Leang, C., Butler, J.E., Kim, B.C., and Lovley, D.R. (2007). Importance of *c*-Type cytochromes for U(VI) reduction by *Geobacter sulfurreducens*. *BMC Microbiol* **7,** 16. doi: 10.1186/1471-2180-7-16.

Shi, L., Squier, T.C., Zachara, J.M., and Fredrickson, J.K. (2007). Respiration of metal (hydr)oxides by *Shewanella* and *Geobacter*: a key role for multihaem *c*-type cytochromes. *Mol Microbiol* **65,** 12-20. doi: 10.1111/j.1365-2958.2007.05783.x.

Shrestha, P.M., Nevin, K.P., Shrestha, M., and Lovley, D.R. (2013a). When is a microbial culture "pure"? Persistent cryptic contaminant escapes detection even with deep genome sequencing. *MBio* **4,** e00591-00512. doi: 10.1128/mBio.00591-12.

Shrestha, P.M., Rotaru, A.E., Aklujkar, M., Liu, F.H., Shrestha, M., Summers, Z.M., Malvankar, N., Flores, D.C., and Lovley, D.R. (2013b). Syntrophic growth with direct interspecies electron transfer as the primary mechanism for energy exchange. *Environ Microbiol Rep* **5,** 904-910. doi: Doi 10.1111/1758-2229.12093.

Shrestha, P.M., Rotaru, A.E., Summers, Z.M., Shrestha, M., Liu, F., and Lovley, D.R. (2013c). Transcriptomic and genetic analysis of direct interspecies electron transfer. *Appl Environ Microbiol* **79,** 2397-2404. doi: 10.1128/AEM.03837-12.

Shrestha, P.M., and Rotaru, A.E. (2014). Plugging in or going wireless: strategies for interspecies electron transfer. *Front. Microbiol* **5,** 237. doi: 10.3389/fmicb.2014.00237.

Sieber, J.R., Le, H.M., and Mcinerney, M.J. (2014). The importance of hydrogen and formate transfer for syntrophic fatty, aromatic and alicyclic metabolism. *Environ. Microbiol.* **16,** 177-188. doi: Doi 10.1111/1462-2920.12269.

Slobodkin, A.I. (2005). Thermophilic microbial metal reduction. *Mikrobiologiia* **74,** 581-595.

Smith, J.A., Lovley, D.R., and Tremblay, P.L. (2013). Outer cell surface components essential for Fe(III) oxide reduction by *Geobacter metallireducens*. *Appl Environ Microbiol* **79,** 901-907. doi: Doi 10.1128/Aem.02954-12.

Smith, J.A., Aklujkar, M., Risso, C., Leang, C., Giloteaux, L., Holmes, D.E. (2014). Insight into mechanisms involved in Fe(III) respiration by the hyperthermophilic archaeon, *Ferroglobus placidus*. *In Press*.

Stams, A.J., and Plugge, C.M. (2009). Electron transfer in syntrophic communities of anaerobic bacteria and archaea. *Nat Rev Microbiol* **7,** 568-577. doi: 10.1038/nrmicro2166.

Straub, K.L., and Schink, B. (2003). Evaluation of electron-shuttling compounds in microbial ferric iron reduction. *FEMS Microbiol Lett* **220,** 229-233.

Strycharz, S.M., Glaven, R.H., Coppi, M.V., Gannon, S.M., Perpetua, L.A., Liu, A., Nevin, K.P., and Lovley, D.R. (2011). Gene expression and deletion analysis of mechanisms for electron transfer from electrodes to *Geobacter sulfurreducens*. *Bioelectrochemistry* **80,** 142-150. doi: 10.1016/j.bioelechem.2010.07.005.

Sudarsan, N., Lee, E.R., Weinberg, Z., Moy, R.H., Kim, J.N., Link, K.H., and Breaker, R.R. (2008). Riboswitches in eubacteria sense the second messenger cyclic di-GMP. *Science* **321,** 411-413. doi: 10.1126/science.1159519.

Summers, Z.M., Fogarty, H.E., Leang, C., Franks, A.E., Malvankar, N.S., and Lovley, D.R. (2010). Direct exchange of electrons within aggregates of an evolved syntrophic coculture of anaerobic bacteria. *Science* **330,** 1413-1415. doi: 10.1126/science.1196526.

Summers, Z.M., Gralnick, J.A., and Bond, D.R. (2013). Cultivation of an obligate Fe(II)-oxidizing lithoautotrophic bacterium using electrodes. *MBio* **4,** e00420-00412. doi: 10.1128/mBio.00420-12.

Thomas, P.E., Ryan, D., and Levin, W. (1976). An improved staining procedure for the detection of the peroxidase activity of cytochrome P-450 on sodium dodecyl sulfate polyacrylamide gels. *Anal Biochem* **75,** 168-176.

Tor, J.M., and Lovley, D.R. (2001). Anaerobic degradation of aromatic compounds coupled to Fe(III) reduction by *Ferroglobus placidus*. *Environ Microbiol* **3,** 281-287.

Tremblay, P.L., Aklujkar, M., Leang, C., Nevin, K.P., and Lovley, D. (2012). A genetic system for *Geobacter metallireducens*: role of the flagellin and pilin in the reduction of Fe(III) oxide. *Environ Microbiol Rep* **4,** 82-88. doi: 10.1111/j.1758-2229.2011.00305.x.

Tremblay, P.L., Summers, Z.M., Glaven, R.H., Nevin, K.P., Zengler, K., Barrett, C.L., Qiu, Y., Palsson, B.O., and Lovley, D.R. (2011). A *c*-type cytochrome and a transcriptional regulator responsible for enhanced extracellular electron transfer in *Geobacter sulfurreducens* revealed by adaptive evolution. *Environ Microbiol* **13,** 13-23. doi: 10.1111/j.1462-2920.2010.02302.x.

Ueki, T., Leang, C., Inoue, K., and Lovley, D.R. (2012). Identification of multicomponent histidine-aspartate phosphorelay system controlling flagellar and motility gene expression in *Geobacter* species. *J Biol Chem* **287,** 10958-10966. doi: 10.1074/jbc.M112.345041.

Ueki, T., and Lovley, D.R. (2010a). Genome-wide gene regulation of biosynthesis and energy generation by a novel transcriptional repressor in *Geobacter* species. *Nucleic Acids Res* **38,** 810-821. doi: 10.1093/nar/gkp1085.

Ueki, T., and Lovley, D.R. (2010b). Novel regulatory cascades controlling expression of nitrogen-fixation genes in *Geobacter sulfurreducens*. *Nucleic Acids Res* **38,** 7485-7499. doi: 10.1093/nar/gkq652.

Van Der Zee, F.P., Bisschops, I.A., Lettinga, G., and Field, J.A. (2003). Activated carbon as an electron acceptor and redox mediator during the anaerobic biotransformation of azo dyes. *Environ Sci Technol* **37,** 402-408.

Vargas, M., Kashefi, K., Blunt-Harris, E.L., and Lovley, D.R. (1998). Microbiological evidence for Fe(III) reduction on early Earth. *Nature* **395,** 65-67. doi: 10.1038/25720.

Vargas, M., Malvankar, N.S., Tremblay, P.L., Leang, C., Smith, J.A., Patel, P., Snoeyenbos-West, O., Nevin, K.P., and Lovley, D.R. (2013). Aromatic amino acids required for pili conductivity and long-range extracellular electron transport in *Geobacter sulfurreducens*. *mBio* **4,** e00105-00113. doi: 10.1128/mBio.00105-13.

Vinogradov, E., Korenevsky, A., Lovley, D.R., and Beveridge, T.J. (2004). The structure of the core region of the lipopolysaccharide from *Geobacter sulfurreducens*. *Carbohydr Res* **339,** 2901-2904. doi: 10.1016/j.carres.2004.10.004.

Von Canstein, H., Ogawa, J., Shimizu, S., and Lloyd, J.R. (2008). Secretion of flavins by *Shewanella* species and their role in extracellular electron transfer. *Appl Environ Microbiol* **74,** 615-623. doi: 10.1128/AEM.01387-07.

Voordeckers, J.W., Kim, B.C., Izallalen, M., and Lovley, D.R. (2010). Role of *Geobacter sulfurreducens* outer surface *c*-type cytochromes in reduction of soil humic acid and anthraquinone-2,6-disulfonate. *Appl Environ Microbiol* **76,** 2371-2375. doi: 10.1128/AEM.02250-09.

Weber, K.A., Achenbach, L.A., and Coates, J.D. (2006a). Microorganisms pumping iron: anaerobic microbial iron oxidation and reduction. *Nat Rev Microbiol* **4,** 752-764. doi: 10.1038/nrmicro1490.

Weber, K.A., Pollock, J., Cole, K.A., O'connor, S.M., Achenbach, L.A., and Coates, J.D. (2006b). Anaerobic nitrate-dependent iron(II) bio-oxidation by a novel lithoautotrophic betaproteobacterium, strain 2002. *Appl Environ Microbiol* **72,** 686-694. doi: 10.1128/AEM.72.1.686-694.2006.

Weinberg, Z., Barrick, J.E., Yao, Z., Roth, A., Kim, J.N., Gore, J., Wang, J.X., Lee, E.R., Block, K.F., Sudarsan, N., Neph, S., Tompa, M., Ruzzo, W.L., and Breaker, R.R. (2007). Identification of 22 candidate structured RNAs in bacteria using the CMfinder comparative genomics pipeline. *Nucleic Acids Res* **35,** 4809-4819. doi: Doi 10.1093/Nar/Gkm487.

Williams, K.H., Bargar, J.R., Lloyd, J.R., and Lovley, D.R. (2013). Bioremediation of uranium-contaminated groundwater: a systems approach to subsurface biogeochemistry. *Curr Opin Biotechnol* **24,** 489-497. doi: 10.1016/j.copbio.2012.10.008.

Yan, W.L., Herzing, A.A., Kiely, C.J., and Zhang, W.X. (2010). Nanoscale zero-valent iron (nZVI): Aspects of the core-shell structure and reactions with inorganic species in water. *J Contam Hydrol* **118,** 96-104. doi: DOI 10.1016/j.jconhyd.2010.09.003.

Yi, H., Nevin, K.P., Kim, B.C., Franks, A.E., Klimes, A., Tender, L.M., and Lovley, D.R. (2009). Selection of a variant of *Geobacter sulfurreducens* with enhanced capacity for current production in microbial fuel cells. *Biosens Bioelectron* **24,** 3498-3503. doi: 10.1016/j.bios.2009.05.004.

Yu, N.Y., Wagner, J.R., Laird, M.R., Melli, G., Rey, S., Lo, R., Dao, P., Sahinalp, S.C., Ester, M., Foster, L.J., and Brinkman, F.S. (2010). PSORTb 3.0: improved protein subcellular localization prediction with refined localization subcategories and predictive capabilities for all prokaryotes. *Bioinformatics* **26,** 1608-1615. doi: 10.1093/bioinformatics/btq249.

Zhang, T., Bain, T.S., Nevin, K.P., Barlett, M.A., and Lovley, D.R. (2012). Anaerobic benzene oxidation by *Geobacter* species. *Appl Environ Microbiol* **78,** 8304-8310. doi: 10.1128/AEM.02469-12.

Zhang, T., Tremblay, P.L., Chaurasia, A.K., Smith, J.A., Bain, T.S., and Lovley, D.R. (2013). Anaerobic benzene oxidation via phenol in *Geobacter metallireducens*. *Appl Environ Microbiol* **79,** 7800-7806. doi: 10.1128/AEM.03134-13.

Zhang, T., Tremblay, P.L., Chaurasia, A.K., Smith, J.A., Bain, T.S., and Lovley, D.R. (2014). Identification of genes specifically required for the anaerobic metabolism of benzene in *Geobacter metallireducens*. *Front Microbiol* **5,** 245. doi: 10.3389/fmicb.2014.00245.